IDENTIFICATION OF CATALYSTS FOR THE BENEFICIATION OF PTFE PYROLYSATES

by

Gerard Jacob Puts

A Dissertation Submitted in
Partial Fulfilment of the Degree

Master of Engineering
in Chemical Engineering

at the

University of Pretoria

April 2014

Acknowledgements

The author would like to acknowledge the organisations and individuals listed here for their assistance during the course of this research:

Prof. Philip Crouse, for sponsoring and mentoring me;

The Department of Science and Technology, for funding this research;

Dr Bruno Ameduri, for many fruitful discussions and comments;

Shawn Brits, Louise Roux and Gerry Olivier from SepSci, for training me on the instruments and for their rapid response to mitigate instrumentation breakdowns; and

Dr Wiebke Grote of the Department of Geology for the XRD analyses.

IDENTIFICATION OF CATALYSTS FOR THE BENEFICIATION OF PTFE PYROLYSATES

Synopsis

This dissertation relates the results of the preliminary investigation into the catalytic interaction of PTFE with various inorganic materials, with the primary goal of find catalysts that will greatly increase the yield of the high value pyrolysis products, most notably hexafluoropropylene and octafluorocyclobutane.

This dissertation is divided into three parts, *viz.*: A review on the literature concerning PTFE pyrolysis; a brief description of facilities built for this research; and the results of the experimental work.

The experimental work was conducted with a hyphenated TGA-FTIR system in which samples of commercial PTFE mixed with catalyst were pyrolysed. Some sulfates, fluorides and common oxides of the fourth period- and group 13 metals were used as catalysts.

It was found that the fluorides of the fourth period metals Zn, Cu, Ni, Co, Fe and Mn are generally inert with respect to reformation of the gas phase. The sulfates of these metals produced mixed results with $NiSO_4$ increasing the yield of hexafluoropropylene whilst $CuSO_4$ and $CoSO_4$ produced unidentified side products and the rest being inert. The oxides also produced mixed results with CuO readily oxidising PTFE to CO_2.

Among the group 13 metals, the fluoride, sulphate, and common oxide of aluminium gave the best results, converting the PTFE pyrolysates almost completely to hexafluoropropylene and hexafluoroethane. Reaction mechanisms for the conversion of the pyrolysates on Al_2O_3 are proposed.

No impact was noticed on the yield of octafluorocyclobutane or the yield of the octafluorobutene isomers.

Research recommendations include: Metal oxides examined here should be tested further by examination of the metals in their 3+ and 2+ oxidation states, where the applicable oxide has not been covered; the phosphates of the metals examined here should also be studied to determine if the presence of a phosphorous atom will affect the reactivity; and ab initio work should be conducted to gain insight as to which crystal surfaces are responsible for the catalytic effects of the relevant materials.

The work detailed here was limited to a qualitative investigation of the PTFE/catalyst system and does not include deep theoretical treatment of such topics as pyrolysate mass transfer and catalyst surface conditions.

Table of Contents

List of Figures

List of Tables

Research Outputs

Articles in Peer-reviewed Journals

Puts, GJ, Crouse, PL **(2014)** "The influence of inorganic materials on the pyrolysis of polytetrafluoroethylene. Part 1: The sulfates and fluorides of Al, Zn, Cu, Ni, Co, Fe and Mn." *Journal of Fluorine Chemistry*, under review.

Puts, GJ, Crouse, PL **(2014)** "The influence of inorganic materials on the pyrolysis of polytetrafluoroethylene. Part 2: The common oxides of B, Al, Ga, In, Zn, Cu, Ni, Co, Fe, Mn, Cr, Zr and La." *Journal of Fluorine Chemistry*, under review.

Book Chapters

Puts, GJ, Crouse, PL, Ameduri, B **(2014,** in print**)** *Thermal degradation and pyrolysis of polytetrafluorethylene*, Chapter 5 in: Handbook of Fluoropolymer Science and Technology, John Wiley, New York.

Conference Contributions

Puts, GJ, Crouse, PL **(2013)** *Die invloed van koper- en nikkel-gebaseerde katalisators op die pirolise van PTFE*, SAAWK Studentesimposium 2013, Pretoria, South Africa, November 2013.

Puts, GJ, Crouse, PL **(2013)** *The Effects of copper- and nickel-based catalysts on the PTFE pyrolysis ocess*, SACI Conference 2013, East London, South Africa, December 2013.

Nomenclature

Abbreviation	Description
TFE	Tetrafluoroethylene
PFE	Hexafluoroethane
HFP	Hexafluoropropylene
OFCB	Octafluorocyclobutane
OF1B	Octafluoro-1-butene
Cis-OF2B	Cis-octafluoro-2-butene
Trans-OF2B	Trans-octafluoro-2-butene
PFIB	Perfluoro-isobutene
TGA	Thermogravimetric analyser (analysis)
IR	Infrared
FTIR	Fourier-transform infrared
UV/Vis	Ultraviolet/Visible
GC/MS	Gas-chromatography/mass-spectrometry
NMR	Nuclear magnetic resonance
XRD	X-ray diffraction
XRF	X-ray fluorescence

1 Introduction and Research Motivation

Fluoropolymers possess excellent thermal stability and are nearly completely inert to chemical attack. Polytetrafluoroethylene (PTFE), discovered in 1938 by Roy J. Plunkett at I.E. du Pont de Nemours and Company, is the world's most used fluoropolymer, accounting for 44% of the fluoropolymers market (29 000 metric tons) in 2008 with an estimated global trade value of 367 million US Dollars (Heyes *et al*, 2009).

Applications exploiting the extraordinary properties of the material are wide-ranging and include gaskets, thread-seal tape, pipe liners, bearings, gears, slide plates, filter bags, medical prosthetics, and architectural material (Drobny, 2001; Scheirs, 1997). A few common commercial products made from PTFE are illustrated in Figure 1.

Figure 1: Various common PTFE products.

Due to the difficulties in producing the monomeric materials, and large market demand, fluoropolymers are high-value products. The price for unprocessed PTFE amounted to $16000/ton in 2012, compared to $1500/ton for high density polyethylene.

There are four types of PTFE resins commercially available, *viz.* granular, fine powder, dispersions, and micronized powder. Granular PTFE is prepared by suspension polymerisation, while fine- and micronized powders as well as dispersions are mostly prepared *via* emulsion polymerisation. Granular PTFE constitutes the bulk of the PTFE market, accounting for some 45 % of PTFE production in 2008.

Suspension polymerisation produces predominantly high-molecular-weight PTFE. The emulsion process can be tuned to produce a wide range of molecular weights. Emulsion polymerisation requires the use of perfluorinated surfactants, the most common of which is perfluorooctanoic acid. These perfluorinated surfactants have been shown to impact the environment negatively and are being phased out.

Unlike most other polymers, high molecular weight PTFE cannot be melt processed (Schildknecht, 1952: 491 – 494) and PTFE products are prepared predominantly by mechanical working of a pressed preform, during which a considerable amount of waste material is produced. The mass of waste generated can account for as much as 50 % of the final mass on products of complex geometries (Meissner *et al.*, 2004).

As a consequence, PTFE waste cannot be reprocessed *via* the usual methods employed for plastics recycling and presents both an economic loss as well as a serious ecological problem.

The literature indicates that PTFE may be chemically recycled by pyrolysis to regain high-value fluorinated chemicals (Simon & Kaminsky, 1997), *viz.*: tetrafluoroethylene (TFE), hexafluoropropylene (HFP), and octafluorocyclobutane (OFCB) are important commercial compounds, with TFE being the monomer from which PTFE is made, while HFP is used as a comonomer for producing polymers such as FEP and Viton (Carlson and Schmiegel, 2005). OFCB is primarily used as an etch gas in the

electronics industry. OFCB is of special importance in this role as it preferentially etches SiO_2 (Mezzapelle, 2007).

The pyrolysis process always produces a mixture of gaseous products and recovery of the components requires expensive separation techniques such as cryogenic distillation.

Also, some of the products that can be produced during the pyrolysis process are highly toxic; the generation of PFIB is a prime example (Marhevka *et al.*, 1982). The perfluorobutenes (PFIBs) mainly cause pulmonary oedema, but can also affect the heart muscle.

Any attempt to maximise the yields of the higher value products invariable produces significant quantities of these materials. Furthermore, the general recycling route proposed for PTFE entails PTFE Waste → TFE → New PTFE. The reluctance of commercial entities to engage in energy intensive pyrolysis recycling of PTFE suggests that this process is not economically feasible at present.

From the reviewed pyrolysis literature (Puts *et al.*, 2014) it is clear that there has been very little work done on the catalytic benefication of the pyrolysates to specific products.

Such catalytic reformation would be of immense importance to the fluorochemical industry due to its application in the manufacture of monomeric material and the improvement of the economics of the PTFE recycle process.

The present work was undertaken to attempt to remedy this matter by screening of numerous materials for catalytic activity relating to the reformation of PTFE pyrolysates to specific products, shifting of the product yield to higher order fluorocarbons or *in situ* elimination of any toxic by-products.

This document is structured to present:

1. A review of the literature regarding the pyrolysis of PTFE, in a form slightly modified from that which was presented previously (Puts *el al.*, 2014);
2. A description of the facilities developed for this project;

3. The experimental methods by which the research was conducted;
4. The results of the investigation, with discussion;
5. The conclusions drawn from the results; and
6. Recommendations for future research are also provided.

It must also be stressed that due to the pilot nature of this research, the focus is on experimental work rather than detailed theoretical discussions.

2 Literature Review

The review of the literature regarding PTFE pyrolysis is made difficult by the considerable overlap between the reactions involved and fluoro-organic chemistry in general. Care has been taken to remain within the bounds of the gas phase regime and divergence into the realm of solution chemistry was kept to a minimum. Accordingly, some applicable literature may have been missed.

The literature on PTFE pyrolysis is divided into four sections, *viz.*:

1) Literature that deals directly with pyrolysis;
2) Literature that deals with the *autogenous* reactions of the pyrolysis products under pyrolysis conditions;
3) Literature that deals with the catalysed reactions of the pyrolysis products; and
4) Literature that deals with co-pyrolysis reactions of PTFE with various substances.

It should be noted that the reactions of the main pyrolysis products must be discussed alongside the actual pyrolysis process as it is not possible to decouple one from the other. The reactions of the various pyrolysis products with reactive gases are discussed alongside the catalysed reactions as there is considerable overlap between the two, especially where homogenous catalysis is concerned.

2.1 Overview of Pyrolysis Methods

The practical aspects of pyrolysis, *e.g.* reaction conditions, experimental techniques and so forth, are grouped together as *pyrolysis methods*. Four methods of pyrolysis are reported in the literature, *viz.*:

(i) reduced pressure or vacuum pyrolysis;
(ii) ambient pressure pyrolysis;
(iii) inert-gas assisted pyrolysis; and
(iv) reactive-gas assisted pyrolysis.

Homogeneous Pyrolysis:

Vacuum pyrolysis and ambient pressure pyrolysis are essentially the same operation, but these methods have traditionally been dealt with separately due to the design of the laboratory setup. For industrial applications this point is moot and these two methods may be grouped together as homogeneous pyrolysis, which may occur either as batch- or as continuous processes.

For batch processes, the reactor (a quartz tube or a steel pressure vessel) is charged with a fixed mass of PTFE, flushed with an inert gas (usually argon or nitrogen) and then either evacuated or pressurised to the desired operating conditions. The pressurising gas may be inert or may consist of pyrolysis gases. The reactor is then heated to the desired temperature by means of an electric furnace (Meissner *et al.*, 2004; Marhevka *et al.*, 1982; Hunadi & Baum, 1982; Choi & Park, 1975; Madorsky *et al.*, 1953; Lewis & Naylor, 1947).

Only one instance of the flash pyrolysis (addition of PTFE after the reactor has reached operating temperature) has been reported (Bhadury *et al.*, 2007). The gaseous pyrolysis products are collected in a liquid nitrogen cold trap and separated by distillation.

An example of a laboratory scale batch reactor setup is presented in Figure 2.

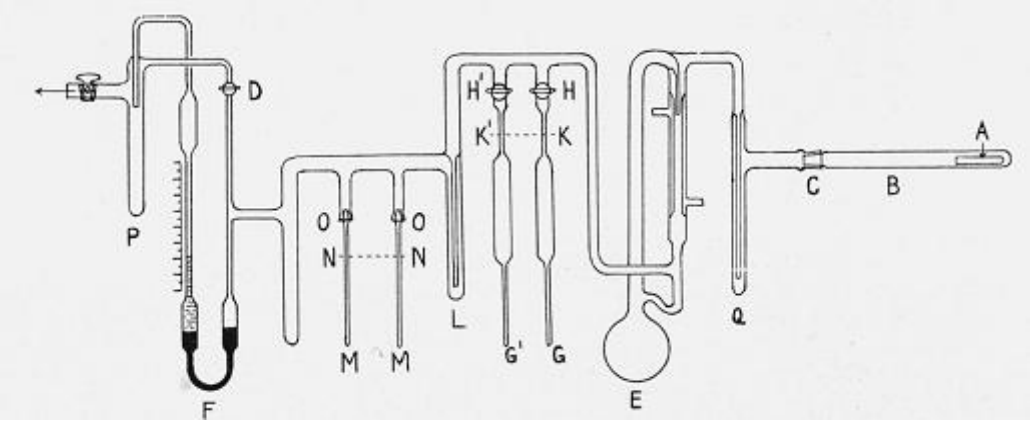

Figure 2: A schematic representation of a batch pyrolysis reactor system. Image taken from Madorsky *et al.* (1953).

For continuous pyrolysis, only metal reactors (steel or nickel) are used and PTFE is fed into the reactor with a screw feeder. The gaseous products are either collected using a scaled up cold trap, or fed directly into other processes (Van der Walt *et al.*, 2008; Meissner *et al.*, 2004). Continuous systems suffer a serious drawback in that it is very difficult to maintain a pressure seal at the PTFE inlet, resulting in the inclusion of air in the reactor atmosphere, which results in PTFE combustion rather than pyrolysis and produces a mixture of mostly undesired products, such as CF_4, CO_2 and CF_2O. An example of a continuous pyrolysis reactor system is presented schematically in Figure 3.

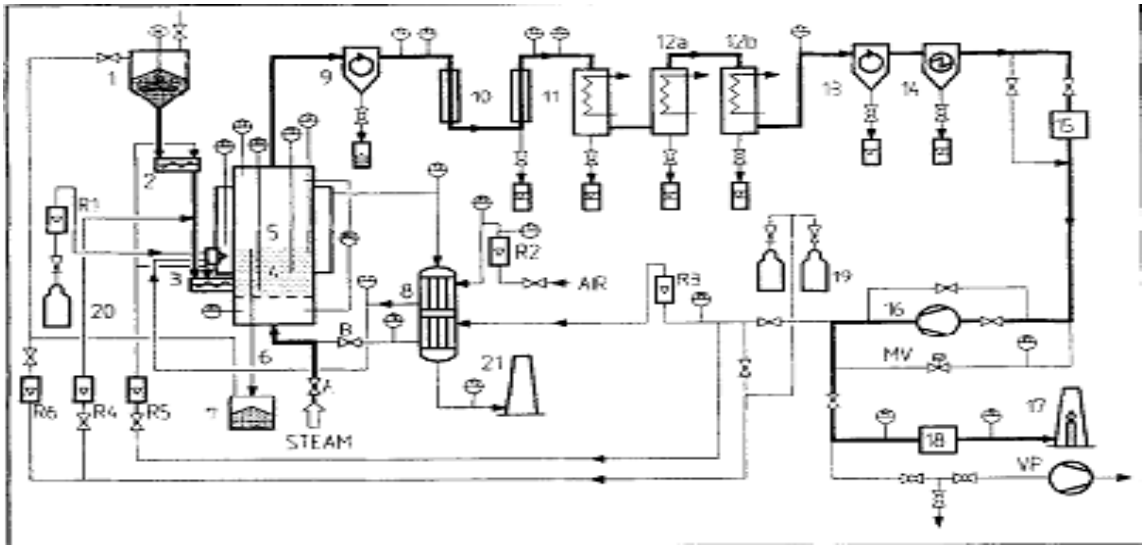

Figure 3: A schematic representation of a continuous pyrolysis reactor system. Image taken from Simon & Kaminsky (1998).

Table 1 summarises available data concerning the products obtained through homogenous pyrolysis of PTFE and their relative yields in relation to pyrolysis conditions. The data in the table were collated from several publications.

Table 1: Distribution of Products obtained from the Homogeneous Pyrolysis of PTFE as Functions of Temperature and Pressure.

101325 Pa Absolute Pressure

Temperature	TFE	HFP	OFCB	PFIB	Perfluorates	Ref.
600 °C	15.9 %	25.7 %	54.3 %	4.1 %	-	A

83600 Pa Absolute Pressure

Temperature	TFE	HFP	OFCB	PFIB	Perfluorates	Ref.
600 °C	32 %	26 %	42 %	-	-	D
700 °C	52 %	24 %	18 %	5 %	-	D

30000 Pa Absolute Pressure

Temperature	TFE	HFP	OFCB	PFIB	Perfluorates	Ref.
600 °C	30.79 %	30.22 %	6.89 %	-	32.1 %	B
700 °C	12.17 %	28.32 %	3.76 %	15.47 %	40.28 %	B
800 °C	1.17 %	40.60 %	-	6.93 %	51.3 %	B

5500 Pa Absolute Pressure

Temperature	TFE	HFP	OFCB	PFIB	Perfluorates	Ref.
600 °C	85.7 %	14.3 %	<4 %	-	-	A
700 °C	82.1 %	17.9 %	<4 %	-	-	A

670 Pa Absolute Pressure

Temperature	TFE	HFP	OFCB	PFIB	Perfluorates	Ref.
500 °C	96.8 %	2.9 %	-	-	-	C
600 °C	97 %	3 %	-	-	-	A

A. Lewis & Naylor, 1947. **B.** Van der Walt *et al.*, 2008. **C.** Madorsky *et al.*, 1953.

D. Choi & Park, 1975. Note: The percentages reported here do not necessarily add up to a 100 %.

It is clear that there is a severe lack of correlation amongst the various datasets presented in Table 1. Although much work has been done, a thorough study

reporting the percentage yields at a sufficient number of pressures and temperatures to allow for statistically meaningful analysis has not been conducted. The two main factors which make interpretation of the data in Table 1 difficult, are the fact that the gaseous pyrolysis products self-react, and that that there is a great likelihood that the materials of construction have a catalytic effect. Additional and more exact detail regarding these materials, along with detail regarding reactor and system geometries and operating conditions are required for a definitive analysis.

A few authors have attempted to extract reaction kinetics from their experimental work. Kinetic expressions reported in the literature include both the kinetics of PTFE pyrolysis and the kinetics of the various gas phase reactions. A summary of these kinetics is presented in Table 2.

Table 2: Arrhenius rate constants and reaction orders for the pyrolysis of PTFE and the relevant gas phase reactions of the pyrolysis products.

Reaction Description	Reaction Order	Frequency Factor	Activation Energy	Ref
Dimerisation of TFE to OFCB	Second Order	10.3×10^{7} /s	106.3 kJ/mol	A
Breakdown of OFCB to TFE	First Order	8.9×10^{15} /s	310 kJ/mol	A
HFP formation from TFE	Second Order	9×10^{8} /s	126.7 kJ/mol	B
PTFE depolymerisation	First Order	4.7×10^{18} /s	336 kJ/mol	C
PTFE depolymerisation	First Order	3×10^{19} /s	347.3 kJ/mol	D
PTFE depolymerisation	First Order	4.122×10^{21} /s	349.1 kJ/mol	E
PTFE combustion	First Order	2.038×10^{18} /s	299.6 kJ/mol	E

A. Atkinson & Trenwith, 1953 **B.** Atkinson & Atkinson, 1957. **C.** Madorsky *et al.*, 1953.

D. Siegle *et al.*, 1964. **E.** Conesa & Font, 2001.

It must be noted that variability in the analysis techniques used to identify and quantify the reaction products cannot be ruled out as a source of uncertainty in the

product compositions and the reaction constants. For example, Bhadury *et al.* (2007) reported the use of a modern GC/MS system, whereas Madorsky *et al.* (1953) used a distillation technique with the identifications being made by boiling point and quantification done *via* partial pressure calculations.

As yet no-one has attempted any *in situ* measurements of the gas phase composition and, given the batch nature of the analyses done to date, online measurements of the gaseous products as they exit the primary reaction zone will be a major step forward in terms of extraction of reaction kinetics.

Inert gas assisted pyrolysis:

Inert-gas assisted pyrolysis concerns the continuous pyrolysis of PTFE using an inert gas as heat transfer- and product transport medium. The reactor setup and products obtained for this method are similar to those reported for homogenous continuous pyrolysis. This method is preferred over homogeneous continuous pyrolysis as it allows for better control of the product residence time in the reactor and facilitates the exclusion of air from the pyrolysis system.

It was reported by Simon and Kaminsky (1997) that while any inert gas can theoretically be used, nitrogen is usually preferred as it does not condense in a cold trap and gives TFE yields upwards of 75%. The same authors reported the use of steam as inert gas. They indicated that steam should be used for any inert gas assisted pyrolysis as it gives TFE yields comparable to the nitrogen assisted method, but allows for the easy separation of the product gases from the carrier medium.

While the work of Simon and Kaminsky has resulted in a patent (Hintzer *et al.*, 1995) and an indication of the intent to construct a pilot plant, no commercial recycling of PTFE waste has been conducted using either inert gas assisted or homogeneous pyrolysis. Work similar to that of Simon & Kaminsky was reported for laboratory scale production of TFE by Arkles and Bonnett (1974) and by Filatov and co-workers (2011).

Reactive gas assisted pyrolysis:

Numerous research articles report the reactions of TFE with other gaseous species to produce high-value products (Barabanov *et al.*, 2011; Takagi *et al.*, 2000; Tittle, 1972; Fokin *et al.*, 1964; Krespan & Langkammerer, 1962; England *et al.*, 1960; Michaelsen & Wall, 1957). Since TFE is the major product in PTFE pyrolysis, it stands to reason that the use of a gas which is reactive towards TFE, such as SO_2, in place of an inert carrier gas will allow for the continuous production of high value chemicals from PTFE waste.

As yet, no mention has been made in the public-domain literature of this potential method, despite the fact that the procedure is very similar to that proposed for the recycling of PTFE waste by inert gas assisted pyrolysis.

2.2 Mechanism of Polymer Breakdown

The literature contains considerable debate as to how exactly the polymer chain breaks down to gaseous compounds and why no solid residue remains after pyrolysis of pure PTFE.

Several workers have postulated that, since TFE is the main pyrolysis product, the PTFE chain snaps a C-C bond somewhere along its length to produce shorter, radically terminated chains which then cleave off TFE molecules, continuously shortening the chain in the process until the entire chain has "unzipped", as illustrated by the scheme in Figure 4 (Simon & Kaminsky, 1997; Lonfei *et al.*, 1986; Madorsky *et al.*, 1953; Lewis & Naylor, 1947).

This postulate, however, does not account for the formation of HFP, OFCB or PFIB and provides no proper explanation for why only TFE should be liberated.

Confirmation of chain scission and, at least, liberation of a radical species arises from degradation studies achieved using filled PTFE. By electron spin resonance spectroscopy, Fock (1968) found that the carbon black used in carbon filled PTFE contained large numbers of unpaired electrons and that pyrolysis of carbon filled PTFE showed vastly different decomposition rates to neat and bronze filled PTFE. He

concluded that the difference in degradation behaviour is due to radical intermediates being stabilized by the unpaired carbon black electrons.

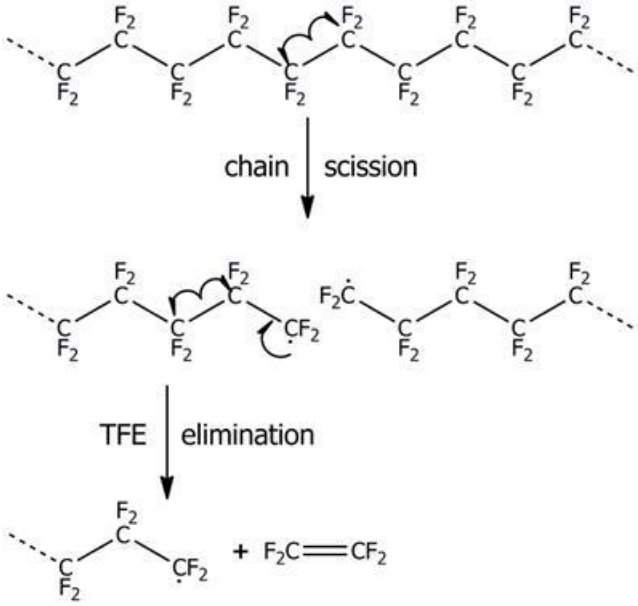

Figure 4: Postulated mechanism for releasing TFE during pyrolysis of PTFE.

As illustrated by Figure 5, the fluorine atoms in a PTFE chain are tightly packed in a 13/6 helical arrangement around the carbon backbone, making the chain far more rigid than its polyethylene hydrocarbon analogue.

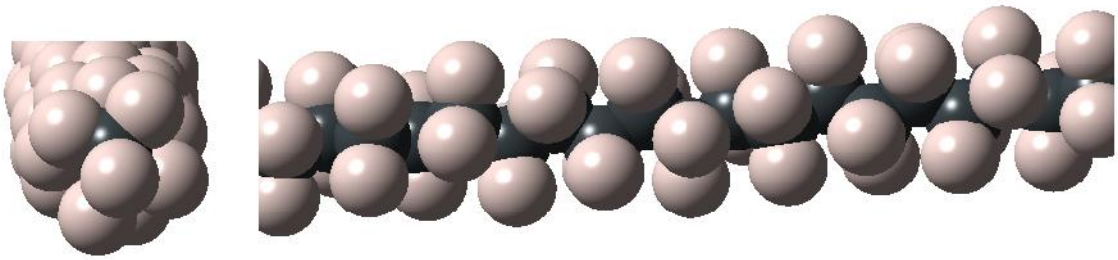

Figure 5: Front- and side-on view of the atomic arrangement in a PTFE chain.

The highly rigid, close packed structure and the great strength of the C-F bond (507 kJ/mol) imply that no fluorine abstraction or internal chain rearrangements of fluorine atoms can occur and products such as HFP and OCFB cannot be directly split from the chain. This is also the reason why no polymer crosslinking (which results in solid residue during polyethylene pyrolysis) occurs in PTFE pyrolysis (Florin *et al.*, 1954).

The nominal bond strength of a C-C bond in a PTFE chain is 359 kJ/mol (Simon & Kaminsky, 1997). The calculations performed by Errede (Errede, 1962) indicate that the strength of the C-C bond falls from 359 kJ/mol to 184 kJ/mol when going from the centre of the fragment to the bond next to the radical carrying carbon, as illustrated in Figure 6.

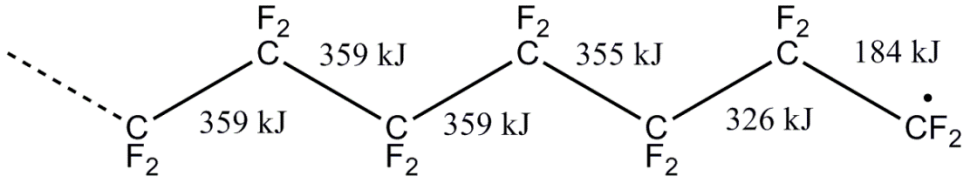

Figure 6: Bond strengths in a PTFE radical fragment.

As the weakest bonds will break first, it becomes evident that a [:CF_2] unit rather than a TFE unit will be cleaved from the radical fragment. These radicals are well studied and they have rather long half-lives compared to their hydrocarbon analogues due to the stabilization of the radical pair by the fluorine atoms.

At temperatures below 700 °C and at partial pressures of 1 mmHg the difluorocarbene molecule has a half-life of about 1 second (Laird *et al.*, 1950). This half-life is sufficiently long for reactions other than recombination to occur, which accounts for the variety of pyrolysis products.

The cleavage of difluorocarbene units is supported by the experimental observation that CF_2O is the major product of the combustion of PTFE in air (Odochian *et al.*, 2011; Conesa & Font, 2001; Baker & Kasprzak, 1993; Williams & Clarke, 1982).

We postulate that, during pyrolysis, the PTFE chain undergoes random scission to produce radically terminated fragments which cleave off difluorocarbenes. This mechanism is summarized by the scheme presented in Figure 7.

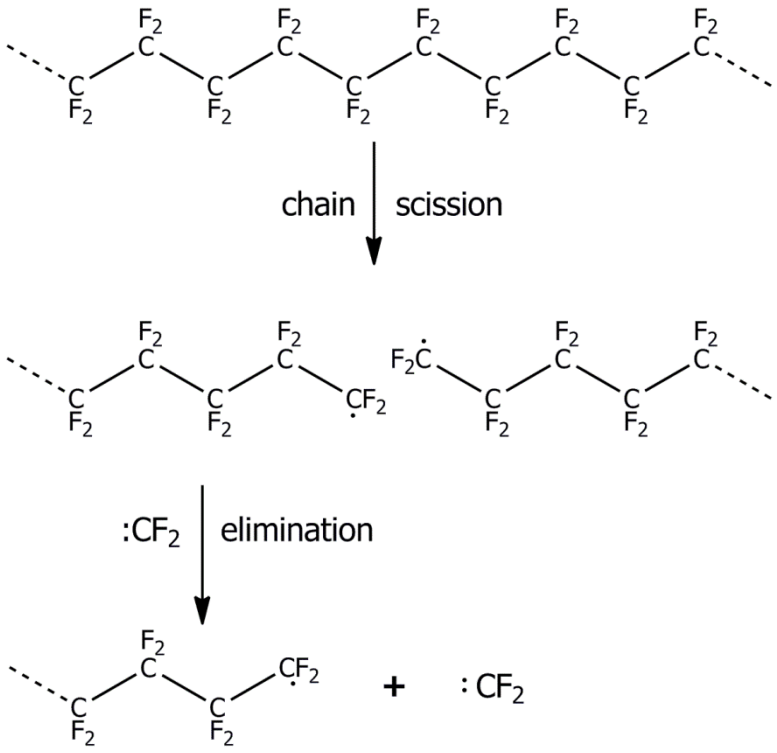

Figure 7: Proposed mechanism for the decomposition of PTFE during pyrolysis.

The thermodynamics of the depolymerisation process has not been studied in detail owing to the lack of thermodynamic data for the polymeric chain. Van der Walt (2007) performed molecular modelling to predict the thermodynamic properties of the polymer chain and the radical intermediates. He calculated the heats of reaction for $C_{10}F_{21}$ releasing [:CF2] or C2F4 as being 190.41 kJ/mol and 218.08 kJ/mol, respectively. These calculations only gave results for a system at 25 °C, but provide

a strong indication that the release of difluorocarbene is, from a thermodynamic point of view, preferable to the direct release of TFE.

The generation of [:CF_2] during pyrolysis of TFE or pyrolysis of CHF_2Cl to TFE is a known fact (Brahms & Dailey, 1996). It has also been experimentally proven that difluorocarbene radicals are released during the thermal breakdown of a number of other small, mostly heterogeneous fluorocarbons in both the liquid and gas phase. Brahms does mention that [:CF_2] is generated during PTFE pyrolysis, but investigation of her reference train reached a dead end in that no mention of any experimental verification of this release could be found in the cited literature.

As pointed out by Penski and Goldfarb (Penski & Goldfarb, 1964), the effect of caging, *i.e.* the solvation and retainment of gases inside the bulk polymer, cannot be ignored during pyrolysis. No studies on this topic other than the one by these authors have been published owing to the great complexity of the issue. However, it stands to reason that this effect only becomes important at high pressures. Under extreme vacuums the diffusion of the gaseous species through the bulk material is simply too rapid for solvation to have any real effect.

The possible effects of polymer chain geometry on the mechanism of breakdown should also be considered. Most solid PTFE exists in highly crystalline form with the crystalline phase consists of regular foldings of polymer chain that form parallel layers known as lamella, shown schematically in Figure 8.

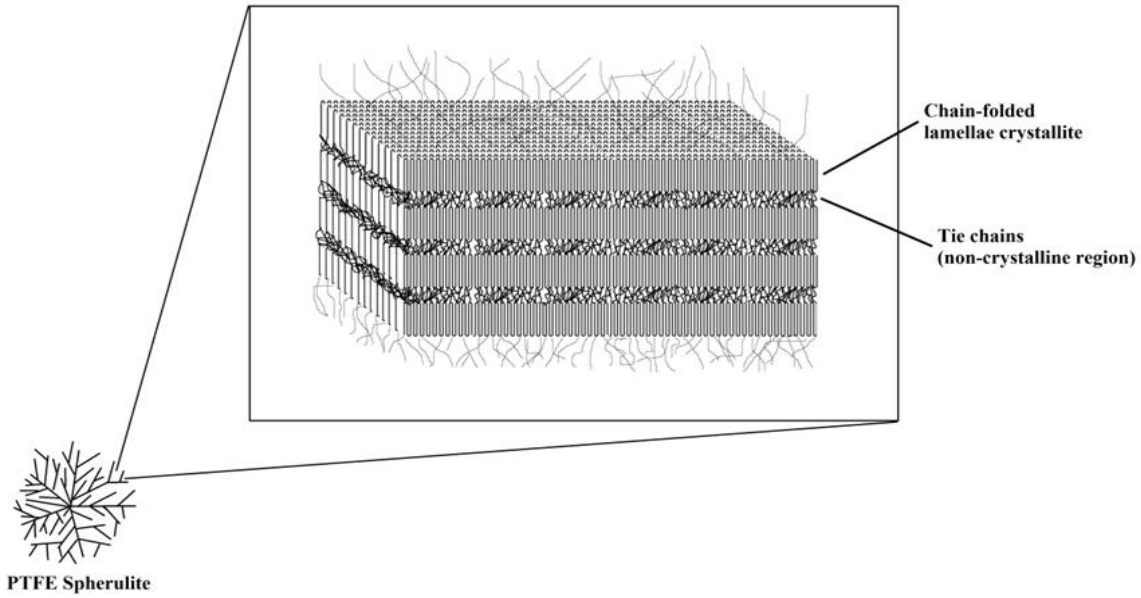

Figure 8: PTFE chain arrangements in crystalline PTFE.

Bends in the polymer chain are accompanied by a disturbance of the helical arrangement, resulting in sites of higher steric strain and non-minimum electronic energy states. This disturbance of the helix has been noted even in the molten state and the polymer melt has been shown by X-ray diffraction to be closely packed and entangled. Observations related to the crystallinity of processed PTFE confirm the presence of interlamellar entanglement (Drobny, 2001: 37).

Given this complex geometry in the molten state, the assumption that all parts of the chain are equally likely to break is suspect, but there has been no study done to determine if there is a preference for scission to occur at specific points in the chain, such as bending sites in the lamellae. However, it stands to reason that sites of steric strain should be the place where scission primarily occurs.

The previously mentioned observations then indicate that PTFE chain breakdown occurs via chain scission at the bending sites of lamellar folds followed by release of [:CF_2] which recombine to form various gaseous products.

It must however be said that without direct experimental confirmation or rebuttal of [:CF_2] release, all the mechanisms proposed for gaseous product formation are enlightened speculation at best.

2.3 Autogenous Reactions of Pyrolysis Products

The difluorocarbene radicals produced by PTFE pyrolysis undergo a number of autogenous gas phase reactions and these range from simple recombination to multistep rearrangements. Much literature exists on the topic and many conflicting mechanism have been proposed (Odochian *et al.*, 2011; Garcia *et al.*, 2007; Buravtsev & Kolbanovsky, 1999; Buravtsev *et al.*, 1994a; Buravtsev *et al.*, 1994b; Lonfei, 1986; Morisaki, 1977; Lewis & Naylor, 1947).

A species by species account of the mechanism of formation of all major products, taking into account the proposed mechanism of PTFE pyrolysis, is laid out below.

2.3.1 Mechanism of Tetrafluoroethylene Formation

As indicated by Table 1, the main pyrolysis product under vacuum conditions is TFE. It is formed by the recombination of two [:CF_2] units. Buravtsev's observation of a TFE biradicaloid during the decomposition of TFE and the recombination of difluorocarbene indicates that TFE is formed *via* the mechanism displayed schematically in Figure 9 (Buravtsev *et al.*, 1994a; Buravtsev *et al.*, 1994b).

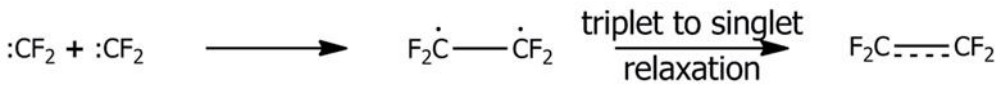

Figure 9: Mechanism of TFE formation from difluorocarbene.

It should be noted that the biradicaloid is not the same as a 1,2-biradical. There is still sufficient sharing of the electrons between the carbons that the electrons cannot

be said to be wholly localized to specific carbons. Then this bond takes on a character intermediate between that of a 1,2-biradical and a π-bond and is considerably more labile that the double bonds found in simple unsaturated hydrocarbons.

2.3.2 Mechanism of Octafluorocyclobutane Formation

Atkinson and co-workers discovered an equilibrium between OFCB and TFE (Atkinson & Trenwith, 1953). They postulated that TFE forms a dimer with itself which exists long enough for the double bond to open up and allow for cyclisation to occur between the TFE units, as detailed schematically in Figure 10.

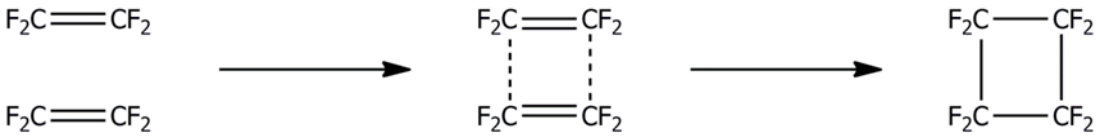

Figure 10: Atkinson's postulate for the mechanism of formation of OFCB from TFE.

The dimer formation is extremely unlikely as it would require a side-on collision between TFE molecules. Being electron rich, the likelihood this occurring in such a way that a stable dimer could form before coulombic repulsion pushes them apart is very small and would result in low yields of OFCB.

Work by a number of authors shows that OFCB comprises a large percentage of the product when pyrolysis occurs at 500 °C – 700 °C (Bhadury *et al.*, 2007; Simon & Kaminsky, 1997; Madorsky *et al.*, 1953; Lewis & Naylor, 1947). They also noted a decrease of OFCB yield with increase in reaction pressure, which, according to Atkinson's postulate would favour increasing OFCB yield. This indicates that the dimer postulate is incorrect.

An *ab initio* investigation by Wang and Borden (Wang & Borden, 1989) into the nature of the π-bond in TFE revealed that the 1,2 biradicaloid of TFE does not keep

the theoretical planar configuration of the ground state. The carbon atoms only barely conform to SP^2 hybridisation and have significant SP^3 character and take on a distorted tetrahedral form.

These facts indicate that OFCB is produced by collision of TFE biradicaliods to form 1,4-perfluorobutane biradicals which undergo cyclization *via* rotation of the bond between the second and third carbons followed by bonding of the terminal radicals, as detailed schematically in Figure 11.

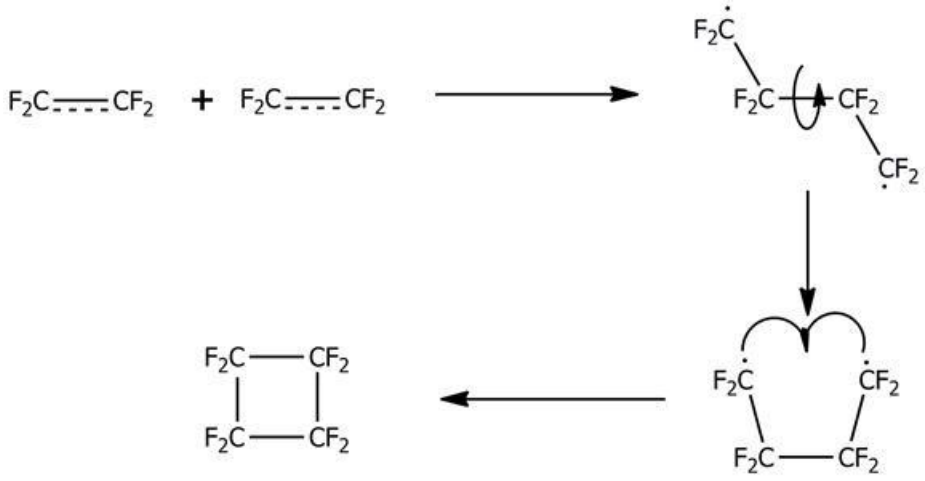

Figure 11: Buravtsev's mechanism for the formation of octfluorocyclobutane from TFE.

As yet, no study has been conducted to determine the energy barrier for this rotation, nor how it correlates to the experimental activation energies reported for Atkinson's postulate.

It is interesting, however, that the activation energy for the reverse reaction in Atkinson's postulate is 310 kJ (Atkinson & Trenwith, 1953), which is only 40 kJ less that the energy required to rupture a C-C bond in a long $(CF_2)_n$ chain.

It is well known from organic chemistry that cyclobutanes are under great steric strain and will readily break a C-C bond to revert to a linear conformation. It stands to reason that the experimental activation energy for the reverse reaction is the energy required to rupture a C-C bond in OFCB.

Lacher and co-workers studied the dimerization of TFE and trifluorochloroethylene (TFCE) (Lacher *et al.*, 1952). The results indicated a difference of 3.8 kJ/mol in activation energy between the dimerization of TFE with itself and the dimerization of TFE with TFCE and a difference of 84 J between TFE-TFCE and TFCE-TFCE.

It is expected that there will be an increase of the rotational energy barrier with increase in substituent size. As a result, the findings of Lacher and co-workers strongly support the existence of the mechanism detailed in Figure 11.

Indeed, Hoffmann and Woodward (1965) using Lacher and other's observations discovered the general rule that for [2+2] cycloadditions it is not possible to form products by direct dimer type bonding and any product formation must go through a multistep diradical mediated mechanism.

Although the word "postulate" is used here, the mechanism described is strongly supported by experimental evidence.

2.3.3 Mechanism of Hexafluoropropylene Formation

Two major postulates for HFP formation are reported in the literature (Garcia *et al.*, 2007; Buravtsev *et al.*, 1999; Simon & Kaminsky, 1997; Morisaki, 1977; Atkinson & Atkinson, 1957). These postulates are summarised in reaction Equations 1 and 2.

$$OFCB \rightarrow HFP + :CF_2 \qquad \textbf{(Eq. 1)}$$

$$TFE + :CF_2 \rightarrow HFP \qquad \textbf{(Eq. 2)}$$

There are several other minor postulates presented in literature, all of which are variations on the above. No mechanisms have been reported for these postulates by the authors and no mechanisms could be found in literature for the formation of HFP. The reaction in Equation 1 would, however, require fluorine rearrangement in

the 1,4-biradical that intermediates OFCB formation, and the reaction in Equation 2 would require the simultaneous addition of carbene and rearrangement of fluorine in the 1,3-biradical which would form from the reaction of TFE and [:CF_2].

No spectroscopic proof of the 1,4 and 1,3 radical rearrangements has been found at the relevant temperatures, despite a rather thorough investigation by Kolbanovskii (Kolbanovskii *et al.*, 1990). Kolbanovskii did however discover that a 1,2 fluorine shift occurs in TFE at temperatures in the region of 750 °C to produce [:CF-CF_3].

It is known from organic chemistry that HFP is not sterically strained and thus more stable than OFCB and should theoretically form first. This is however not the case (Bhadury *et al.*, 2007; Moon *et al.*, 2004; Miller, 1951; Lewis & Naylor, 1947; Harmon, 1946). Given that HFP yields only become significant above 750 °C, a modification of the postulate in Equation 2 to include Kolbanovskii's observations is required to explain HFP formation. This mechanism is detailed schematically in Figure 12.

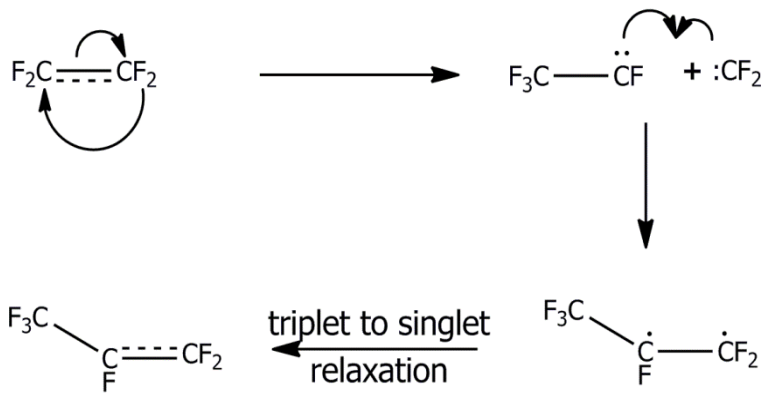

Figure 12: Proposed mechanism of HFP formation during the pyrolysis of TFE.

Gelblum (Gelblum *et al.*, 2010) mentions the intermediaries presented in Figure 12 in a patent concerning the optimised production of HFP, further substantiating the presented reaction scheme.

The double bond in HFP possesses a biradicaloid nature similar to that of TFE, but with a somewhat more pronounced electron division in favour of a localised electron on the centre carbon.

In a review of spectroscopic work on this topic, Buravtsev did not detect [:CF-CF_3] during decomposition of HFP and subsequently rejected the formation mechanism presented in Figure 12 in favour of a mechanism which admits direct [:CF_2] addition to TFE biradicaloids and requires internal fluorine and electron rearrangement within the newly formed 1,3 biradicals to give 1,2 biradicaloids, which then relax to give HFP, as presented schematically in Figure 13 (Buravtsev & Kolbanovskii, 2001; Buravtsev *et al.*, 1999). He indicated that this mechanism was energetically more favourable than the mechanism of Figure 12. However, he did not in any way report the method by which his calculations were performed, making them potentially suspect.

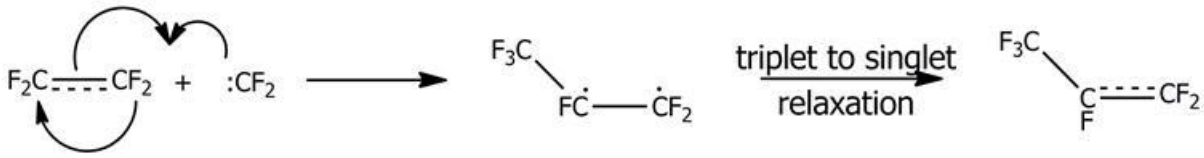

Figure 13: Buravtsev's HFP formation hypothesis (Buravtsev *et al.*, 1999).

His work fails to take into account that OFCB, which is less stable than HFP, is preferentially formed over HFP at lower temperatures and higher pressures during pyrolysis of PTFE, in an environment where high concentrations of both TFE and [:CF_2] are present, which would favor HFP formation according to his postulate. Until this discrepancy is explained, the mechanism, as given in Figure 13, will be accepted as valid.

2.3.4 Mechanism of Formation of Perfluorobutenes

No mechanism could be found in the literature that accounts for PFIB formation. Given that its production only becomes significant at 900 °C and 1 bar pressure, one can argue that 1,2-fluorine shift could occur within HFP to produce a high temperature radical intermediate stable enough to react with [:CF_2] and produce PFIB, as detailed by the postulate indicated in Figure 14.

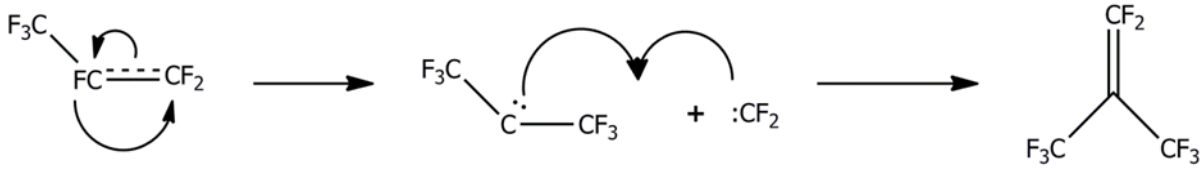

Figure 14: Proposed mechanism for PFIB formation during the pyrolysis of PTFE.

Two other butene isomers are formed besides PFIB, *viz.* perfluoro-1-butene and perfluoro-2-butene. However, as with PFIB, a mechanism of formation from TFE or other pyrolysis products is lacking.

However, German *et al.* (1988) did observe a 1,2 shift in perfluoro-2-butene that resulted in the isomerisation of perfluoro-2-butene to perfluoro-1-butene, detailed schematically in Figure 15.

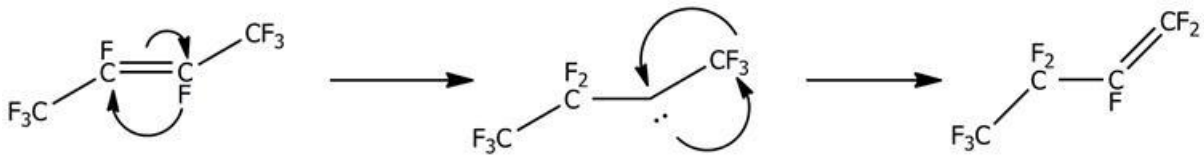

Figure 15: Mechanism of the isomerisation of Perfluoro-2-butene (German *et al.*, 1988).

This isomerisation proves the existence of an internal carbene radical and supports the mechanism in Figure 14. This mechanism does not support Buravtsev's postulate

for the formation of HFP as this mechanism is in two steps while Buravtsev's postulate requires simultaneous addition and fluorine rearrangement.

Additionally, they also indicated a possible mechanism for the formation of perfluoro-2-butene from TFE, presented in Figure 16.

Figure 16: Postulated mechanism for the formation of perfluoro-2-butene from TFE (German *et al.*, 1988).

However, it must be made clear that this mechanism is a postulate only, and that no spectroscopic observation has yet been reported for this.

2.3.5 Remarks on the Autogenous Reactions

The preceding discussions make it clear that the autogenous reactions are in no way fully understood and that considerable work must be carried out to harmonise the available data. Indeed, the author suspects that a complete experimental overhaul must be committed in order to clear up the controversies in the literature.

Nevertheless, one can conclude that the autogenous reactions of the pyrolysis products occur via radical mediated mechanisms, that the lifetimes of these radicals are strongly dependant on the temperature of the reaction zone and that any rearrangement reactions occur primarily via 1,2 fluorine shifts.

2.4 Catalytic Reactions of the Pyrolysis Products

TFE is the major product generated during PTFE pyrolysis and all attempts at catalytic beneficiation of pyrolysis off gas should focus on reformation or reaction of

TFE. HFP is also considered as it is the second most abundant unsaturated compound produced.

An overview of the various catalytic reactions of TFE and HFP reported in literature is presented in the subsections below. A discussion on the mechanisms of catalysis is presented in its own section after the overview.

2.4.1 Heterogenous Catalytic Reactions of Tetrafluoroethylene

Only five investigations into catalytic reformation of TFE have been reported (Filatov *et al.*, 2011; Gelblum *et al.*, 2001; Dmowski *et al.*, 1976; Choi & Park, 1975; Miller, 1951).

Filatov (2011) pyrolyzed PTFE intimately mixed with CoF_3 and found that the yields of gaseous products were greatly reduced, but that the yield of perfluoroparaffins (6 to 26 carbons in length) was greatly improved.

Gelblum (2001) pyrolyzed various CHF gasses in a reactor line with the noble metals (gold, platinum and palladium as well as the alloy Inconel®) and found that there is a definite shift in equilibrium towards the production of HFP when using gold *versus* autogenous pyrolysis. Inconel® (a nickel alloy) acts as catalyst and decomposes the pyrolysis gases to carbon, CF_4 and C_2F_6.

Miller (1951) attempted to catalyze TFE to HFP and OFCB by providing a high surface area for TFE to react using nuclear grade graphite as the catalyst. No catalytic action was observed other than some carbon deposits on the walls of the nickel tube.

Dmowski's work (1976) required the use of a solvent, but showed that KF and CsF were capable of making dimeric and trimeric oligomers of TFE and HFP at 20 °C.

Choi and Park (1975) reported that there is a large increase in the yield of TFE (76 to 90%) at 700 °C when using copper instead of Inconel as reactor tube material. A recent Mandarin language paper, a full English translation of which could not be

obtained, also reported greatly increased yields of TFE when R-22 (CHClF) was pyrolyzed over a 60%/40% Ni-Cu catalyst, supporting the findings of Choi and Park.

An analogous examination of the catalytic reactions of ethylene does not reveal any interesting information. Walker (1943) found no catalytic reformation of ethylene to anything other than methane, hydrogen and carbon. Some of the catalysts tested for ethylene are: SiO_2, $Na_2B_4O_7.10H_2O$, NaOH, $Ca(OH)_2$, Fe_2O_3, ZnO, PbO, Na, Ni, Co, Fe and Cr_2O_3. Walker indicated two features: (i) that the decomposition reactions are mediated by a $:CH_2$ radical; (ii) but that this radical is too short-lived and too reactive to undergo any catalytic interaction.

In a somewhat unrelated patent, Karube (2010) showed that CCl_4 readily adds to TFE at 60 °C in the presence of $AlCl_3$, indicating that TFE is at least reactive to other halocarbons.

Moore and Massey (1992) detailed a reaction in which 1,1,2,2-tetrafluoroethane was isomerized to 1,1,1,2-tetrafluoroethane over chromia catalyst at 400 °C, indicating that fluorine shifts may be catalyzed. The same authors also indicated that AlF_3 and NaF may also be used as catalyst. Similar work for TFE has not been reported, though it stands to reason that such a shift would be beneficial to the formation of HFP.

The author's inability to find literature despite a thorough search makes it clear that little work has been done on the reactions of TFE over catalysts.

2.4.2 Heterogenous Catalytic Reactions of Tetrafluoroethylene with Species Containing Hetero-atoms

There is considerably more literature regarding addition reactions of TFE with various other species. Most of these reactions occur in the gas phase.

Ohashi *et al.* (2011) reported the addition of TFE to aryl zinc using palladium as the catalyst. However, this reaction did not proceed without the presence of LiI in the reaction mixture. They theorized that the reaction is catalyzed by a F^- which forms only in the presence of LiI.

Gas phase isomerization of tetrafluoroethane-β-sultone was effected by Barabanov *et al.* (2011) with NH_3, NF_3 and trimethylamine as the catalysts. Similar results were obtained by England and co-workers (1960).

Takagi *et al.* (2000) synthesized perfluoroamines from TFE and HFP using NF_3 as a nitrogen source and KF and NaF as catalysts. Tittle (1972) added AsF_3 to TFE by using SbF_5 as catalyst. Furthermore, Fokin synthesised perfluorothiols by addition of H_2S to TFE and HFP in the presence of alkaline catalysts (1967).

Many more examples of partially fluorinated additions to TFE and HFP or their partially fluorinated versions can be found in the patent literature and while it is superfluous to mention them all, the general trend in this sort of catalysis is the addition over some form of oxidation catalyst, generally a Lewis acid.

2.4.3 Homogenous Catalytic Reactions of Tetrafluoroethylene with Iodine

Syntheses involving TFE and I_2 were reported by Bedford and Baum (1980), but at pressures of 20 to 27 bar and temperatures in the region of 200 °C, also using a batch reactor. In these works, iodine was used both as a reagent and as a catalyst.

Kotov and co-workers (1988) synthesised $C_2F_4I_2$ and $C_4F_8I_2$ directly from PTFE waste by copyrolysis with solid I_2 at atmospheric pressure and 285 °C using a batch reactor. The yields were strongly dependent on the ratio of TFE to initial I_2.

Dindi and co-workers (2004) patented a process of telomerizing TFE with $C_2F_4I_2$ as chain-transfer agent at high pressure and temperature in a batch reactor to produce $I\text{-}(C_2F_4)_n\text{-}I$, where $n \leq 6$. Their method requires TFE pressures of 2.6 to 2.9 MPa and temperatures in the range of 220 °C. Their patent indicated that OFCB is formed during the reaction and must be periodically vented from the reactor as it inhibits product formation.

These iodine-TFE compounds are known as telechelics (or α,ω-difunctional derviatives) and find use as chain transfer agents for the telomerization of TFE, HFP or VDF, well-reported in a recent monograph (Ameduri & Boutevin, 2003) and a

review article (David *et al.*, 2006). No reports of HFP analogues to the iodine-TFE compounds could be found.

2.4.4 Homogenous Catalytic Reactions with Species Based on Sulfur, Phosphorous and Selenium

Lastly, Krespan and Langkammerer (1962) synthesised cyclic 5 and 6 member perfluorothianes using TFE and elemental sulphur in a batch reactor at temperatures ranging from 200 °C to 300 °C and under autogenous pressure. A maximum yield of 61% was obtained for 1,4 – octafluorodithiane and a maximum yield of 15% was obtained for octafluorothiolane. The isolated structures are presented in Figure 17.

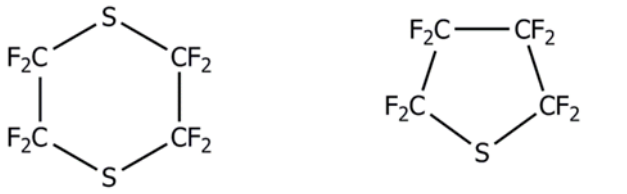

1,4 - Octafluorodithiane Octafluorothiolane

Figure 17: Krespan & Langkammerer's cyclic perfluorothianes.

Both these compounds are volatile liquids, are stable at 300 °C, do not readily react with oxygen, are resistant to attack by acids, bases and free radicals and are reported to have high dielectric strength.

Krespan and Wheland (1994) claimed in a patent that the above mentioned compounds are highly desirable as solvents for the polymerisation of perfluoromonomers. Interestingly, Krespan & Langkammerer (1962) also found that 2-trifluoromethyl-pentafluoro-1,3-dithiolane, the structure of which is presented in Figure 18, was formed as the only by-product during the reactions where sulphur was in excess, constituting some 3% or less of the product mixture.

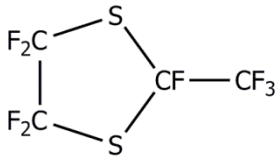

2-trifluoromethyl-pentafluoro-1,3-dithiolane

Figure 18: Molecular structure of 2-trifluoromethyl-pentafluoro-1,3-dithiolane obtained as by-product from the reaction of sulphur with TFE.

Krespan and Langkammerer also produced analogous compounds of selenium and phosphorus using iodine as catalyst in a batch process. The selenides are produced at temperatures in the range of 250 °C as Krespan found that the selenides decompose at higher temperatures. Similarly, the phosphorous containing rings are also decomposed at temperatures above 250 °C. The isolated products are presented in Figure 19.

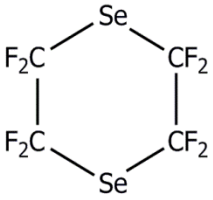

1,4 - Octafluorodiselenide

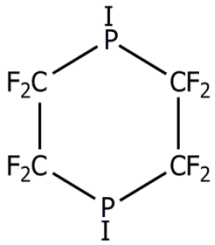

1,4 - Octafluorodiphosphane

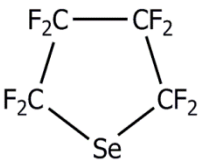

Octafluoroselenide

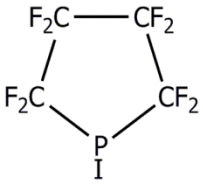

Octafluorophospholane

Figure 19: Cyclic perfluoroselenides and perfluorophosphanes synthesized by Krespan and Langkammerer.

Krespan noted that in all the phosphorus synthesis experiments, iodine satisfies the third valence of phosphorous. No third phosphorus-carbon bonds are formed and the six member phosphorus containing rings take on a puckered, hexane like conformer. Krespan also indicated that the six member phosphorus containing rings are

unreactive to water, but that the octafluorophospholanes are readily hydrolyzed to its phosphorous acid.

Brown (1957) reported the synthesis of the HFP analogue of 1,4-octafluorodithiane by reacting HFP with sulphur at 300 °C and 1 atmosphere pressure. The product had the empirical formula $C_6F_{12}S_2$. He identified this as a cyclic compound, but could not distinguish between the two chiral possibilities. The two possible structures are depicted in Figure 20.

Figure 20: Structural isomers of bis(trifluoromethyl)-perfluorodithiane.

To the best of the author's knowledge no other work reporting similar syntheses using HFP has been reported. Similarly, no work has been reported on the direct reaction of PTFE with sulfur, selenium or phosphorus.

2.4.5 Mechanisms of Catalysis

The reports discussed above indicate that reactions of TFE and HFP were catalyzed by species that either have readily accessible electrons, as in the case of lone pair on trimethylamine and NH_3, or are so polar that the metal atoms are essentially naked, as in the case of KF and NaF (solid bases).

It is known that the lone pair electrons of amines are capable of capturing a carbon radical long enough to convert it to a non-radical species, as is the case with Hindered Amine Light Stabilizers (HALS) (1984). It stands to reason that species with available lone pairs (Lewis bases) stabilize the TFE biradicaloid, allowing the

end opposite to the catalyst to exist as a full radical and subsequently react. Barabanov's (2011) observation of polymer formation is evidence for this terminal radical. Other perfluorinated species capable of forming biradicaloids would undergo similar radical stabilization.

The patent by Karube *et al.* (2010) indicates that a variety of alkaline and alkaline earth metal fluorides and NiF_2 may be used as "promoters" in fluorocarbon rearrangements when doped onto chromia or alumina, but no explanation of their action is given in the literature.

A review by Pearson (1968) on the hard & soft theory of acids and bases indicated that triethylamine, NH_3 and F^- are hard bases while Na^+, K^+ are hard acids but that hardness decreases when going from Na^+ to K^+ to Cs^+. The implication is that the softer the metal is as a Lewis acid, the stronger the F^- will be as a Lewis base. It is obvious that, in light of the better catalysis achieved with CeF than with KF, the reaction proceeds *via* F^- catalyst and not *via* the metal. This is reinforced by the observations made by Ohashi *et al.* (2011).

In the case of chromia, there is considerable electron richness on the chromium atoms, but the much more electron negative oxygen draws these electrons to itself and becomes almost completely ionic, in a sense, approaches O^{2-}. The oxygen anions are readily accessible at the surface of the crystal. Again, we conclude that the reactions are intermediated not by the hard acid Cr^{3+}, but by the strong basic O^{2-}.

The basic catalysis hypothesis is further reinforced by the work of Filatov *et al.* (2011). CoF_3 is a fluorinating agent and it is expected that it would give off fluorine to a fluorocarbon radical to produce small perfluorinated species. This is not the case as long chain fluorocarbons are formed during pyrolysis of PTFE, indicating CoF_3 catalyzes oligomerization.

All of the above is in agreement with what is known from general fluorochemistry regarding the ability of TFE, and fluorocarbons like it, to undergo nucleophilic attack (Banks & Tatlow, 1986).

No explanation could be found for the catalytic action of gold in the patent, but, gold is classified as a very soft Lewis acid and it is assumed that the borderline cases such as gold interact weakly with carbon radicals.

As with gold, copper and nickel are classified as being soft to borderline Lewis acids and are assumed to interact weakly with fluorocarbon radicals. There is a slight difference in the electronegativity between copper and nickel and it stands to reason that an alloy of the two contain some basic metal sites due to this difference.

The addition of iodine and sulphur to TFE also occurs *via* a radical mechanism, but in their cases the reagents act as the catalysts. As indicated by Bedford and Baum (1980), addition of iodine to TFE occurs in three steps, detailed in Figure 21.

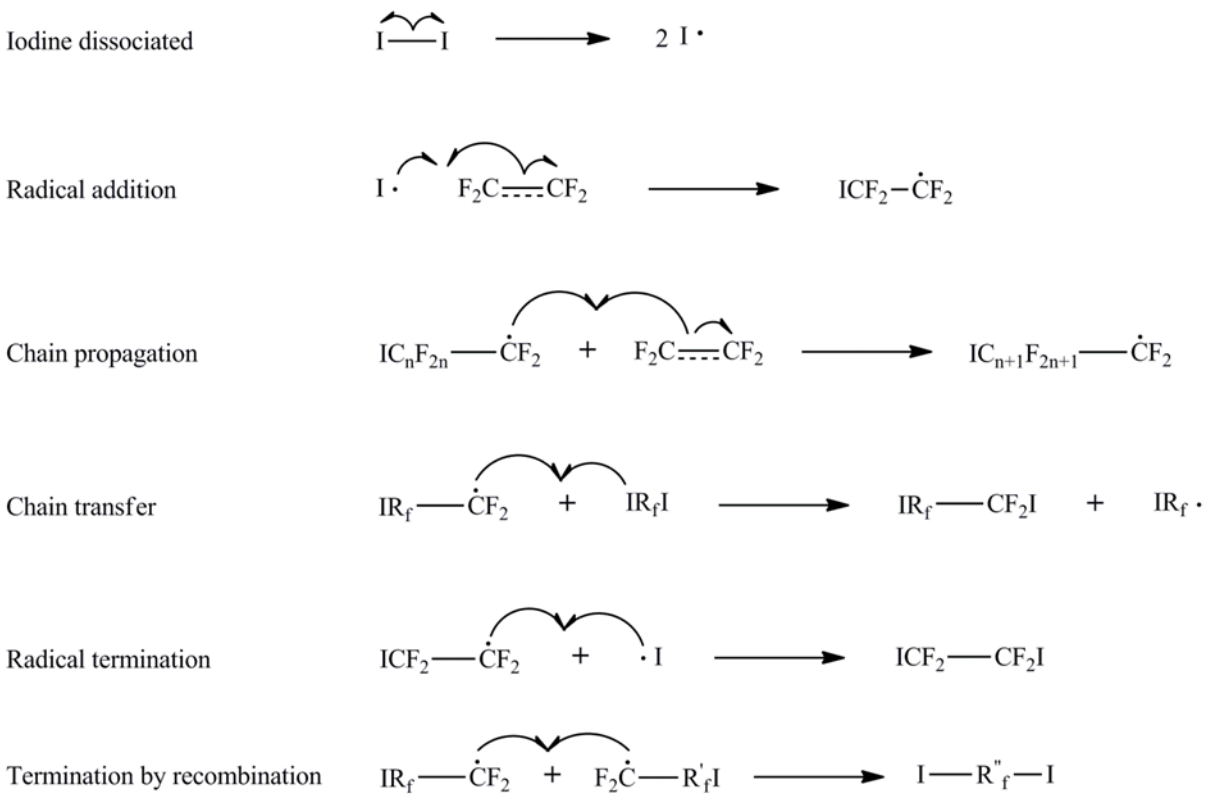

Figure 21: Postulated mechanism for iodine addition to TFE.

Higher order α ω-diiodoperfluoroalkanes are formed by radical addition of TFE to I-CF_2-CF_2˙.

It is interesting to note that Kotov reported that 1,4-diiodoperfluorobutane is formed in larger amounts than the 1,2-diiodoperfluoroethane (44 % *versus* 38 %) but that 1,6-diiodoperfluorohexane and 1,8-diiodoperfluorooctane is formed in significantly smaller amounts (8% and 2%, respectively). This along with Dindi *et al.*'s (2004) observation that OFCB forms in high quantities during the production of diiodoperfluoroalkanes is strongly supportive of the mechanism proposed in Section 2.3.2 for OFCB formation.

It is also interesting to note that the yield of 1,6-diiodoperfluorohexane increased from 8 % to 24 % when the TFE to I_2 ratio was increased from 1 to 2, but that the yield of 1,8-diiodoperfluorooctane only increased to 8% from 2 %. These results would indicate that the radically terminated carbon is not readily available to other TFE molecules and that some telomerisation reactions occurred as mentioned above. This implies that the molecular rotation involved in the proposed OFCB formation mechanism happens quite rapidly.

Thermodynamic calculations for equilibrium composition of the gas phase during the thermal dissociation of iodine, detailed in Figure 22, indicate that there are very few iodine radicals present at 200 °C when the gas is under pressure. This observation explains why Kotov *et al.* (1988) reported yields in excess of 40 % while other literature report low yields.

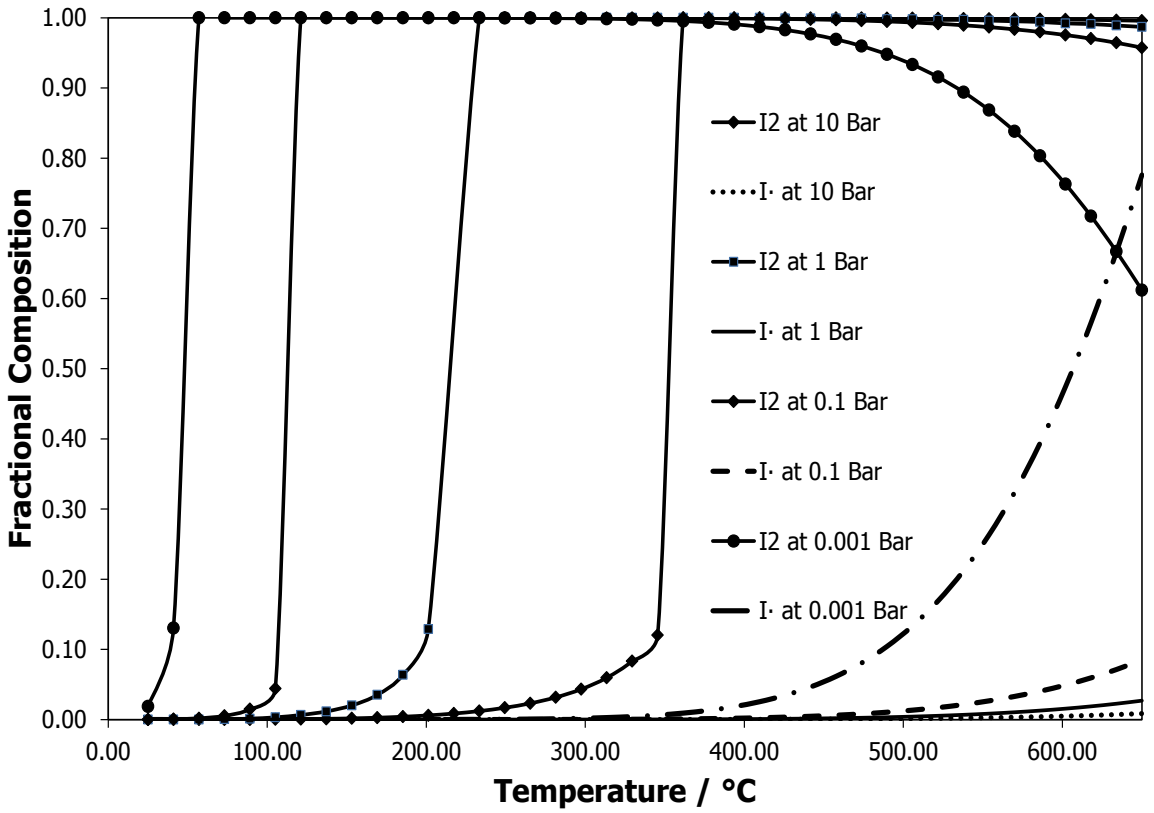

Figure 22: Temperature and pressure dependent equilibrium composition of iodine, calculated using HSC Chemistry (Roine, 2007).

We may conclude that the iodine addition to TFE is catalyzed by the iodo-radicals generated by the thermal homolysis of iodine gas. This catalysis is analogous to the radical initiated catalysis of polymerization.

Krespan (1962) proposed possible radical intermediate mechanisms for the addition of sulphur to TFE, detailed in Figure 23. The central argument here is that sulphur forms a polyatomic radical which attaches itself to TFE while splitting off all the sulphur atoms save the atom attached to the CF_2. This new radical then undergoes further reaction.

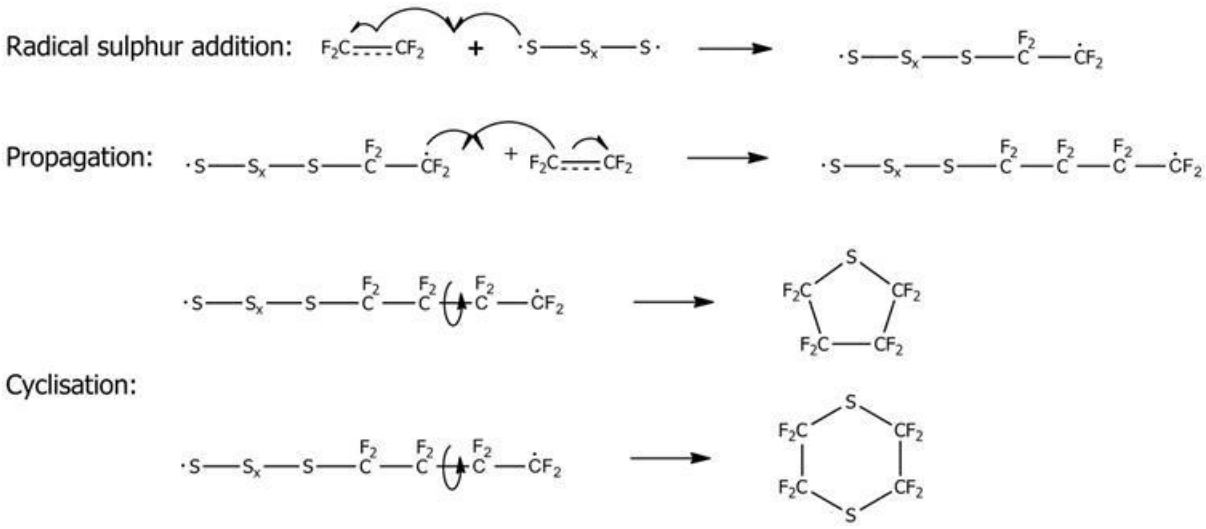

Figure 23: Krespan's mechanism for the addition of sulphur to TFE.

It is known that gaseous sulphur is composed of many sulphur allotropes, but that the main component is disulfur and to a lesser extent, trisulphur (Meyer, 1976). At 1000 K and 1 mmHg pressure, S_2 makes up 99% of the gas phase.

This diatomic sulphur is known to exist as a triplet when in the ground state and readily reacts. Accordingly, the reaction as presented in Figure 23 must be modified to admit that S_2 instead of a polyatomic sulphur chain is added to a TFE molecule.

As indicated by Meyer (1976), the S-S bond is much weaker than that of diatomic oxygen or the C-C bond and while no references could be found on the topic it stands to reason that when S_2 is attached to TFE, the S-S bond will break to afford $\cdot CF_2\text{-}CF_2\text{-}S\cdot$ and [:S] which undergoes further reaction to produce the thianes.

As was the case with iodine, we may conclude that the reactions of TFE and HFP with sulphur is catalysed by sulphur radicals generated by thermal homolysis of S_8.

In summary we may say that the reactions of TFE and other unsaturated perfluorocarbons always occur via radical intermediates and are catalysed by strong bases or other species with unpaired or lone pair electrons.

3 Research Facilities

The Fluoro-Materials Group (FMG), formed under the directives of the South African Fluoro-Expansion Initiative (FEI), is in the process of fully establishing itself within Department of Chemical Engineering at the University of Pretoria (UP).

An important aspect of the group's research involves the synthesis and subsequent characterization of novel fluoropolymers and related fluoro-materials. This endeavour requires that the research group have access to special analytical equipment capable of analysing fluorine containing solid, liquid and gaseous materials, with emphasis on the ability to chemically characterise polymeric materials.

Previous to 2013, most of the experimental and analytical work carried out by the group took place in facilities provided by the Department of Applied Chemistry of the South African Nuclear Energy Corporation (Necsa). In 2012 the National Research Foundation (NRF) decided that the Fluoro-Materials Group should migrate all of its activities to the main campus of the University of Pretoria from Necsa's Pelindaba site.

As part of the work for the catalytic PTFE waste pyrolysis project, an analytical laboratory that meets the stated requirements was set up on the third floor of the Engineering 2 building by the author. This section provides details on said laboratory and includes a discussion on the choice of instrumentation as well as the final set of instruments purchased for this laboratory and, finally, a description of the instrumentation used for this specific project.

Details of the greater commissioning project and a full description of all instrumentation purchased for this laboratory, although available as an internal report, are beyond the scope of this thesis.

3.1 Instrumentation Selection

The selection of equipment for the analysis laboratory was informed not only by the available techniques, their applications and limitations, but also by the generality of the techniques. Reproducibility is crucial, as is standardisation, and the methods must be widely used so that there is good probability of finding comparative data in the open literature.

This subsection provides an overview of the considerations which led to equipment selection as well as a description of the selected equipment.

3.1.1 General Methods of Material Analysis

The analytical laboratory has, as stated previously, the main operational aim of characterisation of fluoropolymers. Polymer characterisation may be classed into two main branches, *viz.*: physiomechanical- and chemical characterisation (Cheremisinoff, 1996).

Physiomechanical properties include tensile strength, flexural modulus, Young's modulus, rheological properties and the like. These properties are determined via tensile testers, dynamic mechanical analysers and rheometers, *etc*.

While these properties are always a function of the chemical nature of the polymer, knowledge of them are not critical to knowledge of the chemical identity of the polymer and it is possible to produce polymers with widely different molecular structures which are similar in mechanical behaviour. Observe, for example, the similarities in chemical inertness and frictional behaviour between high density polyethylene and polytetrafluoroethylene.

The primary questions regarding the nature of a polymer lie with its structure, its molecular identity. That is:

- What is its repeating unit?
- What is its average molecular mass?
- How is the chain terminated? and,
- What physical conformation do the polymer chains take on?

General questions of similar nature may be asked of any material. For example, the identification of an organic compound starts with the determination of which functional groups are present, followed by determination of the ratio of chemical elements to each other within the material and ends with the determination of arrangement of the functional groups within the compound.

The most common techniques used for materials characterisation, with emphasis on polymeric materials, are discussed below.

3.1.1.1 Spectroscopic Methods

By far the most common way of identifying the functional groups within a material is through spectroscopic methods, in particular the use of Infrared Spectroscopy (IR) (Stuart, 2002). This method holds true for all materials, but is particularly applicable to material of an organic nature.

Materials identification, therefore, starts with infrared analysis. Contemporary IR instrumentation of the Fourier transform type are readily available from various manufacturers and the inclusion of a FT-IR spectrometer is a non-issue in any materials analysis laboratory.

Other spectroscopic methods include UV/Vis analysis, which operates on principals similar to IR, and Nuclear Magnetic Resonance (NMR) spectroscopy (Stuart, 2002).

UV/Vis is usually included alongside IR in a general analysis laboratory and is a recommended tool for polymer analysis. UV/Vis analysis is particularly applicable for the identification of carbonyl groups and compounds with chromaphore groups (Pasto & Johnson, 1969). It is especially useful for the investigation of weathering induced polymer degradation.

NMR is a more difficult, involved technique and the equipment is highly specialised and considerably more expensive. NMR analysis requires its own laboratory, with dedicated infrastructure and because of budget constraints NMR is not included among the general analysis techniques (Keeler, 2002).

3.1.1.2 Pyrolysis Methods

Pyrolysis gas chromatography mass spectrometry or Pyro-GC/MS is the fastest growing, most direct and most practical method for the chemical identification of polymeric materials (Tsugi *et al*, 2011).

This method is the combination of two analytical techniques, *viz.*: Gas-Chromatography (GC) and Mass Spectrometry (MS). The method involves the heating of a sample, polymeric or otherwise, to breakdown temperatures and purging the evolved gasses through a capillary chromatography column (GC part) and eluting the separated, pure components into a mass spectrometer (MS part) for precise identification.

The reproducibility of the results depends on the method of sample heating and apparatus for this technique are usually sold as a single unit with the pyroliser, usually a sample holding chamber with a platinum heating wire, being built into the injector of the GC.

As discussed by Wampler (Wampler, 2007), the Pyro-GC/MS method can be used for more than just synthetic polymers. Biologic materials, such as micro-organisms may also be analysed.

A second pyrolysis method, Pyrolysis-Fourier Transform Infrared Spectroscopy or Pyro-FTIR, is also gaining ground as a routine analysis technique (Wampler, 2007). While it is less informative than Pyro-GC/MS, it has the advantage of being a much faster technique. Once a sample's general behaviour has been determined by Pyro-GC/MS, Pyro-FTIR can be used for quick screening of large sample sets.

3.1.1.3 Thermal Methods

Thermal methods allow for the study of material properties as functions of their temperature or the rate of thermal energy addition. There are two techniques in thermal analysis, *viz.*: Thermogravimetric Analysis (TGA) and Differential Scanning Calorimetery (DSC) (Cheremisinoff, 1996).

TGA entails the observation of sample mass as a function of sample temperature. It is mainly used for degradation studies and determination of volatile content in a polymer sample.

The apparatus consists of a sensitive balance surrounded by a high powered furnace, with temperature monitored by sensitive, highly accurate thermocouples. Temperature is controlled by adjustment of the current fed to the furnace. Various balance and furnace configurations are available.

DSC entails the heating of a sample and monitoring the heat flow to the sample with respect to a standard reference material. The heat flow-temperature-time data obtained by DSC gives insight into the melting, crystallisation and glass transition of a material and is useful for determination of polymer crystallinity. Again, various balance and furnace configurations are available.

Both of these techniques are useful for polymer characterisation and find routine application, although TGA is less useful for chemical characterisation than DSC.

3.1.2 Equipment Acquisition

Actual equipment selection was conducted by screening the various configurations and combinations of the methods described above according to criteria specific to the FMG's needs. These criteria are discussed below, as are the resultant instrumentation specifications.

3.1.2.1 Selection Criteria

Since the FMG's work spans inorganic, organic and polymer materials science, the apparatus must all be capable of multi-application use. In example, in addition to the analysis of the pyrolysis gasses of polymers, the GC/MS system must be capable of handling liquid and gaseous organic samples by themselves. Similarly, the FTIR & UV/Vis instruments must be able to deal with the whole gamut of materials on which spectroscopic analysis will routinely be performed, not just on polymer films.

The instrumentation must also be robust enough to be used with materials which may be corrosive or in heated state. For example, it is possible to eliminate HF from polymeric materials containing both hydrogen and fluorine atoms adjacent to each other (O'Shea *et al*, 1990). The thermal instruments must be capable of dealing with small concentrations of hot, corrosive gasses such as HF during routine operation without adversely affecting the long term performance of the instrument. Similarly, the mass spectrometer must be capable of dealing with fluorine radicals evolved by the ionisation of fluorine containing gasses during analysis of these gasses by GC/MS method.

Simultaneous analysis of samples by many techniques is an optional, but highly desired requirement. In example, the simultaneous analysis of the re-crystallisation of a semi-crystalline polymer, such as polypropylene, by DSC and Raman spectrometry gives data not only on the heat of crystallisation, but also reveals the kinetics of the crystallisation process.

Lastly, the instrumentation must be user friendly and must allow for fast mastery of its operation. It does not help research activities if the instruments are so exceptionally sensitive and prone to breaking that only a trained analytical chemist can drive the instrument. Post-graduate students should be able to analyse their own samples with the minimum of training and supervision.

3.1.2.2 Manufacturer Instrumentation Offering

There are numerous instrumentation companies in operation throughout the world. The most well-known entities which market laboratory instrumentation and operate in South Africa (or have an agent capable of providing aftermarket service) are listed in Table 3, alongside their main field of instrumentation.

Table 3: Instrumentation manufactures.

Manufacturer	Main Application Field
Shimadzu	Chromatography, Thermal Analysis
Perkin Elmer	Chromatography, Spectroscopy, Biosciences, Thermal Analysis
Thermo Scientific	Chromatography, Spectroscopy, Materials Characterisation
Agilent	Chromatography, Spectroscopy, Materials Characterisation

À breakdown of the instrumentation offering for each manufacturer is presented in the tables below. Detailed descriptions of all the instruments are not presented; the reader is referred to the manufacturer's literature for a full review of each.

It is understood that the manufacturers have a number of instruments in each category, but that only the applicable systems are listed. In example, only GC systems capable of GC/MS are considered.

Table 4: Shimadzu instrumentation offering.

Instrumentation Type	Instrument Models
Infrared Spectrometers	IRAFfinity-1, IRPrestige-21 (NIR,MIR & FIR), AIM-8800 IR Microscope
UV/Vis/NIR Spectrometers	UV-3600, UV-2700, UV-2600, UV-1800, UV-1240 (Mini)
GC/MS Instruments	GCMS-TQ8030 (Triple Quadrupole), GCMS-QP2010 Ultra, GCMS-QP2010 SE
TG Analysers	TGA-50, TGA-51
DS Calorimeters	DSC-60 Plus, DSC-60 Plus A

Table 5: Perkin Elmer instrumentation offering.

Instrumentation Type	Instrument Models
Infrared Spectrometers	Spectrum Two, Frontier Optica, Frontier FT-NIR/MIR, Frontier FT-FIR
UV/Vis/NIR Spectrometers	Lambda 650, Lambda 750, Lambda 850, Lambda 950, Lambda 1050
GC/MS Instruments	Clarus SQ 8S, Clarus SQ 8T, Clarus SQ 8C
TG Analysers	Pyris TGA 1, Pyris TGA 4000
DS Calorimeters	DSC 4000, DSC 6000, DSC 8000, DSC 8500

Table 6: Thermo Scientific instrumentation offering.

Instrumentation Type	Instrument Models
Infrared Spectrometers	Nicolet iS5, Nicolet iS10, Nicole iS50
UV/Vis Spectrometers	Evolution 201, Evolution 220, Evolution 300, Evolution 600
GC/MS Instruments	Trace 600, Trace 700, Trace 800
TG Analysers	None
DS Calorimeters	None

Table 7: Agilent instrumentation offering.

Instrumentation Type	Instrument Models
Infrared Spectrometers	Cary 610, Cary 620, Cary 630, Cary 660, Cary 670, Cary 680
UV/Vis/NIR Spectrometers	Cary 5000, Cary 6000i
GC/MS Instruments	Agilent 5977A
TG Analysers	None
DS Calorimeters	None

Of all the manufacturers, only Perkin Elmer offers ready-to-use combination or "hyphenated" systems. The individual instrumentation offered by Perkin Elmer may

be combined to give Pyro-GC/MS, Pyro-FTIR, TGA-FTIR-GC/MS, TGA-FTIR, TGA-GC/MS or DSC-FTRaman/FTIR.

3.1.2.3 Final Equipment Specification

As noted previously, multi-application use and simultaneous analysis are core requirements for the laboratory. For this reason, Perkin Elmer was chosen as instrument supplier.

While Perkin Elmer does supply a pyrolysis unit for their GC/MS units, it was judged that more information could be extracted from experiments if the heating rate, final temperature and nature of the sample atmosphere could be adjusted. Also, the ability to know the rate of mass loss at specific temperatures, as well as knowledge of the off gasses for specific mass loss events will allow for a much deeper investigation and understanding of material behaviour, as opposed to the simple analysis data obtained by flash pyrolysis.

For these reasons, it was decided that the GC/MS would not be ordered with a pyrolysis unit, but would instead rely on the TGA to act as pyrolysis instrument.

Again, as noted previously, corrosive gasses may be given off during experiments and it would be detrimental to the lifespan of the GC columns if all gaseous products were analysed using GC/MS as part of the standard practice. It is also understood that any analysis that requires use of the GC/MS system will take considerably longer than a simple TGA analysis.

For these reasons it was decided that the standard TGA-FTIR-GC/MS would be split into two independent systems, *viz.*: TGA-GC/MS or TGA-FTIR. This arrangement allows for quick routine work with the TGA or TGA-FTIR system, keeping the GC/MS or FTIR instrument free for independent work, as the case may be, while still allowing for very accurate work with the TGA-GC/MS system.

Due to the nature of research, it was judged that the top-of-the-line, highly modifiable instruments in each category would be purchased to allow for future

expansion of the laboratory's capabilities with additional "add-in" modules for the instruments.

Due to budget constraints, as well as the fact that the Department of Chemical Engineering already owns a number of these instruments, it was decided to forgo the purchase of a DSC instrument at this time. Instead, a smaller FTIR was purchased with the remaining funds to allow for the processing of greater volumes of routine IR analyses tasks.

Table 8 gives the specifics on the models purchased in each category.

Table 8: Purchased instruments specifications.

Instrumentation Type	Purchased Model
FTIR	Perkin Elmer Spectrum 100 and Spectrum Two
UV/Vis/NIR	Perkin Elmer Lambda 750 S
TGA	Perkin Elmer TGA 4000
GC	Perkin Elmer Clarus 680
MS	Perkin Elmer Clarus SQ 8C

The chemical characterisation laboratory is then capable of: FTIR, UV/Vis/NIR, TGA, TGA-FTIR, TGA-GC/MS and GC/MS.

At the time of writing, the group was also in the process of purchasing a number of other instruments, *viz.*: a breakdown potential tester, a Shore A hardness tester and a planetary ball mill. These instruments, along with the dynamic mechanical analyser unit already in the department's possession were not included here as they do not relate directly to the chemical characterisation of fluorinated materials.

3.2 Instrumentation Overview

A technical overview, as extracted from the manufacturer literature and personal experience, is presented for the TGA-FTIR hyphenated system.

3.2.1 Spectrum 100

The Perkin Elmer Spectrum 100, of which an isometric view is given in Figure 24, is a versatile infrared analyser capable of handling solids, liquids and gaseous material.

Figure 24: Isometric view of the Spectrum 100. Image courtesy of Perkin Elmer.

The Spectrum 100 may be fitted with a number of optical systems, depending on when the instrument was manufactured. The optical specifications for the FMG unit are presented in Table 9.

Table 9: Optical systems specification for the Spectrum 100.

Optical Subsystem	Component	Spectral Range
IR source	Gas laser unit	8000 cm^{-1} to 30 cm^{-1}
Beam splitter	KBr splitter	15700 cm^{-1} to 400 cm^{-1}
Transmission windows	KBr window discs	15000 cm^{-1} to 370 cm^{-1}
Detector	Deuterate triglycine sulphate	15700 cm^{-1} to 250 cm^{-1}

The optimum spectral range of the instrument goes from **7800 cm^{-1} to 450 cm^{-1}**. The instrument may scan in resolution intervals of **0.5, 1, 2, 4, 8, 16, 32 and 64 cm^{-1}** and operate at scan speeds of **0.1, 0.2, 0.5, 1, 2 and 4 cm^{-1}/s**. Scan resolutions of 4 cm^{-1} are preferred as this is the native instrument resolution.

The KBr optics in the FMG's instrument are slightly degraded and produce significant noise when attempting to analyse at wavelengths below 550 cm^{-1}. It is recommended that the Spectrum 100 be used with a scan range of 7800 cm^{-1} to 550 cm^{-1}.

The Spectrum 100 has an operation temperature range of 10 to 50 °C and can function in environments of up to 90% relative humidity at 25 °C.

The instrument may be operated in transmission, split beam or ratio mode and the software allows the option of compensation for atmospheric H_2O and CO_2. The instrument also comes with a filter wheel that allows for the use of custom wavelength filters, blank or no filter is the default setting. At present, only a polystyrene filter disc is installed and is used for the instrument self-validation.

It is possible to replace the beam splitter and transmission windows with other ceramics such as CsI or CaF_2 to achieve a greater infrared range, going as far down as 260 cm^{-1}. This allows for limited work in the far infrared, where the IR fingerprint spectra of most fluoroceramics and organoclays are situated. However, the other

optical systems are all sensitive to water and will degrade rather rapidly. For work in very humid environments, ZnSe is recommended as optical material, though Perkin Elmer does not manufacture transmission windows or beamsplitters in this material.

The Deuterated Triglycine Sulphate (DTGS) detector is of the photoelectric type. These types of detectors are the most common types used for IR detection, but there are many types of detectors commercially available. Rogalski (Rogalski, 2010) provided a comprehensive review of the physical characteristics of the various detectors and detection methods and should be consulted for more advanced information. Perkin Elmer also provides $LiTaO_3$, HgCdTe and photoacoustic detectors and these detectors are easily interchanged with one another.

An application note by Thermo Scientific (Thermo Scientific, 2007) gives a rough guide to the operational characteristics of the various commercial detectors and indicates that while HgCdTe type detectors are more sensitive than DTGS, they are less practical as they require liquid nitrogen cooling. Similarly, $LiTaO_3$ works better at higher temperatures, but is less sensitive and responsive. Unless there is a real, practical need for another detector, the DTGS detector is considered sufficient for any detection application.

Figure 25 illustrates the internal arrangement of the various components within the instrument housing.

The laser unit powers a source module, which acts as a wavelength restrictor, that shines a very coherent (exact coherence value is unknown) beam of infrared radiation onto the beamsplitter.

From here the beam is redirected *via* a set of highly polished SiO_2 coated metal mirrors through the filterwheel and out of the lefthand window into the sample chamber. The beam passes through the fitted module, into the righthand window, where it is reflected onto the detector.

This configuration implies that it is not possible to rig the instrument to work as a diffractive type spectrometer.

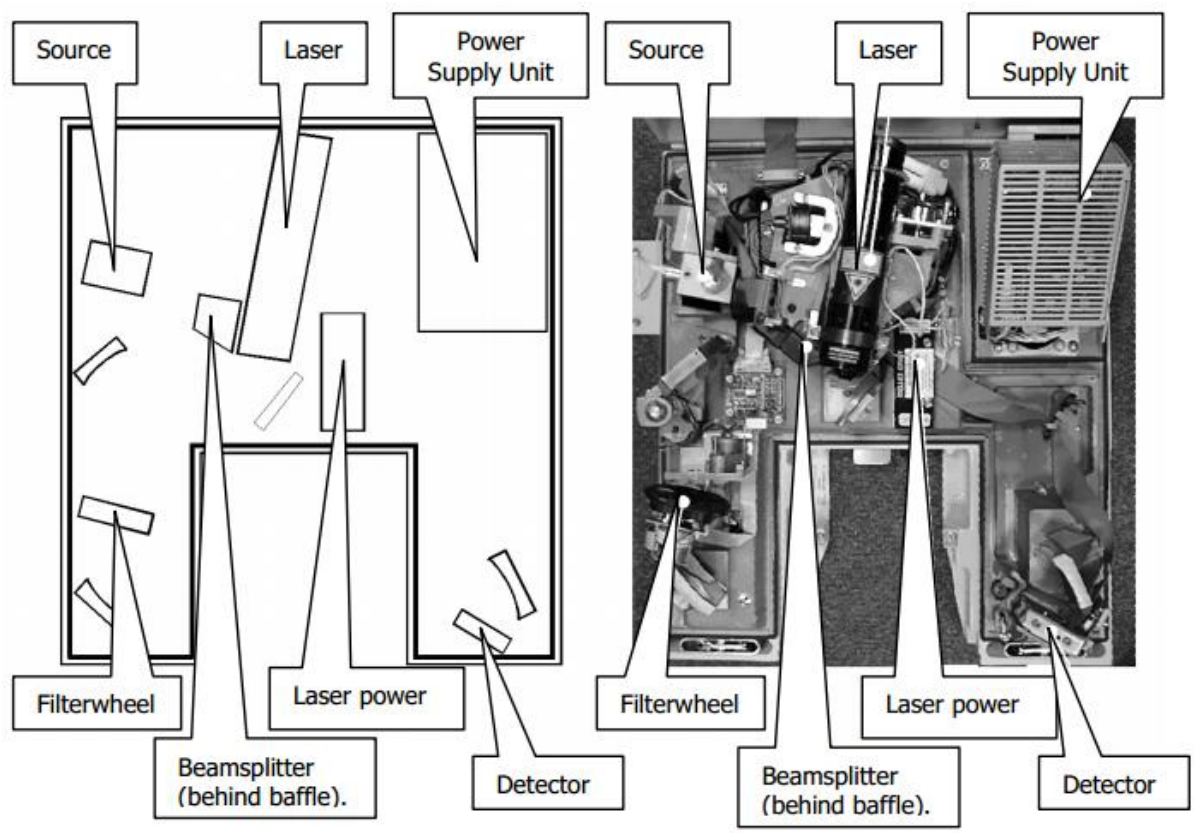

Figure 25: Internal arrangement of the Spectrum 100.

Sample chamber

The sample chamber of the spectrometer, pictured in Figure 26, allows for a number of sample holder modules. The FMG has in its possession the film holder (with oil cell and ambient gas cell attachments), universal ATR, horizontal ATR and the heated gas cell modules.

It must be noted that these modules are all "hot-swappable" and they can be rapidly and easily changed out without having to power down the spectrometer.

The sample chamber is purgable, as is the instrument internals. Similarly, all modules installed in the sample chamber can be purged, with the instrument accepting any inert gas as purgant, although dry nitrogen is preferred.

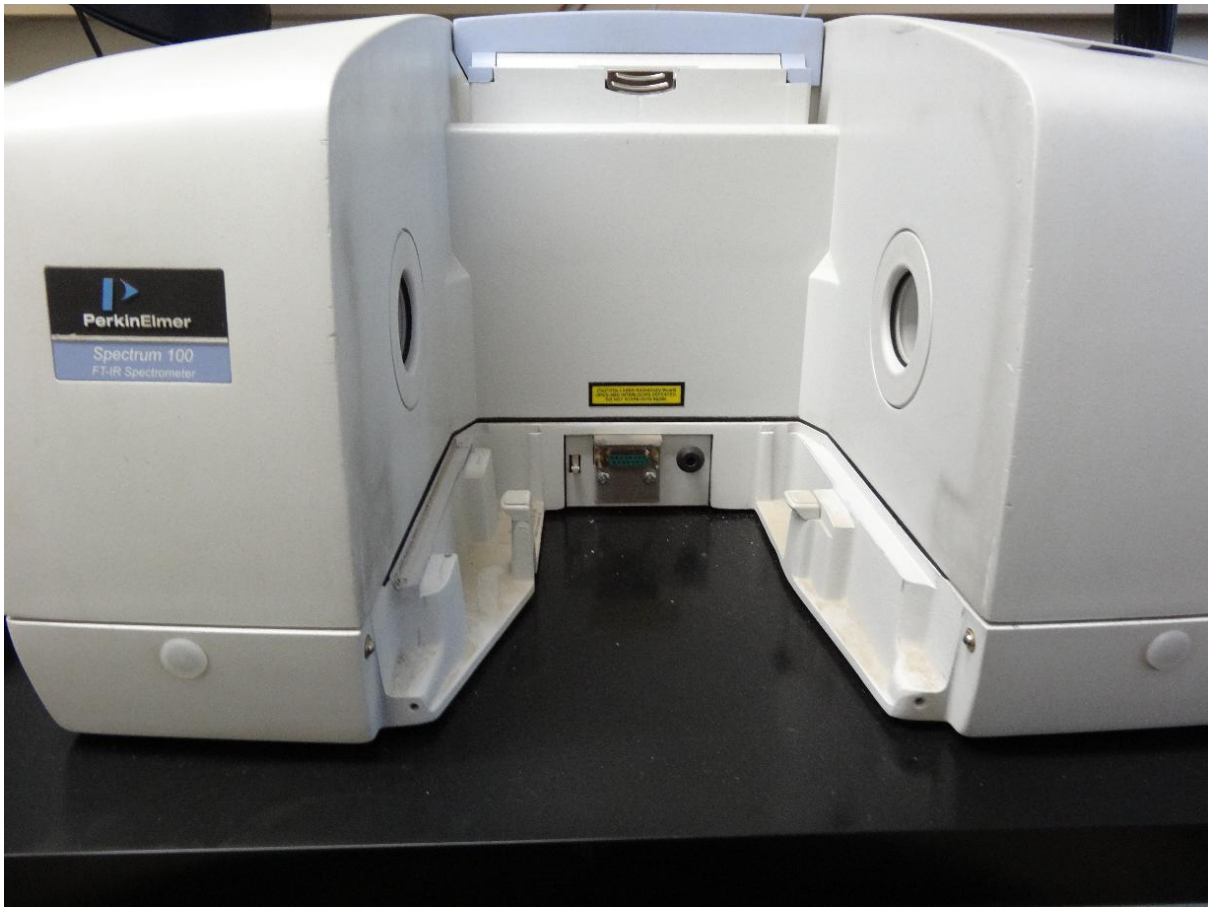

Figure 26: Spectrum 100 sample chamber.

Heated gas cell

The heated gas cell used for TGA-FTIR is shown in Figure 27. The cell consists of a metal tube wrapped in heating cloth with KBr windows fixed to the cylinder ends. The cylinder is connected at the top to a heated transfer line and at the bottom to a 1/4" PFA outlet tube.

The transfer line consists of a steel tube fixed within a metal mesh support tube wrapped in a heating cloth and insulated from the nylon cover by a layer of mineral wool. The transfer line and the gas cell may be heated independently of each other from 50 °C up to a maximum temperature of 325 °C in 1 °C steps.

As with the other modular attachments, the volume surrounding the cell as well as the space in between the cell windows may be purges with N_2. The outlet of the cell

is connected via PFA tubing to a mass flow controller and diaphragm pump, housed in a control box along with the temperature controllers for the cell and transfer line.

The pump can provide a vacuum to the TGA of about 400 mBar and a maximum flow of 200 ml/min can be maintained.

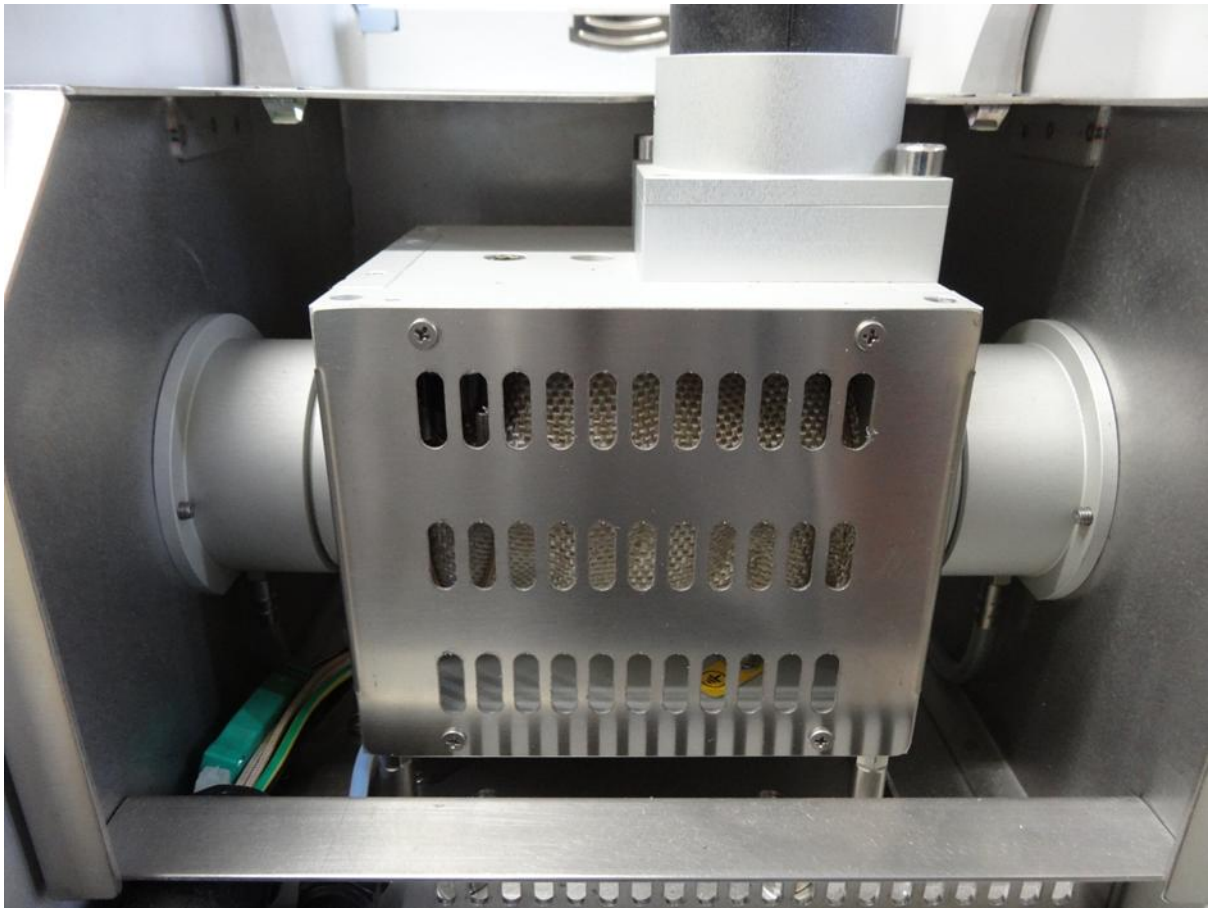

Figure 27: Heated gas cell.

The KBr optics of the gas cell gives the cell a working wavelength range of **4000 cm^{-1} to 450 cm^{-1}**. This limit holds true even when using wider range optics in the Spectrum 100 and while it is possible to change the cell windows to accommodate other materials, it is not recommended as the cell will be exposed to hot H_2O and the windows corroded during the course of normal operations. Also, the optical path length is specified as 10 cm.

3.2.2 TGA 4000

The Perkin Elmer TGA 4000, of which an isometric view is given in Figure 28, a robust, dynamic thermal analysis tool suited for the study of inorganic and polymeric materials.

Figure 28: Isometric view of the TGA 4000.

The TGA 4000 was designed to be a compact, easy to use bottom balance type thermal analyser that allows for quick sample change while maintaining a wide thermal operation range, a wide range of heating rate options and superior sensitivity.

The instrument is essentially a highly sensitive balance surmounted by an accurate high-powered furnace enclosed in a cooling jacket, all of which is enclosed in a plastic case. The furnace and the balance are thermally isolated from each other and the sample is brought into contact with the balance by means of a thermally non-conductive stem that passes through the furnace and into the balance unit.

The internal arrangement of the instrument is sketched in Figure 29 and a top down view of the furnace is presented in Figure 30.

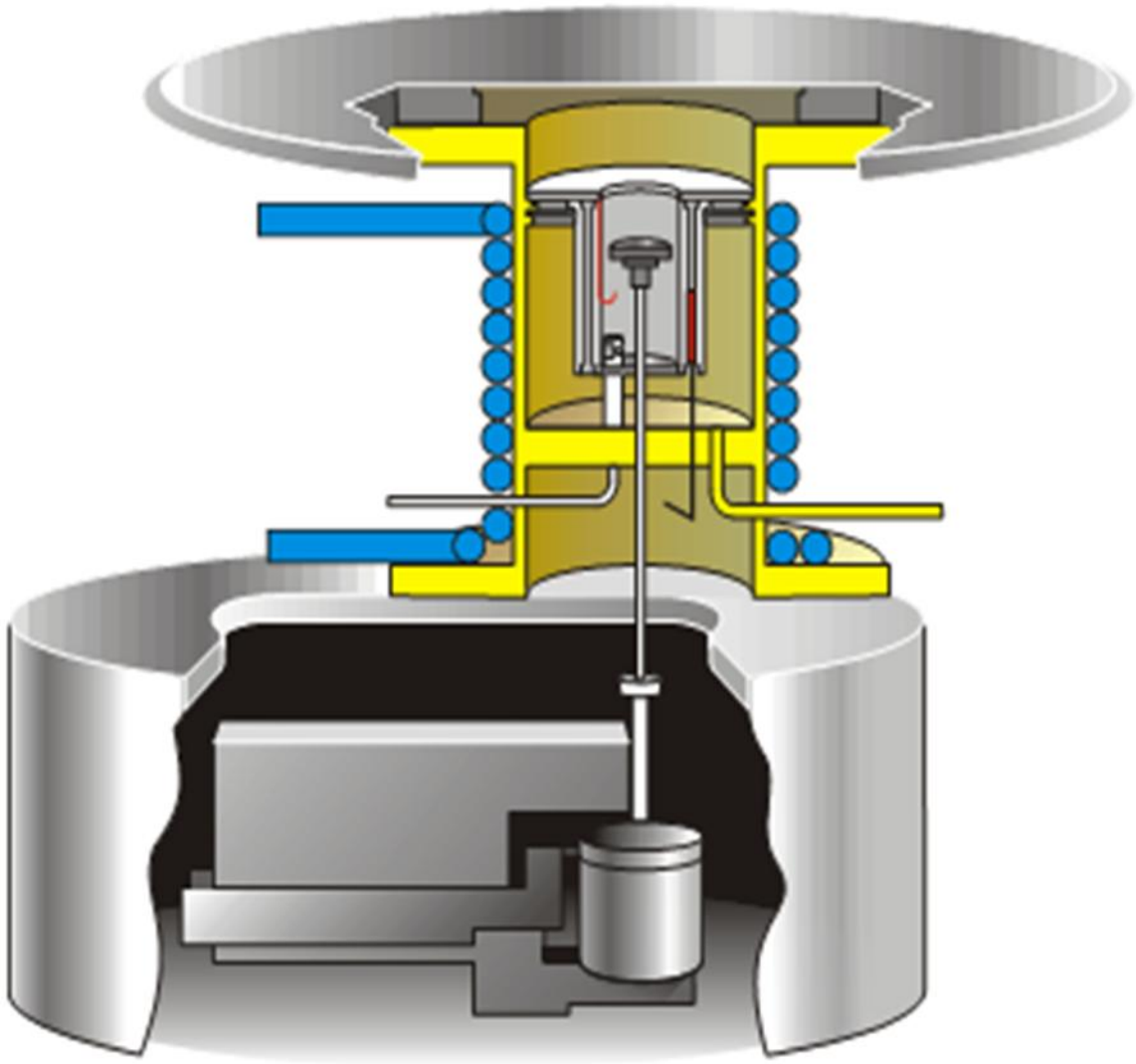

Figure 29: Internal arrangement of the TGA 4000.

Figure 30: Top down view of the furnace with sample pan in place.

Table 10 summarises the hardware specifications for the TGA 4000. The author has found that the manufacturer specifications are slightly off, owing to the difference in ambient conditions between Pretoria and the place where the instrument was manufactured.

Table 10: Specifications of the TGA 4000.

Subsystem	Specification Area	Specification
Balance	Capacity	Maximum of 1500 mg
	Sensitivity	Weight change of 1 µg
	Accuracy & precision	± 0.02 % and ± 0.01%
Furnace	Temperature Range	Ambient to 1000 °C
	Scan Rate	0.1 °C/min to 200 °C/min
	Cooling Time	1000 °C to 100 °C in 10 min

For example, the minimum heating rate is reported as 0.1 °C/min, but the author has found that the heating rate becomes subject to serious variability if a heating rate below 2 °C/min is used.

Similarly, the maximum temperature is specified to be 1000 °C, however, there are constraints in the software that prohibit the user from specifying this as end temperature. The real maximum specifiable temperature is 999 °C.

The author has, however, noticed that there is a 20 °C temperature overshoot during heating at maximum rate and it is therefore recommended that the maximum temperature never be set higher than 950 °C.

It has also been noticed that increase in sample mass results in a decrease in balance sensitivity.

The sample temperature is monitored by way of a dual thermocouple system whereby one thermocouple monitors the temperature of the sample stem a small distance away from the actual sample and the second thermocouple monitors the temperature at the furnace wall. From these readings a sample temperature is obtained.

Furthermore, both the sample balance and the furnace area are purgable with gases. The balance is always purged with nitrogen, while the furnace purgant may be specified. Currently, the TGA 4000 is set up to allow for the use of oxygen, nitrogen and instrumentation air as purge gases.

It must be noted that while the furnace purge rate may be specified from 1 ml/min to 200 ml/min, **the balance purge is fixed at 150 ml/min.** The mass-flow controller is accurate to ±1 ml/min. The balance purge rate has been optimised for both TGA-FTIR and TGA-GC/MS work and should preferably not be changed from its present setting.

The exhaust gases from both the furnace and the balance merge at the outlet of the furnace and exit the instrument through the furnace top plate (or heated transfer line, if used) and the side exhaust port.

When using the heated trunk, it must be remembered that the furnace gases will be diluted with 150 ml/min of nitrogen before being sucked into the trunk. Any gas which is not sucked up by the trunk is pushed out at the exhaust port. This dilution may affect the results of the gas phase FTIR analysis and care should be taken that the furnace purge not be set so high that it dilutes the product gases to the point that they are not observable by the FTIR spectrometer. In practice it has been found that a furnace purge rate of 50 ml/min is the limit beyond which the purge becomes too dilute to be detected.

It is possible to use helium instead of nitrogen as purge gas. However, the mass flow controller is not calibrated for its use and the relevant physical properties must be given to the Pyris software suite when specifying helium as purge gas.

The cooling jacket is of the continuously recirculating, fixed temperature type. Sample heating or cooling is effected by controlling the power to the furnace so that it is higher or lower than the cooling supplied by the jacket.

The cooling liquid is a 50/50 mixture of ethylene glycol and distilled water and is pumped from the chiller to the back of the TGA where it circulates through the cooling jacket before being returned to the chiller.

At present, the chiller is set to 15 °C. Under no circumstances must this value altered and most especially, the temperature must never be set lower than this value or else water condensation will occur within the balance and furnace, which will damage the instrument. Should the temperature or flow rate from the chiller be adjusted, the furnace must be recalibrated or damage to the instrument will occur from temperature overshoots.

Like the furnace, the sample stem and crucibles are made of sintered alumina. The crucibles come in one size only, namely 150 µl, an example of which is detailed in Figure 31.

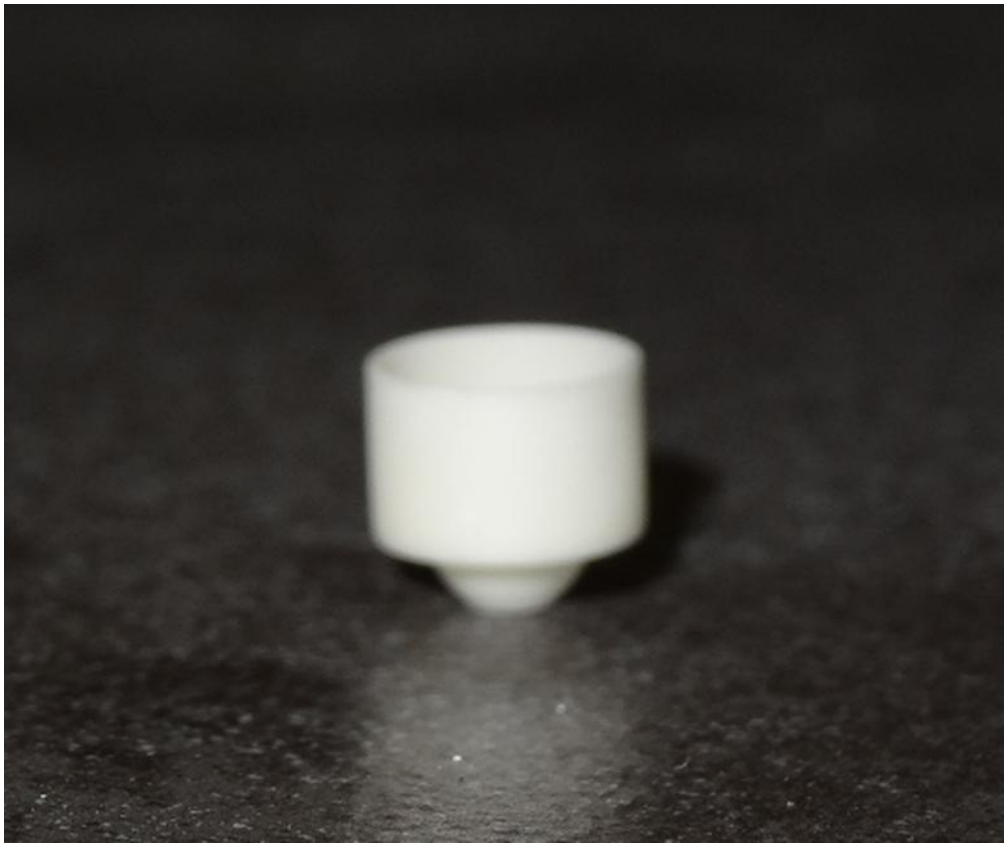

Figure 31: Photograph of a 150 µl sample crucible.

While there are many commercial entities available who can supply sample crucibles, no other make of crucible will fit into the TGA 4000 owing to the shapes of the sample stem and crucible.

The author has made contact with the company that supply Perkin Elmer with their crucibles and is at present in negotiation with them for the production of larger size crucibles.

In conclusion, the TGA 4000 is a very robust and useful instrument, capable of dealing with nearly any thermal analysis task.

3.2.3 Hyphenated TGA-FTIR

The final hyphenated system used for this particular project is depicted in Figure 32. This system enables the FMG to analyse the gaseous products evolved from decomposition reactions taking place in the TGA unit in an online fashion.

The ability to perform this analysis opens up an entire new field of analysis in polymer chemistry and, for this particular project at least, allows us to investing the effect that additives have on the degradation behaviour of polymers in a more detailed and informative fashion.

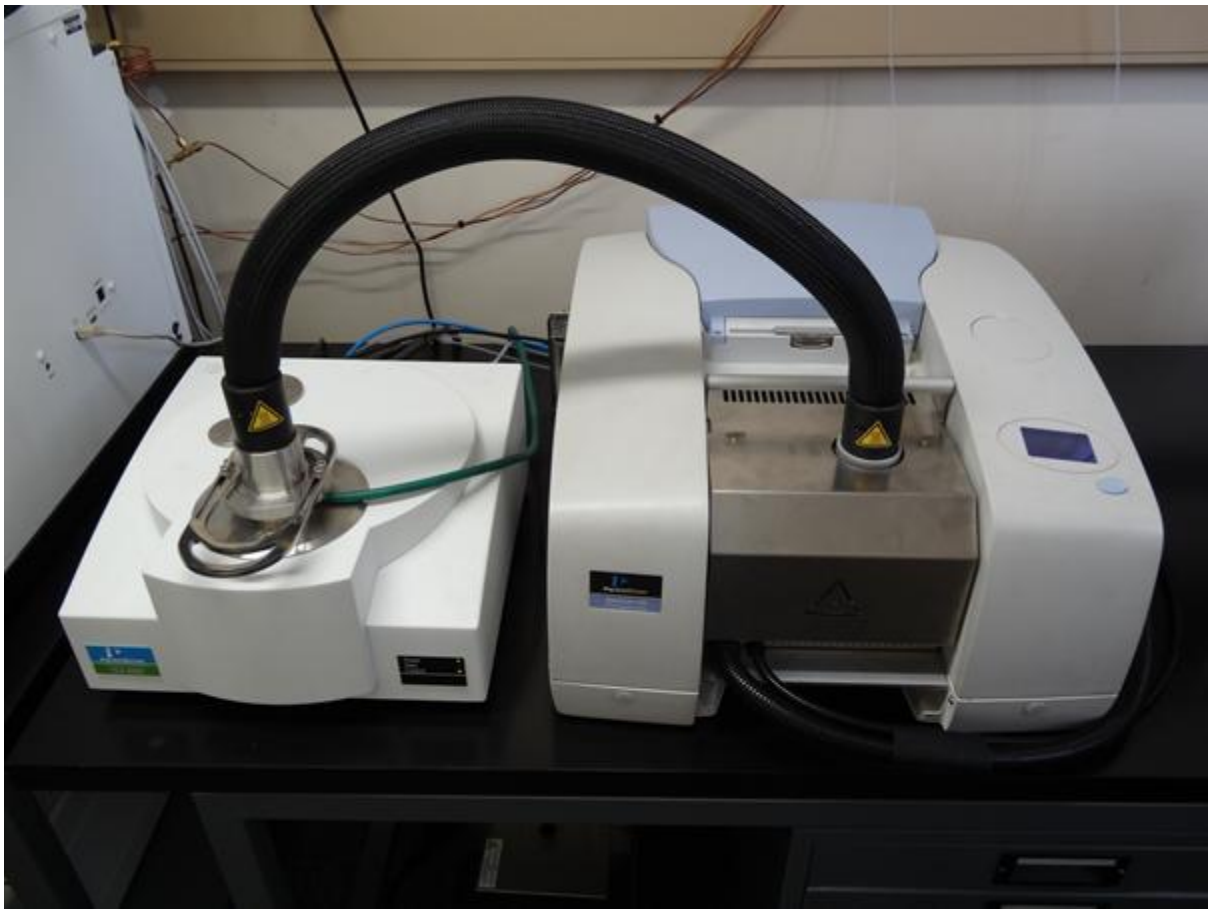

Figure 32: The FMG's TGA-FTIR Hyphenated system.

4 Experimental

4.1 Reagents

The majority of the reagents used in this work were purchased from reliable third party suppliers: Analysis grade (purity >99%) $Al_2(SO_4)_3$, $ZnSO_4$, $CuSO_4$, $NiSO_4$, $CoSO_4$, $FeSO_4$ and $MnSO_4$ we purchased from Saarchem. ACS grade (purity >99%) AlF_3, ZnF_2, CuF_2, NiF_2, CoF_2, FeF_2, MnF_2, Al_2O_3, Ga_2O_3, In_2O_3, CuO, NiO and Fe_2O_3 were purchased from Sigma Aldrich. PTFE 807NX originating from DuPont was used as received. Pharmaceutical grade ZnO (Ph. Eur., BP, USP, 99-100.5%) and high purity V_2O_5 (99.99% trace metal basis) was also purchased from Sigma Aldrich. Cr_2O_3 (purity ≥ 98%) and ZrO_2 (purity > 99%) was purchased from Merck and used as received. La_2O_3 (purity > 99%) was purchased from BDH Chemicals and used as received.

Mn_2O_3 was prepared by calcining 10 g of MnO_2 in air at 800 °C for 24 hours. The Co_3O_4 was prepared by calcining 20 g of $CoCO_3$ in air at 800 °C for 24 hours. The MnO_2 (ReagentPlus grade) and $CocO_3$ was purchased from Sigma Aldrich.

Commercial PTFE (Teflon 807NX) originating from DuPont was used for this work owing to the manufacturer's specification that it is the most pure of the commercially available PTFE types. PTFE produced by the FMG's polymerisation laboratory was not used even though it is chemically more pure that the commercially available products. This was due to the fact that the FMG PTFE has, as yet, not been fully characterised and therefore presents an unknown variable that may affect the results of the study.

All the reagents, except where indicated otherwise, were used as received from the manufacturer. It must be mentioned that many of these reagents were not "fresh" and some of them had been in the FMG's possession for over a year. The reagents were however, properly inspected for degradation before use and all of the old stock were properly stored after their initial use. Degradation of chemical change of the reagents is not a factor in the experimental results.

4.2 Sample Preparation

TGA samples were prepared by grinding 1 g of inorganic material with 1 g of PTFE in a mortar-and-pestle until the mixture appeared macroscopically homogeneous. The mixtures were stored in polytops (air tight class vials) until needed. Some examples of these are given in Figure 33.

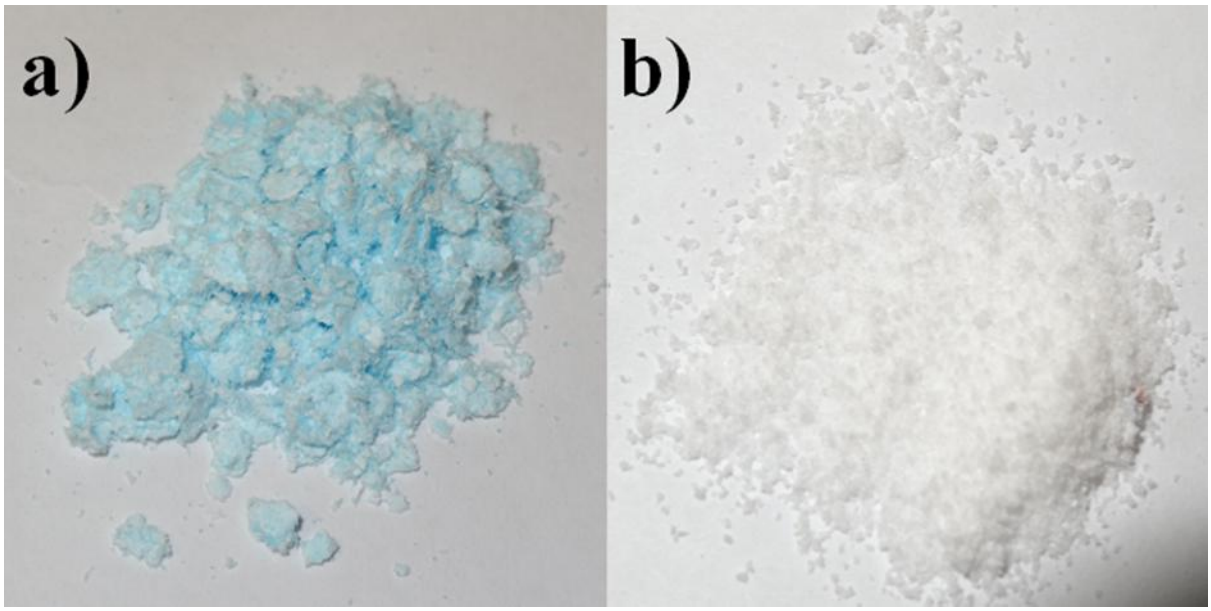

Figure 33: Photographs of a) the $CuSO_4$/PTFE mixture and b) the AlF_3/PTFE mixture.

It goes without saying that the mortar-and-pestle was rigorously cleaned after each grind to prevent cross contamination. Both these items were cleaned using ethanol, distilled water with surfactant and phosphoric acid before being scrubbed with steel wool. The mortar-and-pestle was rinsed with distilled water up to three times after the end of the wash and dried using paper towel.

The TGA crucibles underwent acid cleaning with *aqua regia*, followed by calcination in air at 800 °C and mechanical removal of any remaining deposits by sandpaper abrasion. Finally, the crucibles were rinsed with distilled water and then dried.

It must be mentioned that the grinding process was not conducted with a ball mill or similar apparatus due to the ductility of the PTFE. Attempts to use a ball mill ended in failure with the PTFE coating the grinding balls with no mixing having taken place between the PTFE and the filler materials.

4.3 X-ray Powder Diffraction Analysis

The X-ray powder diffraction analysis conducted on the raw V_2O_5 was performed with a PANalytical X'Pert Powder x-ray diffractometer using Co alpha radiation.

4.4 Quantum Chemical & Thermodynamic Equilibrium Calculations

Quantum chemical calculations were performed with the Spartan 06 software suite (Wavefunction Inc., 2006) using DFT (B3LYP). Each of the expected gaseous product molecules was simulated using the 6-31+G*, 6-311G* and 6-311++G** basis sets. The vanadium fluorides and –oxyfluorides were simulated using the 6-31+G* basis set.

The calculations were performed on a desktop computer supplied by Hewlett-Packard equipped with a 3.2 GHz Intel i7 2600 processor and 16 GB of memory.

The thermodynamic equilibrium composition calculations were performed using Outotec's HSC 6.1 software suite (Roine, 2007).

4.5 TGA-FTIR Analysis

TGA-FTIR experiments were conducted by placing approximately 50 mg of PTFE/filler mixture in α-alumina crucibles followed by pyrolysis using the TGA-FTIR instrumentation setup as described in section 3.2.

The samples were heated at a rate of 20 °C/min from 35 °C to 950 °C in an atmosphere of nitrogen flowing at 20 mL/min. The sampling port area immediately

above the furnace was purged with nitrogen at a rate of 150 mL/min. The heated transfer line and IR gas cell were kept at 225 °C. Transfer of the sample from the TGA to the cell took place at a rate of 40 mL/min, thus diluting the sample with an extra 20 ml/min of nitrogen.

The spectrometer was set to take one scan every 6 s in the range of 4000 cm^{-1} to 550 cm^{-1} at a resolution of 4 cm^{-1}.

Care was taken to insure that the samples taken from the filler/PTFE grind was properly mixed, *i.e.* appeared to be as close to a 50/50 filler/PTFE filler ratio as could be obtained.

5 Results and Discussion

5.1 Generation of IR Reference Spectra for the Product Gases

Infrared spectra for simple fluorinated compounds such as CF_4, TFE, PFE and OFCB are available from NIST (Coblentz Society, 2013), but no literature could be found concerning the infrared spectra for HFP, PFP or the perfluorobutenes. Infrared absorption spectra were, therefore, generated for all the expected product species using DFT (B3LYP) with the 6-31+G*, 6-311G* and 6-311++G** basis sets. The DFT (B3LYP) functional has been shown to predict reasonably accurately the absorption spectra for both small unsaturated fluorocarbons a well as small to medium saturated fluorocarbons (Ignat'eva and Buznik, 2006). It was found that the 6-311G* basis set predicted absorption frequencies closest to the available experimental values. Table 11 compares the calculated absorption frequencies to the experimental frequencies for TFE, PFE and OFCB. presents the calculated absorption frequencies for HFP, PFIB, OF1B and the isomers of OF2B.

Table 11: Experimental and predicted IR absorption frequencies for TFE, PFE and OFCB.

Compound	$\nu_{Calculated}$ (cm^{-1})	$\nu_{Experimental}$ (cm^{-1})
TFE	1324	1324
	1180	1170
PFE	1230	1248
	1107	1114
OFCB	1322	1337
	1275	1286
	1224	1236
	963	960
	565	570

Table 12: Predicted IR absorption frequencies for HFP, PFIB, OF1B, cis-OF2B and trans-OF2B.

$\nu_{Calculated}$ (cm^{-1})				
HFP	**OF1B**	**Cis-OF2B**	**Trans-OF2B**	**PFIB**
1831	1825	1771	1264	1772
1386	1364	1347	1240	1382
1323	1328	1327	1201	1305
1207	1308	1252	1173	1264
1194	1221	1202	883	1231
1155	1215	1166	680	1190
1033	1192	1102		1047
762	1162	954		990
654	1098	717		718
	946			

These calculated infrared absorption frequencies were used to identify the species detected in the gas phase.

It should be noted here that vibrational calculations are not very accurate owing to the inability of the basis sets to deal with the severe electronegativity of fluorine. For example, the experimental vibrations of TFE are at 1324 cm^{-1} and 1170 cm^{-1}, but the *ab initio* calculations predict that the 1170 cm^{-1} will be at 1180 cm^{-1}. These errors are not so large as to make the calculated results useless, but care must be taken when interpreting the experimental results.

5.2 Thermal Behaviour of Pure PTFE

In order to validate the experimental setup and provide a baseline for the filled PTFE experiments, control experiments were carried out using unfilled PTFE.

The thermograms for these experiments, presented in Figure 34, indicate an onset temperature of around 560 °C, in good agreement with the literature. The temperature at which mass loss is first noted was found to be around 450 °C

The degradation also proceeds fairly rapidly, with total decomposition taking approximately 9 minutes at the chosen heating rate of 20 °C/min and no residue remaining in the crucible afterward.

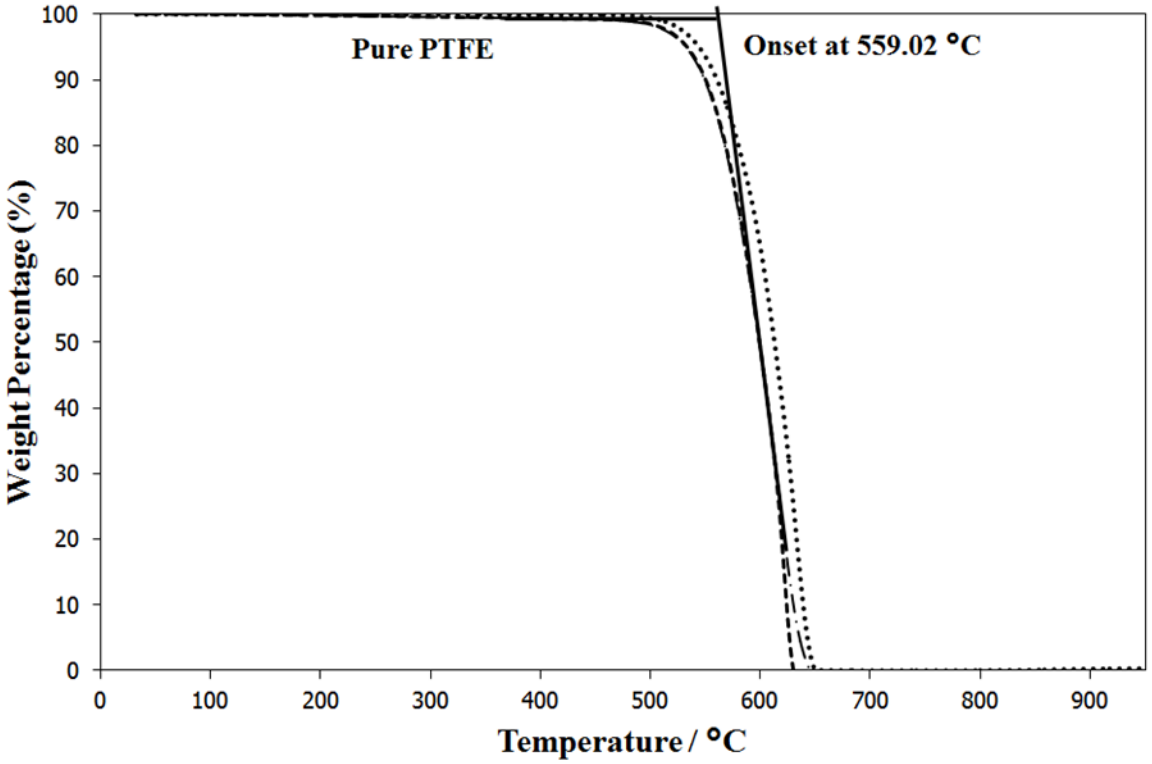

Figure 34: Thermograms for the PTFE control experiments.

The IR spectra for the gas phase were the same for all the control runs, one of which is reproduced in Figure 35. The large bands 1325 cm^{-1} and 1183 cm^{-1} indicate the presence of TFE while those at 1787 cm^{-1}, 1387 cm^{-1} and 1033 cm^{-1} indicate that trace quantities of HFP are also present.

The gas-phase composition determined for the control experiments are in agreement with those reported by Odochian (2011) and Madorski (1953). Keeping in mind that the atmospheric pressure in the laboratory was in the region of 86 kPaa, these results differ strongly with the values reported by Choi and Park (1976) (see Table 1), according to whom, nearly equal amounts of TFE and HFP should be observed.

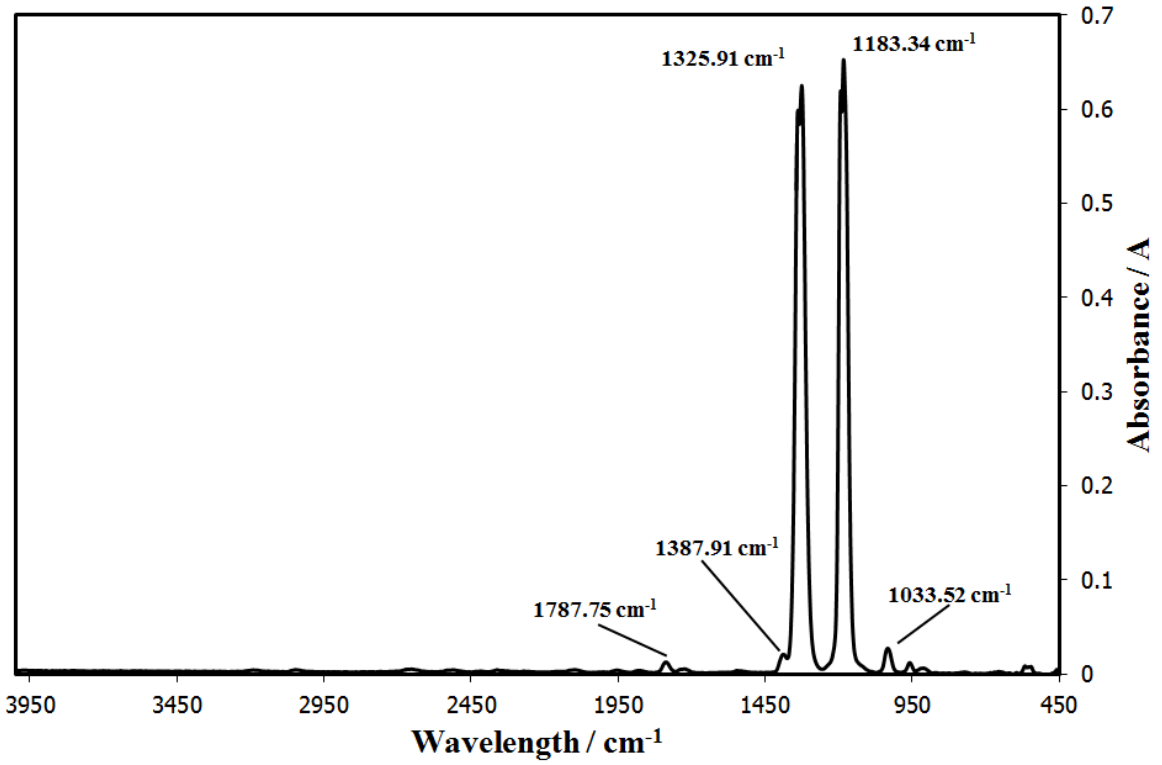

Figure 35: IR Spectrum of the gas phase at maximum absorbance during pyrolysis of pure PTFE.

From this we may state that any fluorocarbon species other than TFE noted in the gas phase is produced by chemical interaction of the PTFE pyrolysates with the filler material.

5.3 Thermal Behaviour of the Neat Filler Materials

Given the relatively high decomposition temperature of PTFE, potential decomposition of the filler material must be considered when interpreting the results of the filled PTFE experiments.

The literature (Weast, 1974) indicates that $Al_2(SO_4)_4$ starts to decompose at 770 °C, $ZnSO_4$ at 680 °C, $CuSO_4$ at 650 °C, $NiSO_4$ at 848 °C, $CoSO_4$ at 735 °C and $FeSO_4$ at 480 °C. $MnSO_4$ melts at 700 °C and decomposes at 850 °C.

Al_2O_3 melts at 2045 °C, Ga_2O_3 melts at 1900 °C, In_2O_3 sublimates at 850 °C, ZnO melts 1975 °C, CuO melts at 1326 °C, NiO melts at 1990 °C, Fe_2O_3 metls at 1565 °C,

Mn_2O_3 decomposes at 1080 °C, Cr_2O_3 melts at 2435 °C and V_2O_3 melts at 690 °C (Weast, 1974). The Co_3O_4 is stable up to 900 °C.

AlF_3 sublimates at 1272 °C (Aigueperse, 2005), ZnF_2 melts at 872 °C, CuF_2 decomposes at 950 °C, NiF_2 sublimates at 1000 °C, CoF_2 melts at 1200 °C, FeF_2 melts at 1000 °C and MnF_2 melts at 856 °C (Weast, 1974).

The metal fluorides and metal oxides, in general, exhibit sharp decomposition or sublimation steps with minimal dissociation at temperatures below their melting or sublimation points, but it is understood that the sulfates have no sharp decomposition point and that near to the reported decomposition temperatures they already exhibit a significant degree of dissociation (Hammerschmidt and Wrobel, 2009).

Thermodynamic-equilibrium composition curves for the solid sulfates are presented in Figure 36.

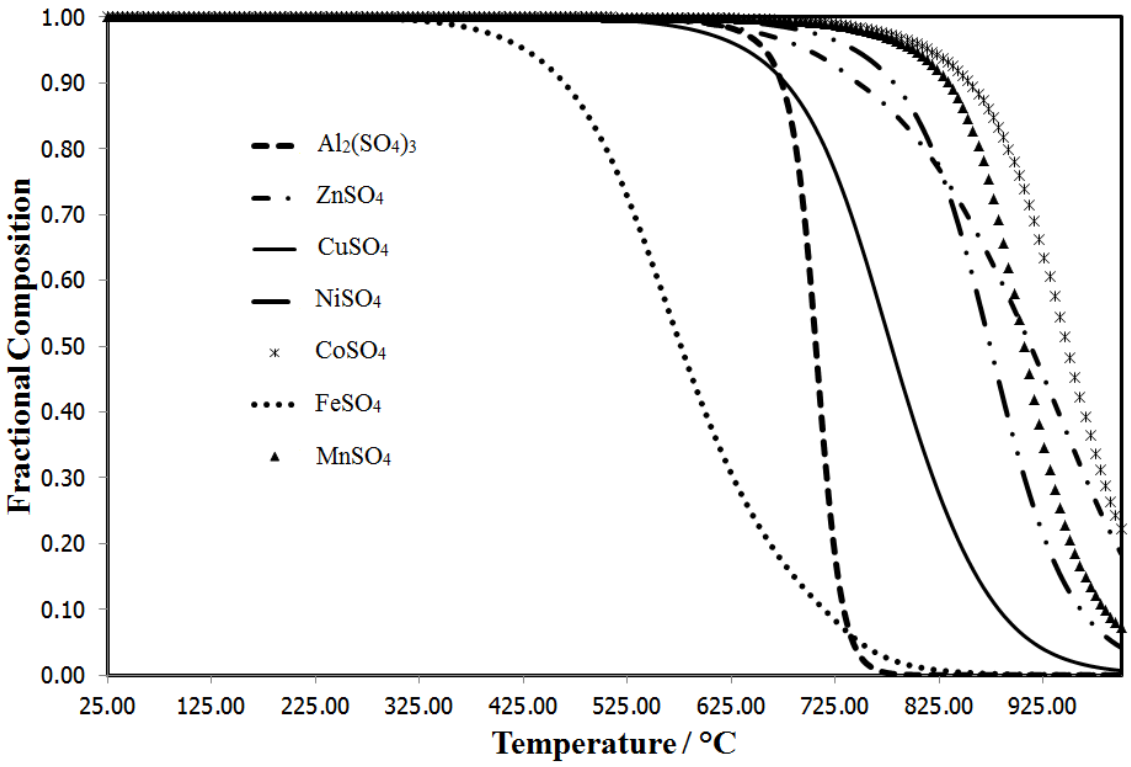

Figure 36: Thermodynamic equilibrium composition of the solid sulfates as a function of temperature.

The graph indicates that all the sulfates except for $FeSO_4$ and $CuSO_4$ should be fully solid during the pyrolysis reaction and, except for the two aforementioned materials, any interactions taking place will be between solid filler and the pyrolysates.

5.4 Thermal Behaviour of PTFE Filled with Transition Metal Sulfates

The thermograms for the pyrolysis of the sulfate filled PTFE samples are presented in Figure 37 and Figure 38, while the infrared spectra of the gas phase, taken at the point of maximum absorbance, are presented in overlaid format in Figure 39 and Figure 40.

With the exception of $CuSO_4$ and $FeSO_4$ filled samples, the onset of degradation temperature does not differ much from that of pure PTFE, varying from 550 °C to 560 °C. The shapes of the degradation curves at the point of PTFE breakdown do not differ significantly from the control case either, implying that these sulfates do not affect the actual degradation process.

The other significant events present on these curves are the dehydration steps for $Al_2(SO_4)_3$, $ZnSO_4$, $CuSO_4$, $CoSO_4$ and $MnSO_4$, which all occur below 400 °C, as well as the bulk breakdown steps for the sulfates themselves, which occur well past the breakdown of PTFE.

$ZnSO_4$ and $MnSO_4$ have no effect on the gas phase, as evidenced by the lack any absorption peaks other than what should be observed for pure PTFE breakdown.

The $Al_2(SO_4)_3$ filled samples show TFE as well as additional peaks at 1386 cm^{-1}, 1280 cm^{-1}, 1244 cm^{-1} and 1034 cm^{-1}, with a small shoulder at 1114 cm^{-1}. Absorption at 1244 cm^{-1} and 1114 cm^{-1} indicate the presence of PFE, while the remaining correspond to HFP.

The $CuSO_4$-filled PTFE samples show peaks for TFE as well as a single side peak at 1244 cm^{-1}. Additionally, there are also peaks at the 600 cm^{-1} and 550 cm^{-1} mark, attributed to the presence of SO_3.

$FeSO_4$ and $CoSO_4$ also produce the side peak at 1244 cm^{-1}. This does not correspond to any of the expected pyrolysis products, and, for the moment, remains unassigned. It was noticed that runs with $CuSO_4$, $FeSO_4$ and $CoSO_4$ produced waxy residues on the inlet of the transfer line with $CuSO_4$ and $CoSO_4$ producing the most significant deposits.

The $NiSO_4$ filled PTFE samples show peaks for TFE as well as side peaks that correspond to the presence of HFP.

All the IR spectra show the presence of CO_2, as indicated by its characteristic absorption band at 2358 cm^{-1} (Coblentz Society, 2013). The production of CO_2 is attributed to a reaction between the pyrolysates and the oxygen atoms at the surface of the sulphate particles. As the filler residues have not been studied, no conclusion can be drawn regarding the fate of the fluorine atoms which are exchanged during this reaction. However, the presence of side bands would indicate that the fluorine atoms are given to other fluorocarbon species, rather than to the filler material.

Additionally, sooty deposits were noticed in the $Al_2(SO_4)_3$ residues. Given that PTFE consists of repeating CF_2 units, the production of saturated fluorocarbons requires fluorine exchange reactions between unsaturated fluorocarbon species to produce perfluorocarbons and $C_{(s)}$. The presence of elemental carbon in the form of soot indicates that this type of exchange has occurred and the production of PFE is thus accounted for.

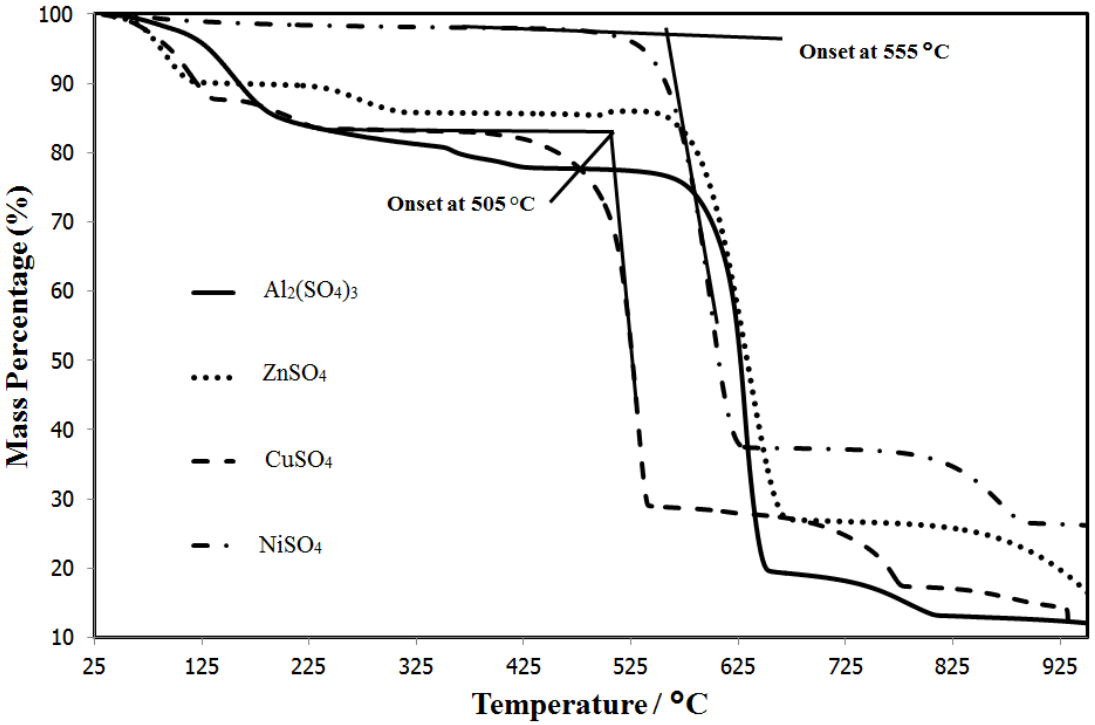

Figure 37: Thermograms for the decomposition of PTFE filled with $Al_2(SO_4)_3$, $ZnSO_4$, $CuSO_4$ and $NiSO_4$.

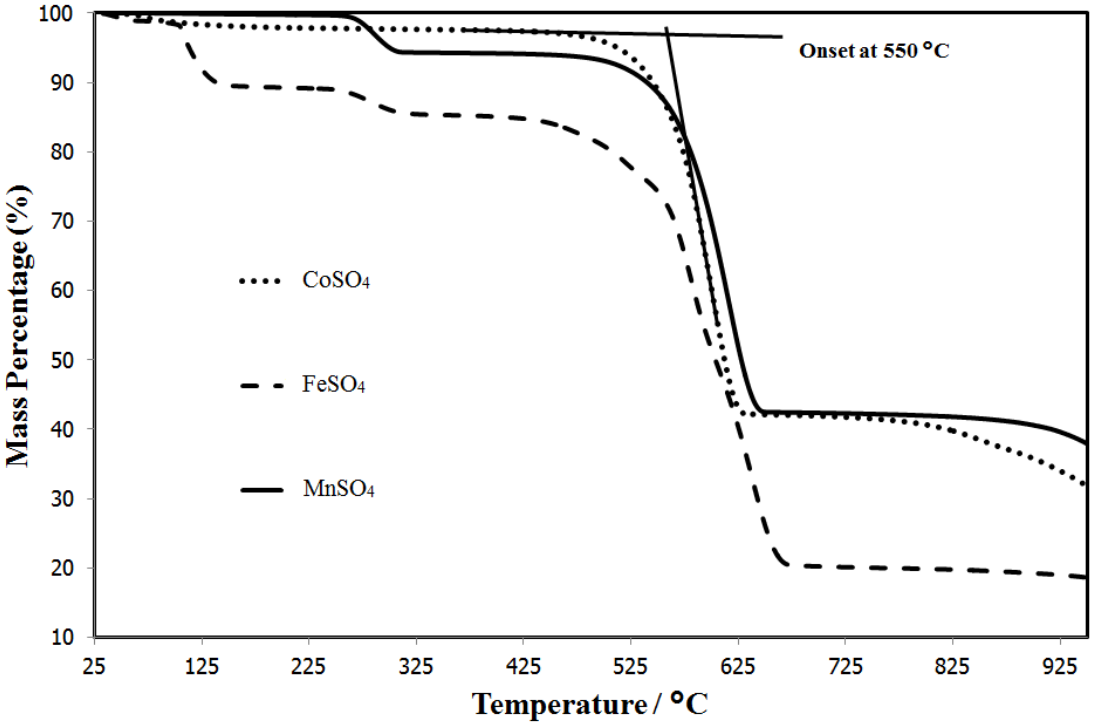

Figure 38: Thermograms for the decomposition of PTFE filled with $CoSO_4$, $FeSO_4$ and $MnSO_4$.

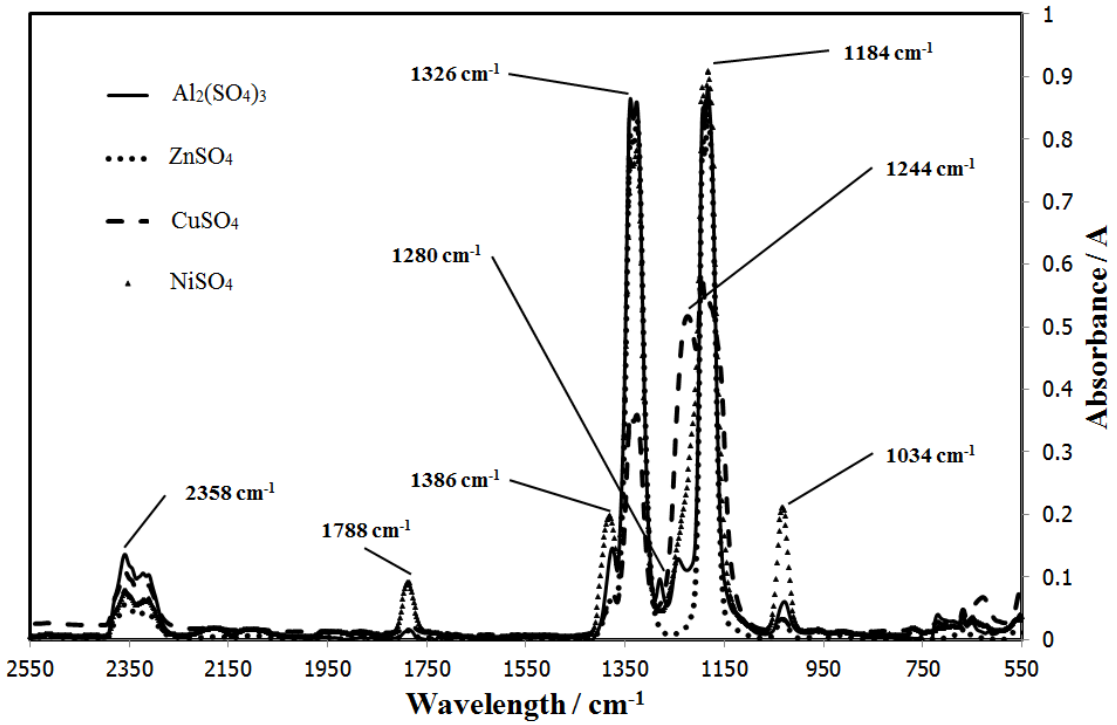

Figure 39: Infrared spectra of the gas phase, taken at the point of maximum absorbance, for the decomposition of PTFE filled with $Al_2(SO_4)_3$, $ZnSO_4$, $CuSO_4$ and $NiSO_4$.

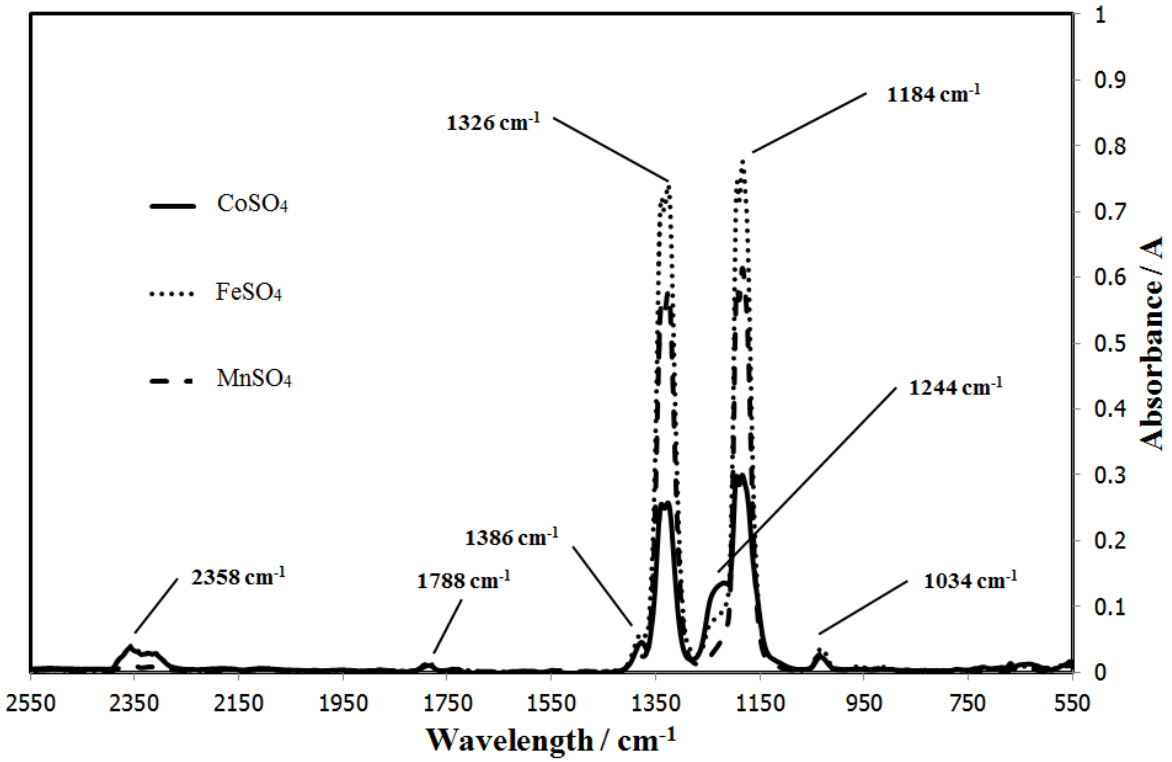

Figure 40: Infrared spectra of the gas phase, taken at the point of maximum absorbance, for the decomposition of PTFE filled with $CoSO_4$, $FeSO_4$ and $MnSO_4$.

5.5 Thermal Behaviour of PTFE Filled with Transition Metal Fluorides

The thermograms for the pyrolysis of the fluoride-filled PTFE samples are presented in Figure 41, while the infrared spectra of the gas phase, taken at the point of maximum absorbance, are presented in Figure 42 and Figure 43.

Except for AlF_3, the onset of degradation temperature is nearly the same for all samples and very close to that of pure PTFE, varying from 565 °C for CoF_2 to 550 °C for CuF_2. Again, except for AlF_3, the slopes of the degradation curves are all similar to the control case. This indicates that these filler materials have no effect on the degradation process.

The AlF_3 filled PTFE show an onset temperature of 530 °C as well as a more rapid degradation rate, as evidenced by the steeper slope of the degradation curve.

Observing the gas phase for the transition metal fluorides, we notice that, in addition to the TFE peaks, there is also some shoulder formation in the region of 1244 cm^{-1}. An interesting trend is exhibited in that NiF_2 produces a large shoulder while the shoulder peaks for the other fluorides are quite muted. This continues the trend seen with the sulfates: Nickel compounds have some special interaction with the pyrolysates.

The peaks present in the spectrum for the AlF_3 filled PTFE do not correspond to any one known pyrolysis product. Assuming that the gas phase is a mixture of compounds rather than comprised of a new, unexpected species, the peaks at 1114 cm^{-1} and 1242 cm^{-1} indicate the presence of PFE. This assignment is confirmed by the presence of sooty deposits in the AlF_3 residue. The remaining peaks then correspond to HFP. Notably absent are the characteristic peaks for TFE, indicating that AlF_3 almost totally reforms the gas phase to HFP.

The marked activity of the aluminium compounds is ascribed to the open P-orbital which can act as electron acceptor. The mechanism of PTFE degradation involves chain scission, a mechanism which is defended in Chapter 2, to produce $:CF_2$ units which then undergo recombination. The $:CF_2$ recombination products undergo

various radical intermediated reactions that produce the products recovered during PTFE pyrolysis. The open P-orbital on the Al cation could arguably capture these radical species, thereby facilitating the fluorine rearrangement reactions that produce the observed products. The reactivity of Co^{2+} is explained by the presence of an unpaired electron in the valence shell which can capture the fluorocarbon radical species generated during pyrolysis.

The reactivity of Co^{2+} and Cu^{2+} is explained by the presence of an unpaired electron in the valence shell which can capture the fluorocarbon radical species generated during pyrolysis.

The apparent difference in reactivity between Al^{3+} and Cu^{2+}/Co^{2+} is attributed to the difference in strength of the metal-fluorocarbon bond with the bond strength with cobalt and copper weaker than with aluminium.

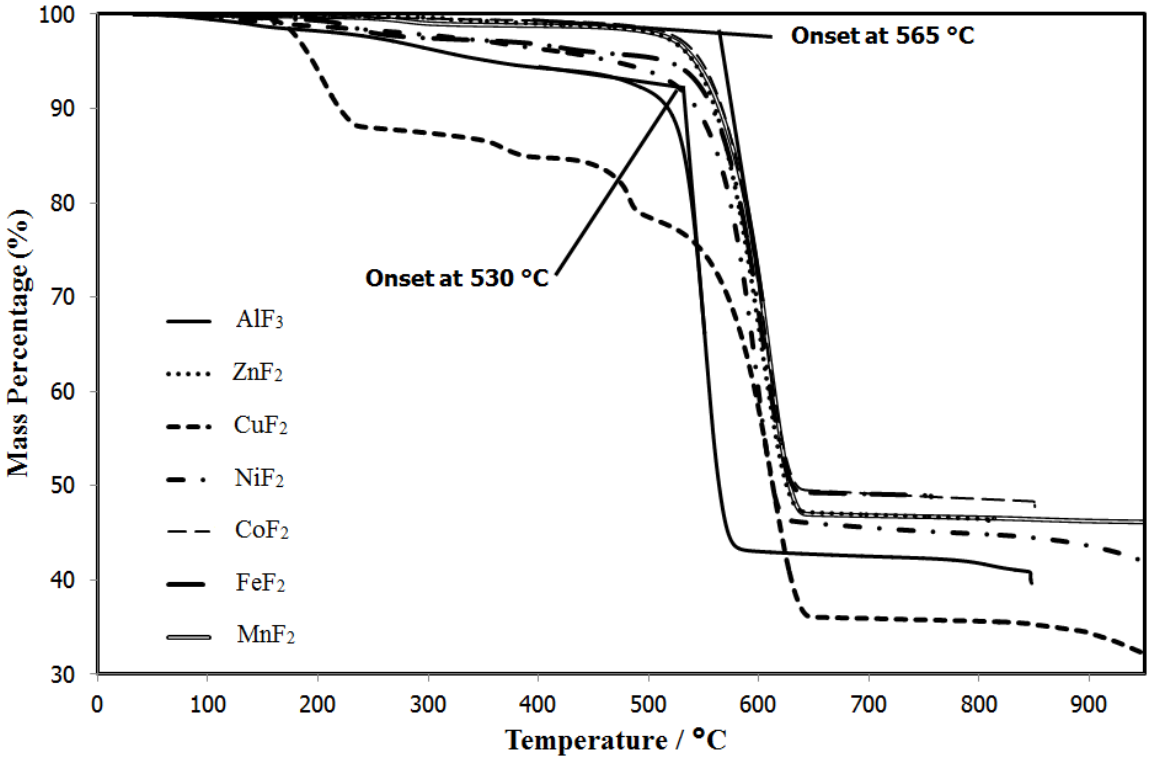

Figure 41: Thermograms for the decomposition of PTFE filled with AlF_3, ZnF_2, CuF_2, NiF_2, CoF_2, FeF_2 and MnF_2.

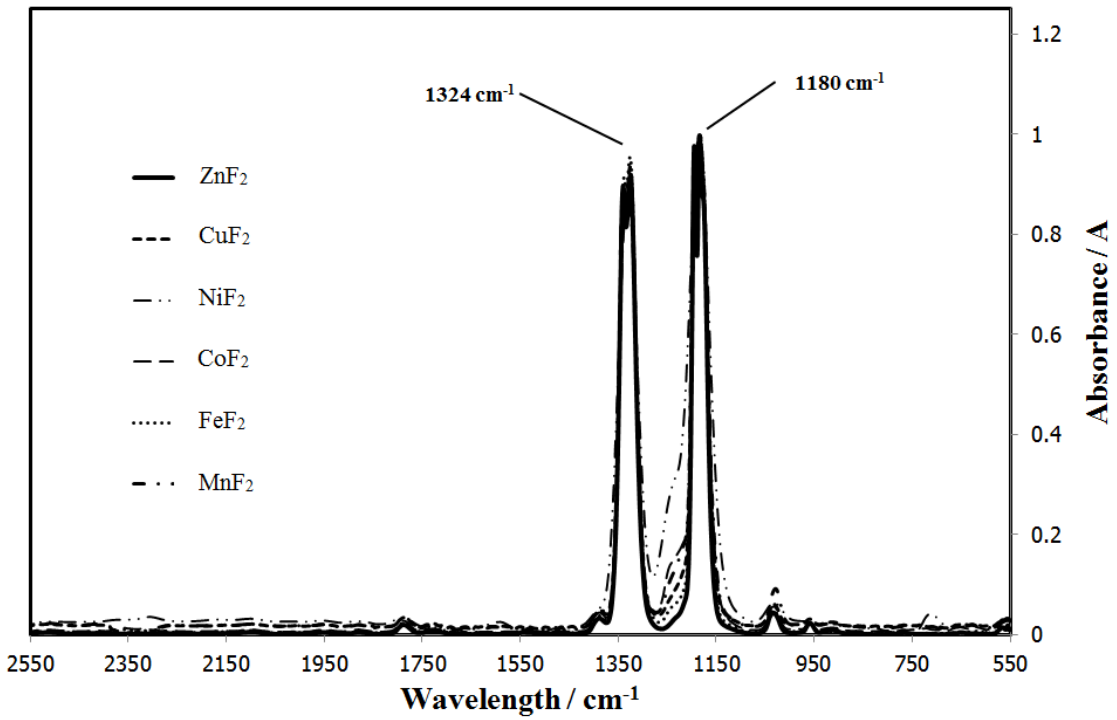

Figure 42: The infrared spectra of the gas phase, taken at the point of maximum absorbance, for the decomposition of PTFE filled with ZnF_2, CuF_2, NiF_2, CoF_2, FeF_2 and MnF_2.

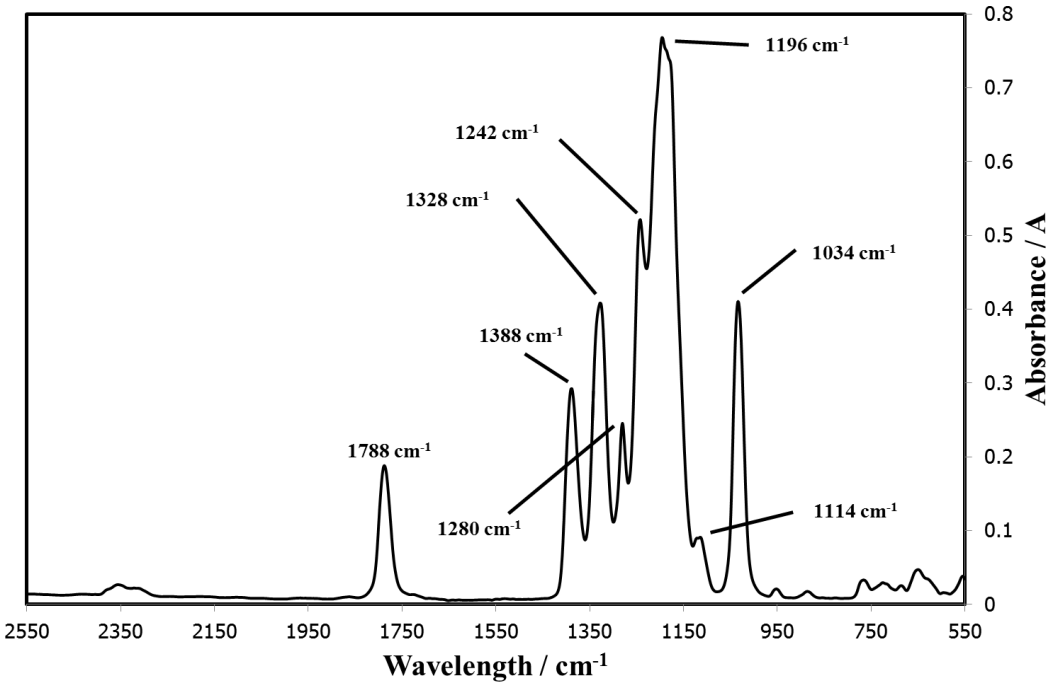

Figure 43: The infrared spectrum of the gas phase, taken at the point of maximum absorbance, for the decomposition of AlF_3-filled PTFE.

5.6 Thermal Behaviour of PTFE Filled with Fourth Period Transition Metal Oxides

The thermograms for the decomposition of PTFE filled with ZnO, CuO, NiO, Co_3O_4, Fe_2O_3, Mn_2O_3, Cr_2O_3 and V_2O_5 are presented in Figure 44. The corresponding IR spectra of the gas phase, taken at the point of maximum absorbance, are presented in Figure 45.

The behaviour of the fourth period metal oxides is interesting in that, except for V_2O_5, the degradation onset temperature does not differ significantly from the pure PTFE control case, being 500 °C for V_2O_5 and 560 °C for the others. More interesting is that CuO and V_2O_5 significantly speed up the rate of degradation, as evidenced by the steep slope of the respective degradation curves. The oxides of Fe and Cr show a slight inhibiting effect on the degradation rate.

The infrared spectra indicate that only CuO, NiO, Cr_2O_3 and V_2O_5 have an effect on the gaseous product distribution. In addition to the characteristic tetrafluoroethylene (TFE) peaks at 1326 cm^{-1} and 1185 cm^{-1}, the CuO filled material exhibits the same side band at 1245 cm^{-1} that was seen for $CuSO_4$. At present the causing species is unknown. It is also noticed that CuO produces a significant amount of CO_2, as evidenced by the characteristic absorption band at 2358 cm^{-1} (Coblentz Society, 2013).

NiO induces some shouldering in the region of 1245 cm^{-1}, similar to what was observed for the fluorides of the fourth period metals, but very little CO_2. The Cr_2O_3 filled material produces a small peak at 1245 cm^{-1} and no CO_2. The V_2O_5 filled material produces a large peak at 1028 cm^{-1} and a strong CO_2 absorption band. ZnO, Fe_2O_3, Co_3O_4 and Mn_2O_3 have no effect on the gas phase other than producing small amounts of CO_2.

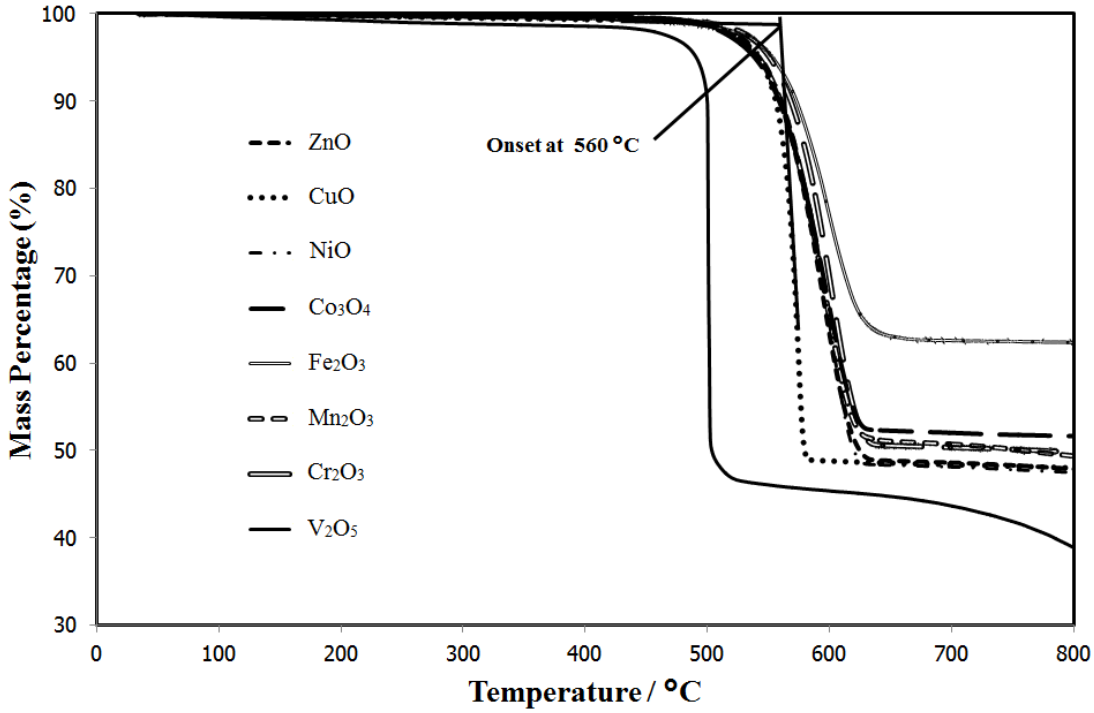

Figure 44: Thermograms for the decomposition of PTFE filled with ZnO, CuO, NiO, Co_3O_4, Fe_2O_3, Mn_2O_3, Cr_2O_3 and V_2O_5.

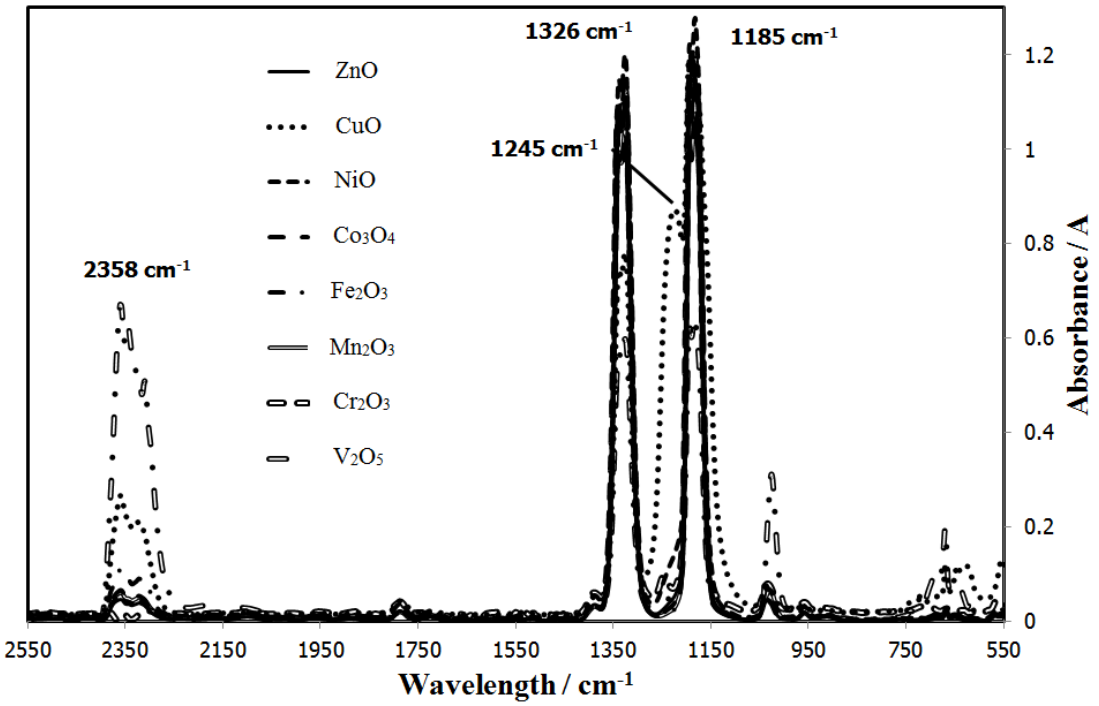

Figure 45: Infrared spectra of the gas phase, taken at the point of maximum absorbance, for the decomposition of PTFE filled with ZnO, CuO, NiO, Co_3O_4, Fe_2O_3, Mn_2O_3, Cr_2O_3 and V_2O_5.

CuO does not undergo oxygen loss under 1000 °C, indicating that the CO_2 observed here is produced by the reduction of CuO by PTFE pyrolysates rather than the combustion of PTFE by free oxygen due to CuO thermal decomposition. The fate of the fluorine atoms exchanged in this reduction is unknown at present, but given the presence of the side peak at 1245 cm^{-1}, it is reasonably assumed that they attach themselves to nearby fluorocarbon species, rather than attach to the surface of the CuO crystals.

The absorption band at 1028 cm^{-1} in the V_2O_5 sample is unaccompanied by absorption bands that correspond to any of the expected pyrolysis products, but does corresponds to the characteristic absorption peak for SiF_4 (Coblentz Society, 2013). The X-ray diffraction pattern of V_2O_5, reproduced in Figure 46, indicate that the V_2O_5 is crystallographically pure, and X-ray fluorescence shows that there is no silicon present in the inorganic material. This makes the assignment of the 1028 cm^{-1} band to SiF_4 highly implausible.

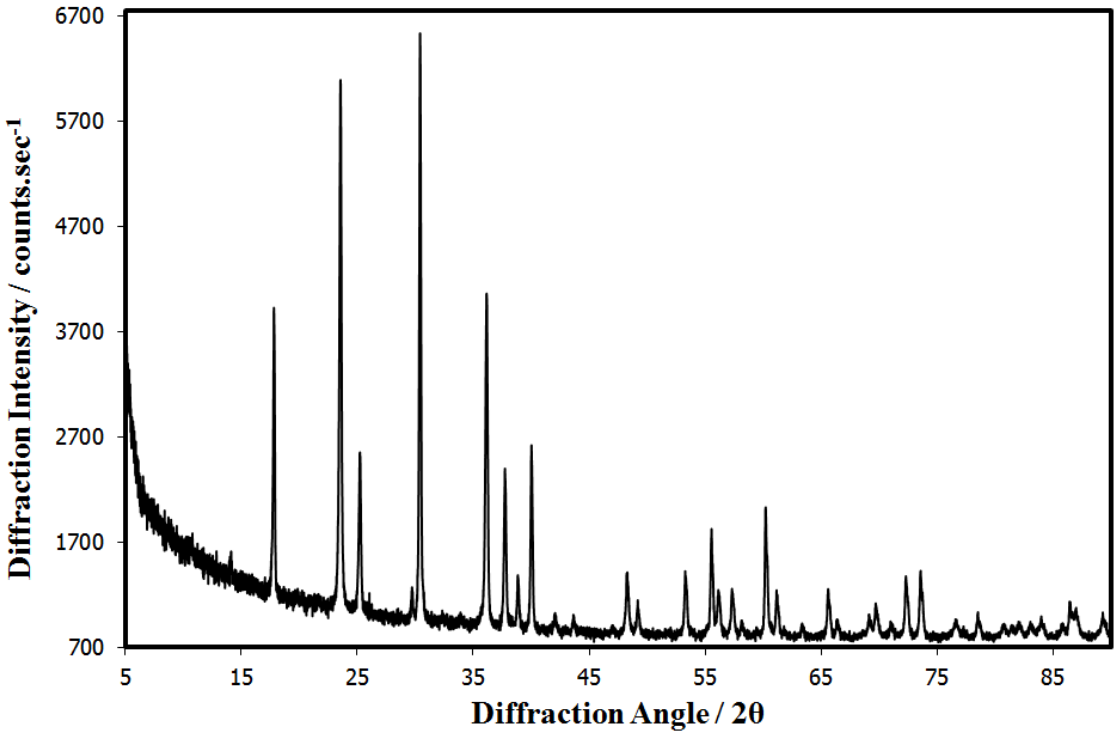

Figure 46: X-ray diffraction pattern showing the characteristic diffraction peaks for V_2O_5, indicating the V_2O_5 is crystallographically pure.

VF_3 and VF_5 are both volatile at temperatures below 1000 °C, with VF_5 boiling at 111 °C and VF_3 sublimating at 800 °C (Weast, 1974), implying that they could potentially be in the gas phase at PTFE pyrolysis conditions. No literature could be found on the infrared absorption of VF_3, however the literature indicates that VF_5 does not have any infrared absorbance bands in the region near 1000 cm^{-1} (Hope, 1990).

Quantum-chemical calculations of VF_3, VF_4 and VF_5 using DFT (B3LYP) with the 6-31+G* basis set indicated that VF_3 has a singular absorption band at around 1950 cm^{-1}, VF_4 at around 760 cm^{-1} and VF_5 exhibiting two absorption bands at around 770 cm^{-1} and 830 cm^{-1} (compare the experimental of 769 cm^{-1} and 801 cm^{-1} (Hope, 1990). The literature indicates that VF_3O boils at 480 °C (Weast, 1974) and absorbs infrared at 1054 cm^{-1}, 806 cm^{-1}, 721.5 cm^{-1}, 308 cm^{-1}, 257.8 cm^{-1} and 204.3 cm^{-1} (Selig and Claassen, 1966). The absorption behaviour of these compounds indicates that the absorption peak at 1028 cm^{-1} cannot be due to any vanadium fluoride or vanadium oxyfluoride. The cause of the band at 1028 cm^{-1} remains unknown at present, but is reasonably assumed to not be caused by SiF_4.

5.7 Thermal Behaviour of PTFE Filled with Group 13 Oxides

The thermograms for the decomposition of PTFE filled with Al_2O_3, Ga_2O_3 and In_2O_3 are presented in Figure 47. The corresponding IR spectra of the gas phase, taken at the point of maximum absorbance, are presented in Figure 48.

The degradation onset temperature is in the region of 550 °C for all three oxides. The rate of degradation for Ga_2O_3 and In_2O_3 does not differ significantly from the control case. However, Al_2O_3 significantly accelerates the degradation rate.

The infrared spectra show that Al_2O_3 produces PFE and HFP similar to what was noticed for AlF_3 and $Al_2(SO_4)_3$. Ga_2O_3 produces some shouldering around 1235 cm^{-1} while In_2O_3 seems to be inert towards the gas phase. Given that all these compounds are Lewis acids, we find that the binding strength of these compounds with fluorocarbon radicals are in the order of $Al_2O_3 >> Ga_2O_3 > In_2O_3$.

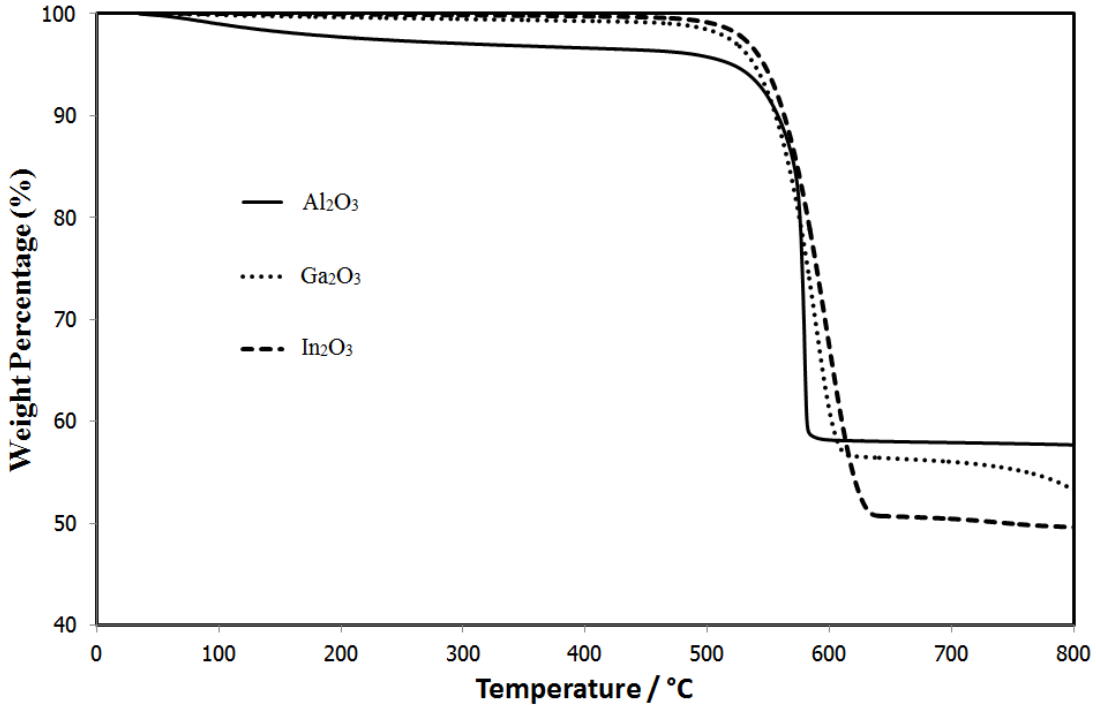

Figure 47: Thermograms for the decomposition of PTFE filled with Al_2O_3, Ga_2O_3 and In_2O_3.

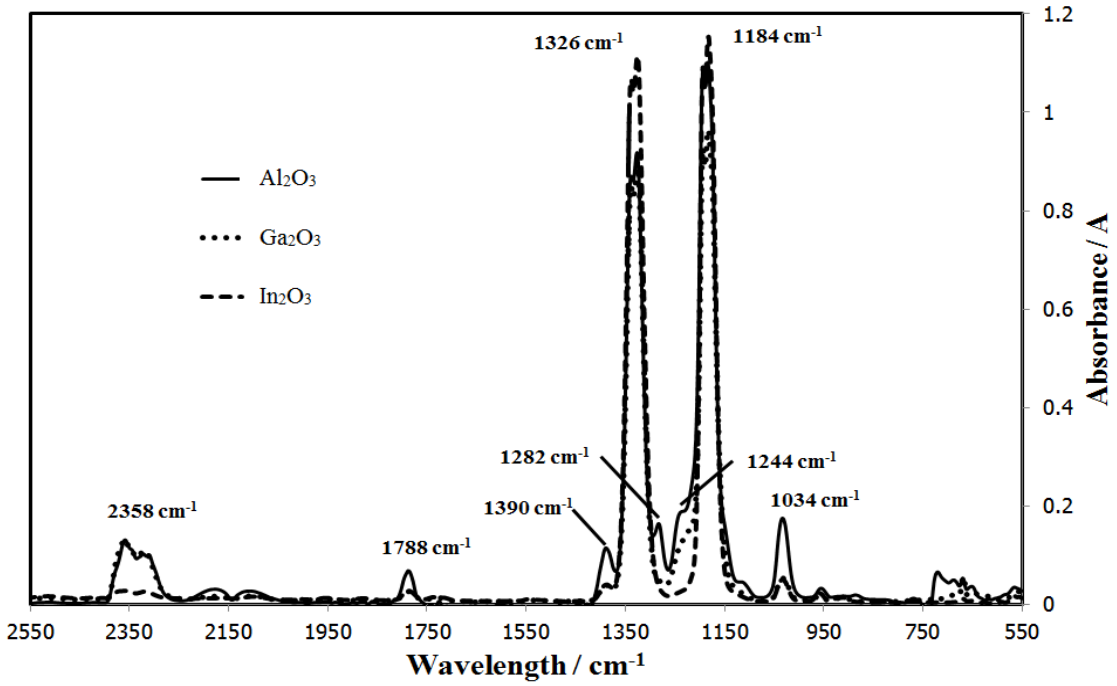

Figure 48: Infrared spectra of the gas phase, taken at the point of maximum absorbance, for the decomposition of PTFE filled with Al_2O_3, Ga_2O_3 and In_2O_3.

Working from the observation made in Section 5.5, a plausible mechanism for the group 13 catalysed reactions involves the chemisorption of :CF_2 onto the metal sites via the insertion of the unpaired electrons into the empty p-orbital of metal atoms at the surface of the catalyst crystal, followed by co-ordination of one radical to an adjacent CF_2 molecule. If a situation arises where two CF_2 units co-ordinate to a central CF_2, fluorine re-arrangement may occur to produce HFP which then desorbs from the catalyst surface. This is illustrated for Al_2O_3 in the reaction scheme given in Figure 49. A plausible mechanism for PFE formation is presented in the reaction scheme in Figure 50.

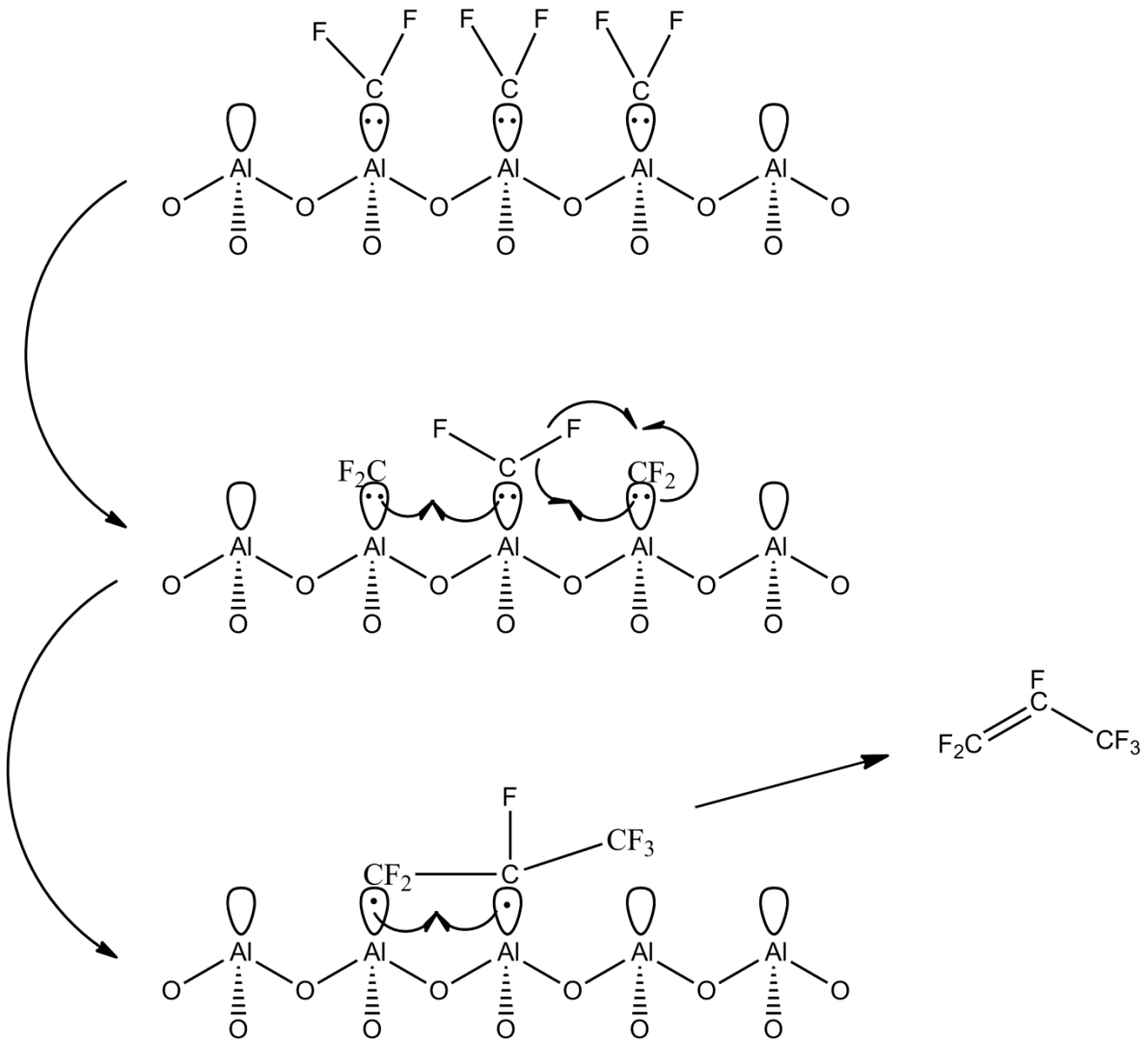

Figure 49: Proposed mechanism for the synthesis of hexafluoropropylene from :CF_2 on alumina.

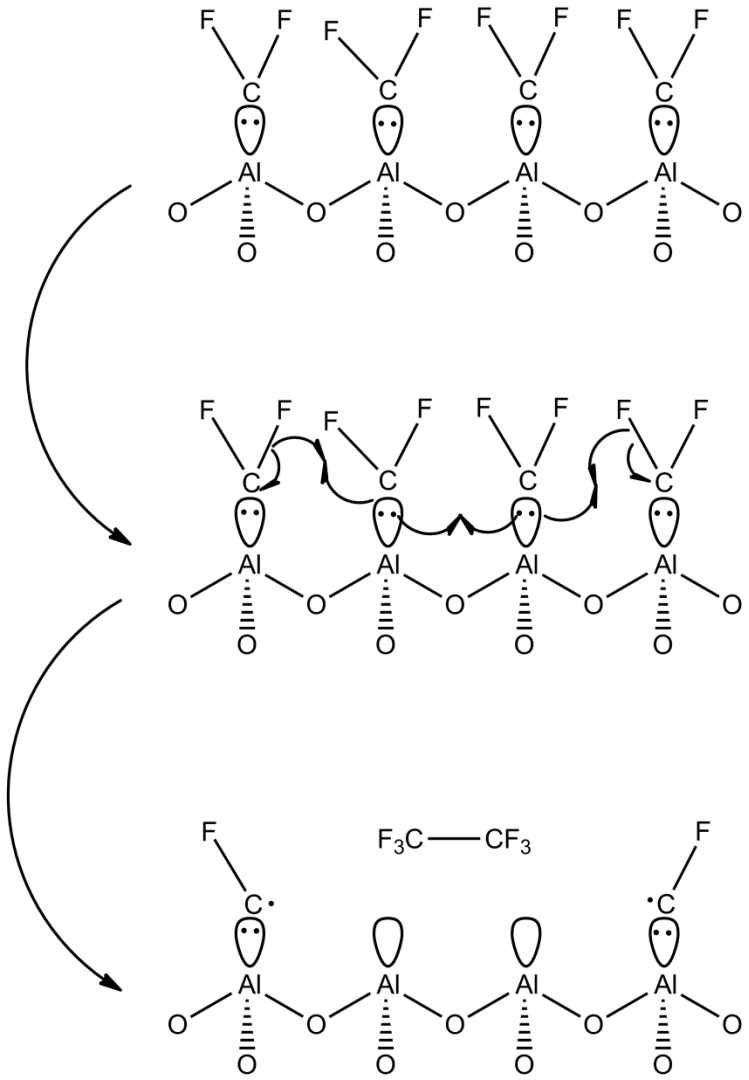

Figure 50: Proposed mechanism for the synthesis of perfluoroethane from :CF_2 on alumina.

The fate of the CF molecules occurring after the rearrangement reaction shown in Figure 50 is difficult to speculate upon, but it is assumed that, given the formation of soot on the catalyst, the CF units undergo another round of fluorine exchange to produce elemental carbon.

The behaviour of B_2O_3 could not be studied as the B_2O_3 melt evaporated completely from the crucible before PTFE pyrolysis occurred.

5.8 Thermal Behaviour of PTFE Filled with ZrO_2 and La_2O_3

The thermograms for the decomposition of PTFE filled with ZrO_2 and La_2O_3 are presented in Figure 51. The corresponding IR spectra of the gas phase, taken at the point of maximum absorbance, are presented in Figure 52.

Zirconia and lanthana are known to be generally unreactive, requiring high temperatures and severe conditions to react. The thermograms indicate that this inertness is exhibited in the presence of fluorocarbon radicals as well, with neither ZrO_2 nor La_2O_3 significantly affecting the degradation onset temperature (found to be 550 °C). The slopes of the degradation curves are somewhat flatter that what is observed for pure PTFE, indicating that ZrO_2 and La_2O_3 have an inhibiting effect on the degradation rate.

The infrared spectra indicates that ZrO_2 and La_2O_3 have no effect on the gaseous product distribution other than La_2O_3 producing some CO_2.

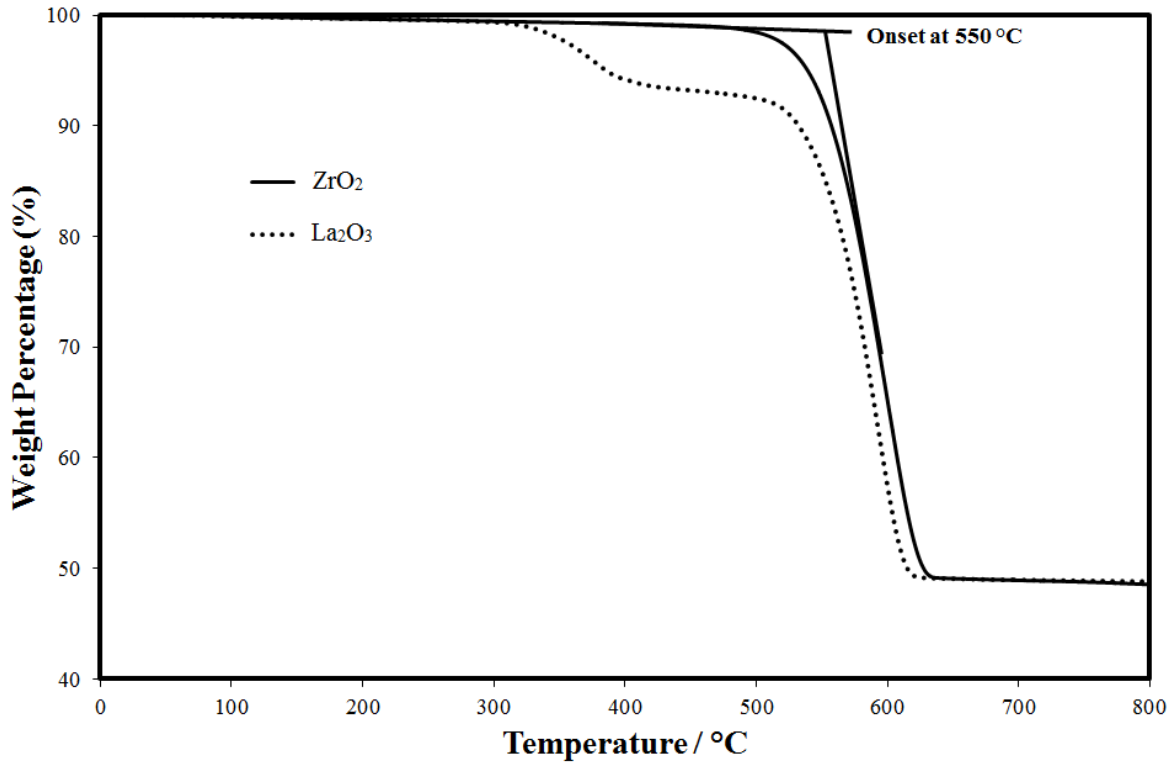

Figure 51: Thermograms for the decomposition of PTFE filled with ZrO_2 and La_2O_3.

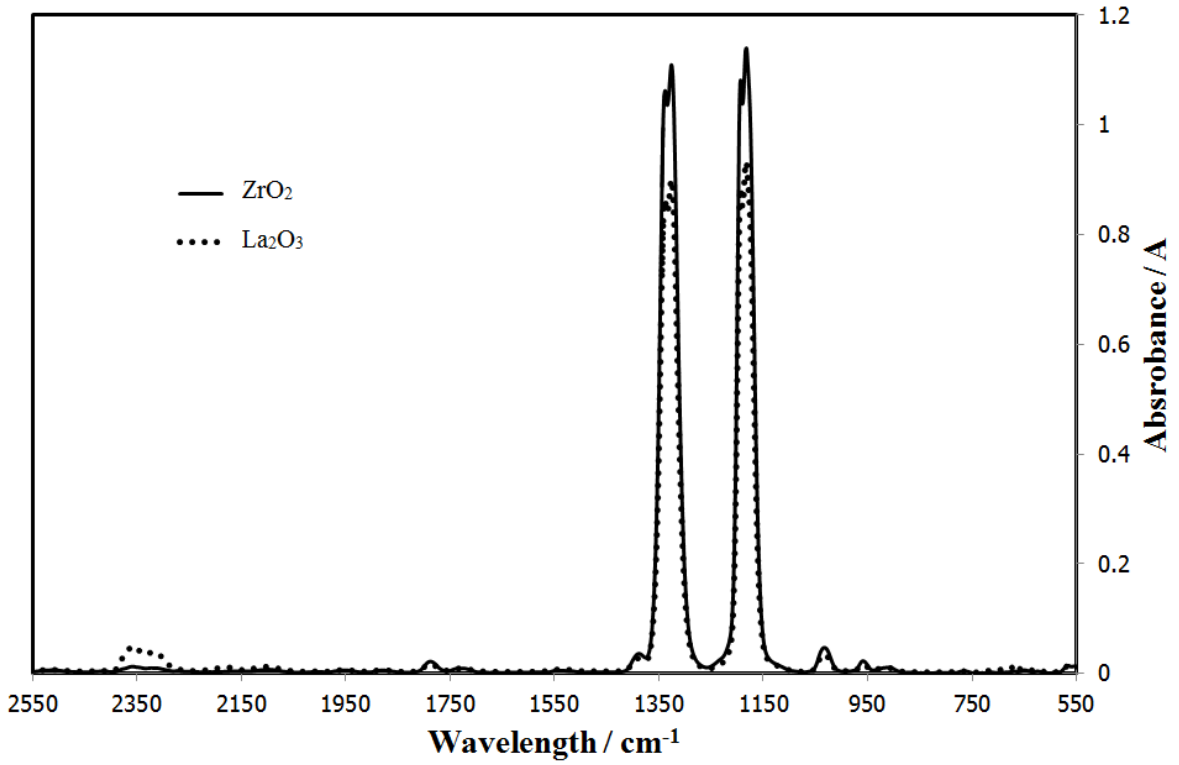

Figure 52: Infrared spectra of the gas phase, taken at the point of maximum absorbance, for the decomposition of PTFE filled with ZrO_2 and La_2O_3.

6 Research Conclusions and Recommendations

The work detailed here has demonstrated that the sulfates of Al, Zn, Ni, Co, Fe and Mn are generally inert with respect to the rate of degradation of PTFE, but that $CuSO_4$ accelerates the degradation rate and lowers the degradation onset temperature by 50 °C. These compounds all affect the composition of the gaseous product stream with $Al_2(SO_4)_3$ and $NiSO_4$ increasing the yield of HFP.

This work has also demonstrated that ZnO, NiO, Co_3O_4, Fe_2O_3, Mn_2O_3, Cr_2O_3, ZrO_2 and La_2O_3 are generally inert with respect to the degradation onset temperature and degradation rate of PTFE. Except for ZrO_2, all these oxides undergo surface reactions with the PTFE pyrolysates to produce CO_2, with NiO and Cr_2O_3 also catalysing some small change in the gaseous composition, but producing predominantly TFE.

It was also demonstrated that CuO and V_2O_5 react in bulk with PTFE at pyrolysis conditions, greatly increasing the degradation rate and producing CO_2, with V_2O_5 decreasing the degradation onset temperature by 60 °C. CuO catalyses some small change in the gas phase. V_2O_5 produces an additional absorption band at 1028 cm^{-1} which does not correspond to any of the known pyrolysis products.

Furthermore, it has been shown that Al_2O_3 shifts the gaseous product distribution to HFP and PFE and that the group 13 metal oxides decrease in reactivity with PTFE when going down the periodic table.

Finally, this work has demonstrated that the fluorides of Zn, Cu, Ni, Co, Fe and Mn are generally inert with respect to the rate of degradation of PTFE, but that AlF_3 accelerates the degradation rate and lowers the degradation onset temperature by approximately 30 °C. All these compounds have some effect on the product stream composition, but that AlF_3 displays the strongest effect on the gas phase, seemingly producing exclusively PFE and HFP in an ratio of approximately 50/50 %.

The questions that originally prompted this investigation now has a first approximation answer: AlF_3, $Al_2(SO_4)_3$, Al_2O_3 and $NiSO_4$ show potential as catalysts for the selective beneficiation of PTFE waste by pyrolysis to hexafluoropropylene.

Furthermore, much of the data reported in this work are completely new and allow for a better understanding of the degradation behaviour of PTFE, provide data on the suitability of filler materials for the functionalization of PTFE *via* nanocomposites and opens up an entirely new field of catalysis research.

The behaviour seen with aluminium compounds have led to the postulation of mechanisms for the formation of HFP and PFE. The mechanisms involves the chemisorption of $:CF_2$ onto the open p-orbitals of the aluminium metal sites followed by co-ordination of two $:CF_2$ units adjacent to a central $:CF_2$ unit. Fluorine exchange reactions then take place which produce the intermediaries that finally desorb to form HFP and PFE.

Finally, it was concluded from the available literature that Lewis bases would be effective catalysts and no mention was made of the possible use of Lewis acids; but the data presented here has indicated that Lewis acids are very effective catalysts.

This work should be continued using a three-pronged attack:

- The reactivity of the metal oxides examined here should be tested further by examination of the metals in their 3+ and 2+ oxidation states, where the applicable oxide has not been covered;
- The phosphates of the metals examined here should also be studied to determine if the presence of a phosphorous atom will affect the reactivity; and
- *Ab initio* work should be conducted to gain insight as to which crystal surfaces are responsible for the catalytic effects of the relevant materials.

Work that would follow on the last point, should anything meaningful arise from such a study, is the examination of heats of adsorption of TFE and HFP onto these materials as well as an examination by reflection infrared absorption techniques to determine the mode of bonding of the adsorbing molecules on to the catalyst surface (similar to what has been done for CO on cobalt in Fischer-Tropsch catalysis).

7 References

Aigueperse, J, Mollard, P, Devilliers, D, Chemla, M, Faron, R, Romano, R, Cuer, JP **(2005)** Fluorine Compounds, Inorganic, in: *Ullmann's Encyclopedia of Industrial Chemistry*, Wiley, Weinheim.

Ameduri, B, Boutevin, B **(2003)** *Well-Architectured Fluoropolymers: Synthesis, Properties, and Applications*, Elsevier, Amsterdam.

Arkles, BC, Bonnett, RN **(1974)** "Method for the Depolymerization of Polytetrafluoroethylene" *US Patent 3,832,411*, Liquid Nitrogen Processing Corporation.

Atkinson, B, Atkinson, VA **(1957)** "The Thermal Decomposition of Tetrafluoroethylene" *Journal of the Royal Chemical Society (Resumed)*, 2086–2094.

Atkinson, B, Trenwith, AB **(1953)** "The Thermal Decomposition of Tetrafluoroethylene" *Journal of the Royal Chemical Society (Resumed)*, 953, 2082–2087.

Baker, BB, Kasprzak, DJ **(1993)** "Thermal degradation of Commercial Fluoropolymers in Air" *Polymer Degradation and Stability*, **42**, 181–188.

Banks, RE, Tatlow, JC (1986) "A Guide to Modern Organofluorine Chemistry" *Journal of Fluorine Chemistry*, 33, 227–346.

Barabanov, VG, Bispen, TA, Ilyin, AN, Kornilov, VV, Krivoshein, AE, Moldavsky, DD, Fenichev, IM, Vasilév, AS, Zubritskaya, NG **(2011)** "The Improved Preparation Method of Difluoro(fluorosulfonyl)acetyl Fluoride" *Fluorine Notes*, **2 (75)**, 1–3.

Bedford, CD, Baum, K **(1980)** "Preparation of α,ω-diiodoperfluoroalkanes" *Journal of Organic Chemistry*, **45**. 347–348.

Bhadury, PS, Singh, S, Sharma, M, Palit, M **(2007)** "Flash pyrolysis of polytetrafluoroethylene in a quartz assembly" *Journal of Analytical and Applied Pyrolysis*, **78 (2)**, 288–290.

Brahms, DLS, Dailey, WP **(1996)** "Fluorinated Carbenes" *Chemical Reviews*, **96**, 1585–1632.

Brice, TJ, LaZerte, JD, Hals, LJ, Pearlson, WH **(1953)** "The Preparation and some Properties of the C_4F_8 Olefins" *Journal of the American Chemical Society*, **75 (11)**, 2698–2702.

Brown, HC **(1957)** "Reactions of Hexafluoropropene with Sulphur" Journal of Organic Chemistry, **22 (6)**, 715.

Bryant, WMD (1962) "Free Energies of Formation of Fluorocarbons and Their Radicals. Thermodynamics of Formation and Depolymerisation of Polytetrafluoroethylene" *Journal of Polymer Science*, 56, 277–296.

Buravstev, NN, Kolbanovskii, YA, Ovsyannikov, AA **(1994)** "1,2 – Biradicals as Intermediates in the Cyclodimerization of Tetrafluoroethylene" *Mendeleev Communications*, **4 (2)**, 48–50.

Buravtsev, NN, Kolbanovskii, YA **(2001)** "Mechanism of Hexafluoropropylene Formation in gas-phase pyrolysis of Tetrafluoroethylene" *Macromolecular Chemistry and Polymeric Materials*, **75 (4)**, 598–605.

Buravtsev, NN, Kolbanovskii, YA, Ovsyannikov, AA **(1994)** "Biradical Intermediates in Tetrafluoroethylene Dissociation and Difluorocarbene Recombination" *Mendeleev Communications*, **4 (5)**, 190–191.

Buravtsev, NN, Kolbanovsky, YA **(1999)** "Intermediates of thermal transformations of perfluoro-organic compounds. New spectral data and reactions" *Journal of Fluorine Chemistry*, **96 (1)**, 35–42.

Carlson, JP, Schmiegel, W **(2005)** Fluoropolymers, Organic, in: *Ullmann's Encyclopedia of Industrial Chemistry*, Wiley, Weinheim.

Carlsson, DJ, Tovborg Jensen, JP, Wiles, DM **(1984)** "Antioxidant Mechanisms of Hindered Amine Light Stabilizers" *Macromolecular Chemistry Supplements*, **8**, 79–88.

Carter, VL, Bafus, DA, Warrington, HP, Harris, ES (1974) "The acute inhalation toxicity in rats from the pyrolysis products of four fluoropolymers", *Toxicology and Applied Pharmacology*, 30 (3), 369–376.

Cheremisinoff, NP (1996) *Polymer Characterisation: Laboratory Techniques and Analysis*, Noyes Publications, New Jersey.

Choi, SK, Park, JD **(1976)** "The Pyrolysis of Polytetrafluoroethylene" *Journal of the Korean Chemical Society*, **20 (2)**, 141–145.

Choi, SS, Kim, YK **(2011)** "Analysis of pyrolysis products formed from ethylene-tetrafluoroethylene heterosequences of poly(ethylene-co-tetrafluoroethylene)" *Journal of Analytical and Applied Pyrolysis*, **92**, 470–476.

Coblentz Society, Inc. **(2013)** Evaluated Infrared Reference Spectra, in: Linstrom, PJ, Mallard, WG, *NIST Chemistry WebBook, NIST Standard Reference Database Number 69*, National Institute of Standards and Technology, http://webbook.nist.gov, (retrieved December 31, 2013).

Conesa, JA, Font, R **(2001)** "Polytetrafluoroethylene Decomposition in Air and Nitrogen" *Polymer Engineering and Science*, **41 (12)**, 2137–2146.

David, J, Boyer, C, Tounar, J, Ameduri, B, Lacroix-Desmazes, P, Boutevin, B **(2006)** "Use of Iodocompounds in Radical Polymerization"*Chemical Reviews*, **106 (9)**, 3936.

Dindi, H, Hagedorn, JJ, Hung, MH **(2004)** "Process for Manufacturing Diiodoperfluoroalkanes", *US Patent 6,825,389*, DuPont Dow Elastomers LLC.

Dixon, GD, Feast, WJ, Knight, GJ, Mobbs, RH, Musgrave, WKR, Wright, WW **(1969)** "Preparation and Thermal Degradation of Copolymers of Tetrafluoroethylene and Perfluoroalkenes" *European Polymer Journal*, **5 (2)**, 295–306.

Dmowski, W, Flowers, WT, Haszeldine, RN **(1977)** "The use of Crown Ethers in the Synthesis of Hexafluoropropene and Tetrafluoroethylene Oligomers" *Journal of Fluorine Chemistry*, **9 (1)**, 94–96.

Drobny JG **(2001)** *Technology of Fluoropolymers*, CRC Press.

England, DC, Dietrich, MA, Lindsey, RV **(1960)** "Reactions of Fluoroolefins with Sulfur Trioxide" *Journal of the American Chemical Society*, **82**, 6181–6188.

Errede, LA **(1962)** "The Application of Simple Equations for Calculating Bond Dissociation Energies to Thermal Degradation of Fluorocarbons" *Journal of Organic Chemistry*, **27 (10)**, 3425–3430.

Ferrero, F, Beckmann-Kluge, M, Spoormaker, T, Schroder, V **(2011)** "On the Minimum Ignition Temperature for the Explosive Decomposition of Tetrafluoroethylene on hot walls: Experiments and calculations" *Journal of Loss Prevention in the Process Industries*, **25**, 293–301.

Filatov, VY, Murin, AV, Kazienkov, SA, Khitrin, SV, Fuks, SL **(2011)** "Depolymerisation of Polytetrafluoroethylene in the Presence of Water Vapor or Fluorine-Transfer Agent" *Russian Journal of Applied Chemistry*, **84 (1)**, 147–150.

Florin, RE, Wall, La, Brown, DW, Hymo, LA, Michaelsen, JD **(1954)** "Factors Affecting the Thermal Stability of Polytetrafluoroethylene" *Journal of Research of the National Bureau of Standards*, **53 (2)**, 121–130.

Fock, J **(1968)** "On the influence of Carbon Black on the Thermal Degradation of Polytetrafluoroethylene" *Polymer Letters*, **6 (2)**, 127–131.

Fokin AV, Skladnev, AA, Studnev, YN, Knunyants, LL **(1964)** "Reactions of FLuoroolefins with Hydrogen Sulfide" *Izvestiya Akademii Nauk SSSR Seriya Khimicheskaya*, **2**, 341–346.

Garcia, AN, Viciano, N, Font, R **(2007)** "Products obtained in the fuel-rich combustion of PTFE at high temperatures" *Journal of Analytical and Applied Pyrolysis*, **80 (1)**, 85–91.

Gelblum, PG, Herron, N, Noelke, CJ, Rao, VNM **(2002)** "Synthesis of Perfluoroolefins" *European Patent WO/2002/006193*, E. I. du Pont de Nemours and Company.

Hammerschmidt, J, Wrobel, M (2009) "Decomposition of metal sulphates – A SO_2 source for sulphuric acid production" *The Southern African Institute of Mining and Metallurgy's Sulphur and Sulphuric Acid Conference*, Johannesburg.

Harmon, J **(1946)** "Polyfluorinated Cycloparafins and process for producing them", *US Patent 2,404,374*, E.I. du Pont de Nemours & Company.

Hayes, T, Furst, K, Richards, H **(2009)** *Industry Study 2496 Fluoropolymers*, The Freedonia Group, Cleveland.

Hintzer, K, Schöttle, T, Staudt, HJ ,Weber, H **(1995)** "Process for the Preparation of Fluorinated Monomers*" European Pat. 0647607 A1*.

Hoffmann, R, Woodward, RB **(1965)** "Selection Rules for Concerted Cycloaddition Reactions" *Journal of the American Chemical Society*, **87 (9)**, 2046–2048.

Hope, EG **(1990)** "Spectroscopic studies on molecular vanadium pentafluoride isolated in inert gas matrices" *Journal of the Chemical Society, Dalton Transactions*, **1990 (3)**, 723–725.

Hunadi, RJ, Baum, K **(1982)** "Tetrafluoroethylene: A Convenient Laboratory Preparation" *Synthesis*, **82 (6)**,454.

Ignat'eva, LN, Buznik, VM **(2006)** "Quantum-chemical calculations of the IR absorption spectra of modified polytetrafluoroethylene forms" *Russian Journal of Physical Chemistry*, **80 (12)**, 1940–1948.

James, R, Rowsell, DG **(1969)** "The preparation of Fluorinated Cyclic Sulphides and Dispulphides" *Chemical Communications*, 1274–1275.

Karube, D, Chaki, T, Shiotani, Y, Sugiyama, A **(2010)** "Process for production of 2,3,3,3-tetrafluoropropene", *WO2010/013795A1*, Daikin Industries, ltd.

Keeler, J (2002) *Understanding NMR Spectroscopy*, Wiley, New York.

Knight, GJ, Wright, WW **(1972)** "Thermal Degradation of Perfluoro Polymers" *Journal of Applied Polymer Science*, **16**, 739–748.

Kolbanovskii, YA, Mamikonyan, ER, Matveyeva, LN, Shchipachev, VS **(1990)** "High-Temperature 1,2-Transfer of F in C_2F_4 in Gas Phase" *Soviet Journal of Chemical Physics*, **7 (4)**, 885–892.

Kotov, SV, Ivanov, GD, Kostov, GK **(1988)** "A Convenient One-Stage Synthesis of Some Diiodoperfluoroalenes by using Tetrafluoroethylene derived from PTFE waste" *Journal of Fluorine Chemistry*, **41 (2)**, 293–295.

Krespan, CG, Langkammerer, CM **(1962)** "Fluorinated Heterocyclic Derivatives of Sulfur, Selenium and Phosphorus" *The Journal of Organic Chemistry*, **27 (10)**, 3584–3587.

Krespan, CG, Wheland, RC **(1994)** "Perfluoroalkyl Sulfide Polymer Solvents for Fluoromonomer Polymerisation", *US Patent 5,286,822*, E.I. Du Pont de Nemours.

Lacher, JR, Tompkin, GW, Park, JD **(1952)** "The Kinetics of the Vapor Phase Dimerization of Tetrafluoroethylene and Trifluorochloroethylene" *Journal of the American Chemical Society*, **74 (7)**, 1693–1696.

Lailey, AF **(1997)** "Oral N-acetylcysteine protects against perfluoroisobutene toxicity in rats" *Human & Experimental Toxicology*, **16**, 212–216.

Laird, RK, Andrews, EB, Barrow, RF **(1950)** "The Absorption Spectrum of CF_2" *Transactions of the Faraday Society*, **46**, 803–805.

Lee, CH, Guo YL, Tsai, PJ, Chang, HY, Chen, CR, Chen, CW, Hsiue, TR **(1997)** "Fatal acute pulmonary oedema after inhalation of fumes from polytetrafluoroethylene" *European Respiratory Journal*, **10**, 1408–1411.

Lewis, EE, Naylor, MA **(1947)** "Pyrolysis of Polytetrafluoroethylene" *Journal of the American Chemical Society*, **69 (8)**, 1968–1970.

Lisochkin, YA, Poznyak, VI **(2006)** "Explosive-Hazard Estimates for Several Fluorine-Containing Monomers and Their Mixtures, Based on the Minimum Ignition Pressure with a Fixed Igniter Energy" *Combustion, Explosion and Shock Waves*, **42 (2)**, 140–143.

Liu, L, Davis, SR **(1992)** "Matrix Isolation Spectroscopic Study of Tetrafluoroethylene Oxidation" *Journal of Physical Chemistry*, **96 (24)**, 9719–9724.

Lonfei, J, Jingling, W, Shuman, X **(1986)** "Mechanisms of Pyrolysis of Fluoropolymers" *Journal of Analytical and Applied Pyrolysis*, **10 (2)**, 99–106.

Madorsky, SL, Hart, VE, Straus, S, Sedlak, VA **(1953)** "Thermal Degradation of Tetrafluoroethylene and Hydrofluoroethylene Polymers in a Vacuum" *Journal of Research of the National Bureau of Standards*, **51 (6)**, 327–333.

Marhevka, JS, Johnson, GD, Hagen, DF, Danielson, RD **(1982)** "Generation of Perfluoroisobutylene Reference Sample and Determination by Gas Chromatography with Electron Capture and Flame Ionization Detection" *Analytical Chemistry*, **54 (14)**, 2607–2610.

Meissner, E, Wroblewska, A, Milchert, E **(2004)** "Technological parameters of pyrolysis of waste polytetrafluoroethylene" *Polymer Degradation and Stability*, **83 (1)**, 163–172.

Meyer, B **(1976)** "Elemental Sulphur" *Chemical Reviews*, **76 (3)**, 367–388.

Mezzapelle, JJ **(2007)** "Etching processes using C_4F_8 for silicon dioxide and CF_4 for Titanium Nitride" *US Patent 7276450 B2*, International Business Machines Corporation.

Michaelsen, JD, Wall, LA **(1957)** "Further Studies on the Pyrolysis of Polytetrafluoroethylene in the Presence of Various Gases" *Journal of Research of the National Bureau of Standards*, **58 (6)**, 327–331.

Miller, WT **(1951)** *Slesser & Schram's National Nuclear Energy Series*, Book 7, Volume 1, Chapter 32, 592–596.

Moon, DJ, Chung, MJ, Kwon, YS, Ahn, BS **(2004)** "Method of a Simultaneous Preparation of Hexafluoropropylene and Octafluorocyclobutane", *US Patent 6,710,214 B2*, *Korea Institute of Science and Technology.*

Moore, GJ, Massey, HM **(1992)** "Tetrafluoroethane Isomerization", *US Patent 5,091,600*, Imperial Chemical Industries plc.

Morisaki, S **(1978)** "Simultaneous Thermogravimetry-Mass Spectrometry and Pyrolysis-Gas Chromatography of Fluorocarbon Polymers" *Thermochemica Acta*, **25 (2)**, 171–183.

National Toxicology Program **(2011)** *Report on Carcinogens*, Twelfth Edition.

Nelson, DA **(1956)** "Pyrolysis process for making Perfluoropropene from Tetrafluoroethylene", *US Patent 2,758,138*, E. I. du Pont de Nemours and Company.

O'Shea, ML, Monterra, C, Low, MJD (1990) "Spectroscopic Studies of Carbons, XVII: Pyrolysis of Polyvinylidene Fluoride", *Materials Chemistry and Physics*, 26 (2), 193–205.

Odochian, L, Moldoveanu, C, Mocanu, AM, Carja, G **(2011)** "Contributions to the thermal degradation mechanism under nitrogen atmosphere of PTFE by TG-FTIR analysis" *Thermochemica Acta*, **526 (1-2)**, 205–212.

Ohashi, M, Kambara, T, Hatanaka, T, Saijo, H, Doi, R, Ogoshi, S **(2011)** "Palladium-Catalyzed Coupling Reactions of Tetrafluoroethylene with Arylzinc Compounds" *Journal of the American Chemical Society*, **133**, 3256–3259.

Pasto, DJ, Johnson, CR (1969) *Organic Structure Determination*, Prentice-Hall, New Jersey.

Pearson, RG **(1968)** "Hard and Soft Acids and Bases, HSAB, Part 1" *Journal of Chemical Education*, **45 (9)**, 581–587.

Penski, EC, Goldfarb, IJ **(1964)** "The Effect of Caging on the Thermal Degradation of Polytetrafluoroethylene" *Polymer Letters*, **2 (1)**, 55–58.

Pohanish, RP **(2002)** *Sittig's Handbook of Toxic and Hazardous Chemicals and Carcinogens*, 4th Edition, Noyes, New York.

Rogalski, Antoni (2010) *Infrared Detectors*, 2de Edition, CRC Press, London.

Roine, A. 2007, HSC Chemistry Ver. 7.0, Outotec, Pori.

Scheel, LD, Lane, WC, Coleman, WE **(1968)** "The Toxicity of Polytetrafluoroethylene Pyrolysis Products" *American Industrial Hygiene Association Journal*, 41 – 48.

Scheirs, J **(1997)** *Modern Fluoropolymers,* Wiley, New York.

Schildknecht, CE **(1952)** *Vinyl and related Polymers*, Wiley, New York.

Selig, H, Claassen, HH **(1966)** "Infrared Spectra of VOF3 and POF3" *The Journal of Chemical Physics*, **44 (4)**, 1404–1406.

Siegle, JC, Muus, LT, Lin TP, Larsen, HA **(1964)** "The molecular structure of Perfluorocarbon Polymers. II. Pyrolysis of Polytetrafluoroethylene" *Journal of Polymer Science: Part A*, **2 (1)**, 391–404.

Simon, CM, Kaminsky, W **(1998)** "Chemical recycling of polytetrafluoroethylene by pyrolysis" *Polymer Degradation and Stability*, **62**, 1–7.

Spartan 06, Wavefunction Inc., Irvine, California, United States of America.

Stuart, BH (2002) *Polymer Analysis*, Wiley, New York.

Takagi, T, Tamura, M, Shibakami, M, Quan, H, Sekiya, A **(2000)** "The synthesis of perfluoroamine using nitrogen trifluoride" *Journal of Fluorine Chemistry*, **101**, 15–17.

Tamayama, M, Andersen, TN, Eyring, H **(1967)** "The Melting and Pyrolysis of Teflon and the Melting of Silver Chloride and Iodine under High Pressure" *Proceedings of the National Academy of Sciences of the United States of America*, **57 (3)**, 554–561.

Thermo Scientific (2007) "Application Note 50808: Detectors for Fourier Transform Spectroscopy", Thermo Fischer Scientific, Madison, Wisconsin.

Tittle, B **(1972)** "The reaction of Tetrafluoroethylene with Arsenic Trifluoride" *Journal of Fluorine Chemistry*, **2**, 449–450.

Tsugi, S, Ohtani, H, Watanabe, C (2011) *Pyrolysis-GC/MS Databook of Synthetic Polymers*, Elsevier, Amsterdam.

Van der Walt, IJ **(2007)** *Recovery of Valuable Products from Polytetrafluoroethylene (PTFE) Waste*, Ph.D. Thesis, North West University, Potchefstroom, South Africa.

Van der Walt, IJ, Grunenburg, AT, Nel, JT, Maluleke, GG, Bruinsma. OSL **(2008)** "The Continuous Depolymerisation of Filled Polytetrafluoroethylene with a Continuous Process" *Journal of Applied Polymer Science*, **109 (1)**, 264–271.

Walker, HW **(1943)** "Catalytic Reactions of Ethylene" *The Journal of Physical Chemistry*, **31**, 961–996.

Wampler, TP (2007) *Applied Pyrolysis Handbook*, 2de Edition, CRC Press, London.

Wang, SY, Borden, WT **(1989)** "Why is the π Bond in Tetrafluoroethylene weaker than that in Ethylene? An ab Initio Investigation" *Journal of the American Chemical Society*, **111 (18)**, 7282–7283.

Weast, RC **(1974)** CRC Handbook of Chemistry and Physics, 55th Edition, Chapter B, CRC Press, Cleveland, Ohio.

Williams, SJ, Clarke, FB **(1982)** "Combustion Product Toxicity: Dependence on the Mode of Product Generation" *Fire and Materials*, **6 (3-4)**, 161–162.